Republic of Iraq
Ministry of Higher Education
And Scientific Research
University of Technology
Mechanical Engineering Department

A CFD SIMULATION OF SOME IRAQI LIQUID AND GASEOUS FUELS COMBUSTION

A THESIS

SUBMITTED TO THE MECHANICAL ENGINEERING DEPARTMENT AT THE UNIVERSITY OF TECHNOLOGY IN A PARTIAL FULFILLMENT OF THE REQUIREMENTS FOR THE DEGREE OF MASTER OF SCIENCE IN MECHANICAL ENGINEERING

By Engineer

Hayder Mohammed Abbas

B.Sc. In Mech. Eng.2002.

SUPERVISED BY

Ass. Prof .Dr. Kutaiba J. Mahdi ***Ass. Prof. Dr Adel M. Saleh***

2013


سُورَةُ الفَاتِحَةِ
بِسْمِ ٱللَّهِ ٱلرَّحْمَٰنِ ٱلرَّحِيمِ ﴿١﴾
ٱلْحَمْدُ لِلَّهِ رَبِّ ٱلْعَٰلَمِينَ ﴿٢﴾
ٱلرَّحْمَٰنِ ٱلرَّحِيمِ ﴿٣﴾ مَٰلِكِ يَوْمِ
ٱلدِّينِ ﴿٤﴾ إِيَّاكَ نَعْبُدُ وَإِيَّاكَ
نَسْتَعِينُ ﴿٥﴾ ٱهْدِنَا ٱلصِّرَٰطَ
ٱلْمُسْتَقِيمَ ﴿٦﴾ صِرَٰطَ ٱلَّذِينَ
أَنْعَمْتَ عَلَيْهِمْ غَيْرِ ٱلْمَغْضُوبِ
عَلَيْهِمْ وَلَا ٱلضَّآلِّينَ ﴿٧﴾

Dedication

To almighty Allah who taught me the first character.

To the Messenger of Allah (Mohammed) and his households and Progeny

(Prays and peace be upon them).

To Imam AL Mahdi Al Muntadhar

(Peace be upon him).

To the person who planned my future life before his death… my father

To my happiness… my mother

To my life and love…my wife & kids.

Hayder Mohammed Abbas

25/10/2013

Acknowledgements

As I produce and present this thesis, I want to present my thankful praying to Almighty Allah for all the assistance in the success of my study and for supplying me with strength and patience to complete it.

Sincere thanks are due to my supervisor Asst. prof. (**Dr. Kutaiba J. Al-Khishali**) for his suggestion to carry out this work, encouragement, kindness and assistance by his correct opinions. Thanks are also to my supervisor Asst. Prof. (**Dr. Adel M. Saleh)** with sincere gratitude and thankfulness. I am deeply thankful to them. I will never forget them forever.

Sincere thanks to Prof. (**Dr. Jack Stein**), North Carolina University and ANSYS CFD consultant in NASA, USA, for his suggestions and support to access to the classified NASA literatures and ANSYS tutorials.

I express my sincere gratitude to prof. (**Dr. Nick Syred**), Cardiff school of Engineering, Wales, UK for his assistance and suggestions to complete my study.

My special thanks go to (**Dr. Mohammed Hamza, Dr. Khalid Abed Al-Hussien, Mr Ahmed Ali and Mr. Kanaan Mohammad**), college of engineering, Qadisiyah university and to Asst. prof. (**Dr. Rafid M. Hanoon**), college of Engineering, university of Thi-Qar. For their support and help.

Great thanks to (**Asst. Prof. Dr.Waheed Shati**, **Dr. Laith Jaafar and Dr. Nabeeh Natiq**), mechanical engineering department, university of Technology, for their support and help.

In addition, my special thanks go to the administration, member of laboratories and all the stuff members of Mechanical engineering department, university of Technology.

My special thanks to all my friends for their support and encouragement.

My great thanks and greetings to my dear parents for the continuous support, patience and pray for me to complete my study.

Special acknowledgement to my darling wife for the support & patience to complete my postgraduate study also thanks to my sons (**Ali and Jaafar**).

Hayder Mohammed Abbas

23/10/2013

Supervisors Certification

We certify that the preparation of this thesis entitled ***"A CFD Simulation of Some Iraqi Liquid and Gaseous Fuels Combustion",*** was prepared by ***"Hayder Mohammed Abbas"*** under our supervision in the Mechanical Engineering Department of the University of Technology in a partial fulfillment of the requirements for the degree of Master of Science in Mechanical Engineering.

Signature:
Name:***Dr. Kutaiba J. Mahdi***
Title: Asst. Prof.
Date: / / 201

Signature:
Name: ***Dr. Adel M. Saleh***
Title: Asst. Prof.
Date: / / 201

Linguistic Certification

I certify that this thesis entitled, **"*A CFD Simulation of Some Iraqi Liquid and Gaseous Fuels Combustion*",** was prepared by "***Hayder Mohammed Abbas***" under my linguistic supervision. Its language was amended to meet the English style.

Name: ***Dr. Arkan Kh. Hussain Al-Taie***

Title: Professor

Date: / / 201

Examination Committee Certification

We, the examining committee, certify that we have read this thesis entitled "***A CFD Simulation of Some Iraqi Liquid and Gaseous Fuels Combustion***" and we have examined the student "***Hayder Mohammed Abbas***" in its contents and in what is related to it, and in our opinion, it meets the standard of thesis for the degree of Master of science in Mechanical Engineering.

Signature:
Asst. Prof. Dr. Kutaiba J. Al-Khishali
Supervisor
Date: / / 2014

Signature:
Asst. Prof. Dr. Adel M. Saleh
Supervisor
Date: / / 2014

Signature:
Asst. Prof. Dr. Sabah J. Hachey
Member
Date: / / 2014

Signature:
Dr. Laith J. Habeeb
Member
Date: / / 2014

Signature:
Asst. Prof. Dr. Abed Alkadhim M. Hassan
Chairman
Date: / / 2014

Approved by Mechanical Engineering Department:

Signature:
Prof. Dr. Jaafar M. Hassan
Dean of Mechanical Engineering Department
Date: / / 2014

Abstract

This thesis describes a study of a 3-D CFD simulation for some Iraqi liquid and gaseous fuels combustion, with some experimental work on the Iraqi Diesel fuel.

This study include the effect of increasing (C/H) ratio in fuels lead to an increase in the overall temperature range of fuels except for the Iraqi Diesel. This may be because of sulfur presence that absorb amount of the heat that generated by combustion process, and showed an increase in the unburned fuels percentage in the exhaust.

The CFD simulation of Iraqi fuels combustion in a boiler are studied using finite volume method with liquid fuels and gaseous fuel. Non-premixed combustion model and probability density function (PDF table) were used to analyze the processes for the liquid fuels (Iraqi Diesel and Light Diesel) and Iraqi LPG. Species transport model was applied for prediction of pure Methane and air mixture combustion.

The Iraqi Diesel and Iraqi LPG fuels with all their properties were added to the FLUENT database while Light Diesel and Methane fuels already found in the FLUENT database .The turbulent kinetic energy (k) with dissipation rate (ε) model are used to solve this turbulent flow process. Then, continuity, momentum and energy equations are numerically analyzed by using the finite volume method (control volume) by FLUENT program.

Initially, applying the discrete phase model, liquid fuels combustion (Iraqi Diesel and Light Diesel) were for the first time solved until the solutions converged. The Methane is solved using species transport model until the solution is converged. In all cases, reasonable results for the different variables like temperature distribution, velocity… etc. were obtained.

The boiler exhaust gas temperature for Iraqi Diesel measured experimentally was 930 K; while for Light Diesel experimentally obtained by

the boiler manufacturer was 948 K. Solving the model using FLUENT program it was found that the exhaust temperatures for Iraqi Diesel was 930.7 K and for Light Diesel was 948.459 K. For Methane combustion, the exhaust gas temperature was 564K experimentally obtained by the boiler manufacturer and computed using FLUENT program to be 564.5 K. All the measured and calculated results were in an excellent agreement.

The results of this study are presented on graphs with suitable discussions of parameters such as temperature, velocity, pressure, and turbulence kinetic energy, to compare among the combustion conditions of the Iraqi Diesel, Light Diesel, Methane and Iraqi LPG.

The maximum flue gases velocity inside the boiler was (34.2, 49.9, 106.39 and 66.63 m/s) for Iraqi Diesel, Light Diesel, Methane and Iraqi LPG respectively. They were all close to the burner.

In addition, this study offers a suitable suggested design for the burner working on Iraqi LPG or any other gaseous fuel to operate the boiler with the same efficiency obtained by Iraqi Diesel fuel.

Comparison between present work and the available literature works was done and showed an excellent agreement.

CONTENTS

Nomenclature

Symbol	Definition	SI Units
A	Area	m^2
A_p	Area of the inside faces of furnace	m^2
C_P	Specific heat at constant pressure	kJ/kg.K
d	Diameter	m
k	Kinetic energy	m^2/s^2
m	Mass	kg
m_a	Mass flow rate of the air	kg/s
M	Molecular weight	kg/kmol
$M_{w,i}$	Molecular weight of species i	kg/kmol
P	The local absolute pressure	Pa
q	Heat flux	W/m^2
R, Z	Radial and axial directions	-
R_{ed}	Reynolds number based on the particle diameter and the relative velocity	Dimensionless
T	Temperature	K
u_{avg}	Average velocity	m/s
u'	Fluctuation velocity at axial direction	m/s

Greek Letters

Symbol	Definition	SI units
ρ	Density	kg/m^3
μ	Dynamic viscosity	$N.s/m^2$
ε_E	Emissivity≈ 0.8	Constant
λ	Thermal conductivity	W/m. K
$\sigma_{T,t}$	Turbulent Prandtl number	Dimensionless
σ	Stefan – Boltzman constant=5.67×10^{-8}	$W/m^2.K^4$
σ_s	Scattering coefficient	m^{-1}
θ	Tangential direction	-
ϕ	Thermal property (U, V, W, T, k, ε)	-

Subscripts

Symbol	Definitions
C.V.	Calorific value
eff	Effective
ε,t	The dissipation rate of the turbulent kinetic energy
d_h	Hydraulic (diameter)
k,t	The turbulent kinetic energy
O	Oxide of combustion
t	Turbulent
w	Wall

Abbreviations

Symbol	Definition
CFD	Computational Fluid Dynamics
C/H	Carbon to Hydrogen ratio
CME B100	Canola Methyl Ester (Biodiesel fuel)
2-D	Two dimensions
3-D	Three dimensions
FVM	Finite Volume Method
LES	Large eddy simulation
LPG	Liquefied Petroleum Gas
NO	Nitrogen oxide
PIV	Particle image velocimetry
PLIF	Planar laser induced fluorescence
PVC	Processing vortex core
RNG	Renormalization group model
TVC	Trapped vortex combustor
UHC	Unburned Hydrocarbon
WSGGM	Weighted sum of gray gases Model
Φ	Equivalent ratio

Figures

Tables

CHAPTER ONE

INTRODUCTION

CHAPTER ONE
INTRODUCTION

1-1 General:

The control of green-house gas emissions has begun to add to the numerous constraints that combustion systems manufacturers have to satisfy. The reduction of fuel consumption becomes a primary requirement as well as meeting current and future emission legislations. Naturally, talking about reduction of fuel consumption means to keep unvaried, sometimes improved, the performance level of current combustion system production. Dealing with system topics exclusively, improving fuel economy to reduce CO emissions means improving the system thermal efficiency. This target can be met following different routes, each of them could be an effective way with different cost-to-benefit ratios. Often, it could be observed, it is helpful to adopt numerous solutions contemporaneously. Examples are fast combustion, lean burn, and gasoline direct injection and so long may be reminded.

Combustion has been the foundation of worldwide industrial development for the past 200 years. Industry relies heavily on the combustion process. Depending on many factors, certain types of fuels may be preferred for certain geographic locations due to cost and availability considerations. Gaseous fuels, particularly natural gas, are commonly used in most industrial heating applications in the United States. In Europe, natural gas is also commonly used along with light fuel oil. In Asia, South America, and Middle East and in Iraq, heavy fuel oils are generally preferred although the use of gaseous fuels is on the rise. The importance of the study of the Iraqi's fuels combustion arise not only from the point of view of the devices that used them to produce energy, but it is also important to the Iraqi economy and environmental concerns.

The fuel choice has an important influence on the heat transfer from a flame. In general, solid fuels (e.g., coal) and liquid fuels (e.g., oil) produce very luminous flames that contain soot particles that radiate the heat load like blackbodies. Gaseous fuels such as natural gas often produce nonluminous flames because they burn so cleanly and completely without producing soot particles.

The type of fuel also has a large impact on pollutant emissions. For example, gaseous fuels generally contain little or no sulfur so SOx emissions are usually small. However, heavy oils often contain significant quantities of sulfur and therefore SO_x and other emissions like CO, UHC and soot are of concern and need to be controlled.

In some cases, the burner may have more than one type of fuel. Dual-fuel burners are typically designed to operate on either gaseous or liquid fuels. These burners are used where the customer may need to switch between a gaseous fuel (e.g., natural gas) and a liquid fuel (e.g., oil), usually for economic reasons. Many practical, important devices, ranging from home oil heaters to chemical rocket motors, involve the burning of liquid particles in a gas.

Spray combustion is a complicated subject because it involves many different processes. A typical sequence of events would be the injection and atomization of liquid fuel, mixing of droplets with oxidizing gas, heat transfer to droplets producing evaporation of liquid. Mixing of fuel vapor with gas possibly followed by gas-phase ignition processes and certainly by either non-premixed or premixed gas-phase combustion-all accompanied by various additional aspects of finite-rate chemistry, such as fuel pyrolysis, production of oxides of nitrogen, and extinction phenomena.

Boilers (which mainly deals with spray combustion) were used extensively in manufacturing, processing, mining and refining industries to provide steam or hot water. The developments of flames for furnaces and

combustors for industrial applications is still very much of an art in which the practical experience of the designer is paramount. This is because of the complex physico-chemical processes involved in flames with defined detailed analytical description [1].

There are two types of boiler ,fire tube boiler by which the fire passes through the tubes and water tube boiler by which the fire surrounding the tubes that contain the water. The size of any boiler depend on the designer view, demand of power, fuel type and burner design. The number of burners may reach 50 depending on the particular design and operational requirements [2]. In this study, the boiler is small, and is a fire tube type with one burner.

A situation may arise in which a considerable amount of unburned fuel is being picked up by the gas and carried out of the boiler; this is known in the industry as carryover. As a result, unburned fuel may be blown out of the boiler, causing efficiency to decrease and emissions problems. Emissions could be caused by unburned hydrocarbon (UHC) and non-uniform heating induced by cold and hot spots, which produce CO and NOx respectively.

In addition, a situation may arise where the superheater tubes break due to excessive heating, which may lead to boiler shutdown and thus increase the expenses incurred. Super-heated steam that has been heated above the temperature corresponding to its pressure contains more energy than does saturated steam at the same pressure and the heat added provides more energy for the turbine for conversion to electric power. Overheating of the super-heater tubes is prevented by using the appropriate materials and designing the unit to accommodate the heat transfer required for a given steam velocity around the super-heater tubes, based on the desired exit temperature. In real applications, however, the operation of the superheater for producing high-pressure, high-temperature steam may result in problems frequently caused by ruptured superheater tubes. The damage or rupture of the superheater tubes may be caused by many possible reasons including, galvanic corrosion, thermal

contraction and expansion, composition of the combustion gases. Accumulations of soot inside the pipes, accumulation of slag inside the pipe or high temperature distribution above material yield temperature and high thermal stress. The damage caused by high temperature can be minimized by providing uniform combustion and temperature distribution and keep fouling resistance low. Installation of soot-blowers remove accumulated soot and other particulates, and optimize the combustion conditions.

Herein, the interest is to study the combustion and aerodynamic of the fuel flow and air incoming into the furnace by burner with axial flow. Also, the effect of the temperature distribution in this furnace and the other properties of gas products in the axial, radial, and tangential directions, for two types of fuel, liquid {Iraqi Diesel ($C_{7.2083}H_{11.199}S_{0.072}$) and Light Diesel ($C_{10}H_{20}$)} and gaseous fuels {Methane (CH_4) and Iraqi LPG ($C_{3.437}H_{8.874}$)} will be studied and this will help industry to improve boiler's efficiency, reduce emissions, avoid rupture of superheater tubes, and understand the thermal flow transport in the boiler.

This study employs the Computational Fluid Dynamics (CFD) scheme by using the ANSYS FLUENT package programs. CFD simulations could provide a clear picture of what is happening at any point within the boiler, making it easy in most cases to identify the problem and develop a solution. A CFD analysis provides fluid velocity, pressure, and temperature values throughout the solution domain for problems with complex geometries and boundary conditions. During the analysis, the geometry of the system or boundary conditions such as inlet velocity and flow rate can be easily changed to view their effects on thermal-flow patterns or species concentration distributions. CFD can also provide detailed parametric studies that can significantly reduce the amount of experimentation necessary to identify problems and to optimize the operating conditions. This will provide better understanding to furnace performance reaching higher efficiencies.

Some of variables such as the temperatures of the boilers walls, exhaust gases and species concentration at outlet are measured experimentally. In addition, the mean velocity of fuel and air are estimated from the mass flow rates that measured experimentally.

1-2 Boiler's principle of work

The type of boiler is a fire tube boiler. The burner inject the air and fuel inside the combustion chamber as the combustion type in the boiler is a non-premixed combustion. The flue gases resulted from the combustion hit the closed end of combustion chamber and are reflected back to the burner side to be collected in a front plenum and then enter the tubes loosing heat to the water that surround them. Then the flue gases are collected again in the rear plenum to exit finally through the chimney to atmosphere, as shown in figure (1-1)

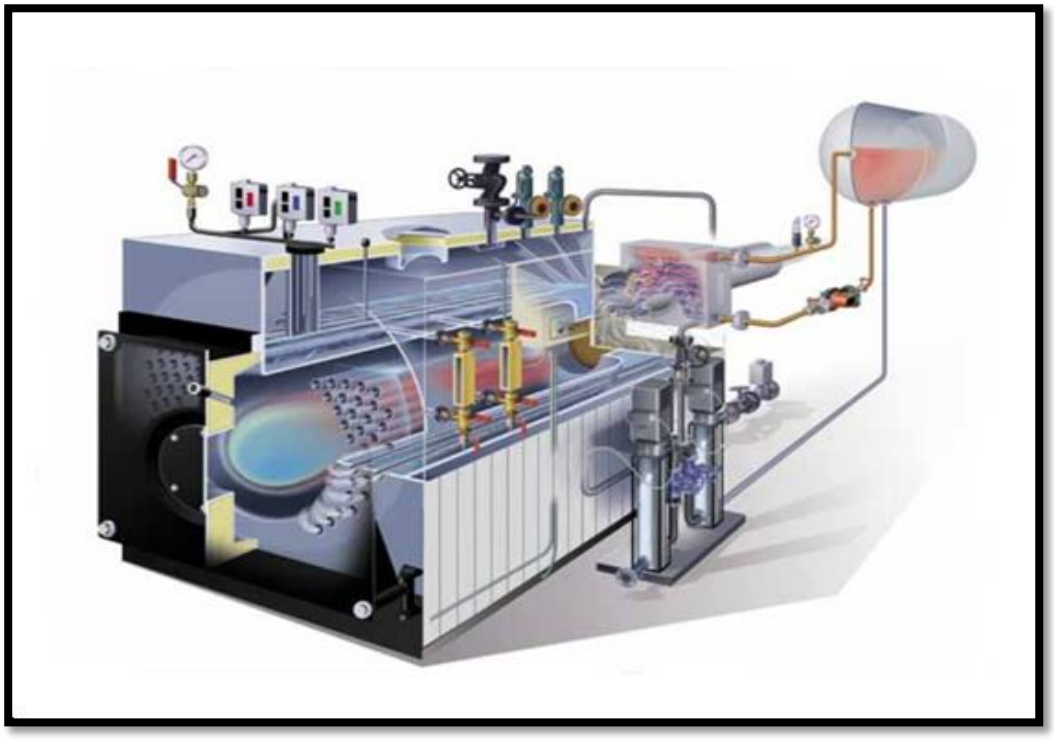

Figure (1-1) The ICI Caldaie boiler.

1-3 Fuel Spray Characteristics:

To burn effectively, a liquid fuel has to be atomized into a fine droplet spray, with droplets appropriately distributed within the combustion chamber. In order

to understand the importance of the problem it is enough to realize that a droplet with a diameter of 1μm contains about 10 billion molecules of fuel, each of which must be combined with several molecules of oxygen [3].

The atomization of a liquid can be accomplished by means of special devices called sprayers, sprinklers, atomizers, injectors…etc., depending on application. According to the kind of energy used for atomization, a few basic types of atomizers can be distinguished: jet atomizers (using the kinetic energy of the liquid jet), swirl atomizers (exploiting the centrifugal forces generated in the fluid by rapid rotation) and blast atomizers (in which the driving energy is that of compressed vapors and gases) [4].

The wide diversity of methods and conditions of atomization and multiplicity of the physical phenomena which accompany the process of droplet formation make it impossible to give any general expressions for droplet size in sprays. The basic mechanism of atomization is essentially the same in all devices. The process involves the formation of small diameter liquid threads, which (due to surface tension) are unstable and break into rows of droplets [3].

Gaseous fuels are usually characterized by clean combustion, with low rates of soot and nitric oxides. The main problem is that of achieving the optimal level of mixing in the combustion zone. A mixing rate that is too high produces narrow stability limits, but a mixing rate that is too low may make the system prone to combustion-induced pressure oscillations. Many different methods have been used to inject gas into conventional combustion chambers, including plain orifices, slots, swirlers, and venture nozzles [5].

1-4 Furnace Flames Technology:

The significant characteristics of turbulent diffusion flames (e.g. length, angle of spread, stability, and radiation from flame) used in furnaces depend largely upon the way in which fuel, air, hot and chemically active combustion

products are mixed. This is because most of the chemical reactions in flames are very fast at elevated temperatures so that the time taken to complete the reaction after the reactants mixed on a molecular scale is negligible. Hence, the overall rate of progress of combustion can be determined by the rate of mixing, with good approximation. The methods of calculating the progress of mixing in flames from design input parameters (burner geometry, momentum flux at source, preheats temperatures, etc.) can be discussed in three broad categories [6]:

I- Predictions based on the laws of turbulent jets, which include mathematical and physical modeling.

II- The use of simplified statistical models of flow in furnaces such as combinations of well stirred and plug flow sections to describe the mixing pattern in combustors, including physical modeling for determining residence time distributions.

III- The solution of the relevant set of partial differential equations of conservation of momentum, mass and energy for turbulent flow.

1-5 Turbulent Models

All flows encountered in engineering practice, both simple ones such as two dimensional jets, wakes, pipe flows and flat plate boundary layers and more complicated three-dimensional ones, become unstable above a certain Reynolds number. Many flows of engineering significance are turbulent so the turbulent flow regime is not just of theoretical interest [7].

Before many decades, direct numerical simulation of turbulent flows at small to moderate Reynolds numbers has been a valuable asset in understanding turbulence phenomena. In such simulations, the motion of eddies ranging in size from the physical system down to the Kolmogorov dissipation length scale are explicitly accounted for [8].

For most engineering purposes, it is unnecessary to resolve the details of the turbulent fluctuations. Only the effects of turbulence on the mean flow are usually sought. For turbulence model to be useful, a general-purpose CFD code must have applicability, be accurate, simple and economical to run. The most common turbulence models are classified as:

(1) Classical models which are based on (time-averaged) Reynolds equations such as:

i- Zero equation model – mixing length model.

ii- Two-equation model – k-ε model.

In two dimensional thin shear layers, the changes in the flow direction are always so slow that the turbulence can adjust itself to local conditions. If the convection and diffusion of turbulence properties is neglected it is possible to express the influence of turbulence on the mean flow in terms of the mixing length. If convection and diffusion are not negligible, a compact algebraic prescription for the mixing length is no longer feasible. The mixing length model lacks this kind of generality. The way forward is to consider statements regarding the dynamics of turbulence. The k-ε model focuses on the mechanisms that affect the turbulent kinetic energy.

There are some advantages of this method:

- Suitable turbulence model for which only initial and/or boundary conditions need to be supplied.
- Excellent performance for many industrially relevant flows.
- Well established, the most widely validated turbulence model [9].

iii- Reynolds stress equation model.

iv- Algebraic stress model.

The classical models use the Reynolds equations and form the basis of turbulence calculations in currently available commercial CFD codes [10].

(2) Large eddy simulations which are turbulence models where the time dependent flow equations are solved for the mean flow and the largest eddies and where the effects of the smaller eddies are modeled. It was argued earlier that the largest eddies interact strongly with the mean flow and contain most of the energy so this approach results in a good model of the main effects of turbulence.

1-6 Thesis Outline :-

This work prescribes the case study of CFD simulation in a boiler in six chapters, starting with the introduction in chapter one to be the scope in general.

The second chapter has the topic of literature survey which is related with many papers and researches accomplished in the thesis field.

The third chapter presents the experimental work of the case study of ICI Caldaie boiler and burner.

Chapter four contain the numerical analysis of all equations and computer programming.

Chapter five illustrates the results of this work compared with literature similar works .The graphs and pictures of these results with discussion and analysis of the predicted values of solving liquid fuels (Iraqi Diesel and Light Diesel) and gaseous fuels (Methane and Iraqi LPG) are presented.

The conclusions of this work with recommendations for further future studies are written in chapter six.

CHAPTER TWO

LITERATURE SURVEY

CHAPTER TWO
LITERATURE SURVEY

2-1 Introduction:

The experiments, applications and developments for many computational, multidimensional, comprehensive combustion studies using different types of fuels are demonstrated in this chapter. Furthermore, many models of combustion in furnaces will be also demonstrated that use the modern computer program analysis. The available computational fluid dynamics (CFD) simulations are used for designing analyzing and optimizing the performance of fossil-fuel combustion and conversion systems.

In this literature, the author took into account to obtain an accurate representation of the flow field in boilers and furnaces since the problems include high numerical resolution, especially at the burner. There were some differences among these results according to the method used, geometry and computer time to convergence.

2-2 Experimental Studies

Najim (1979) [11] measured three components of velocity in an experiment on a cyclone combustor using laser Doppler anemometry and the kinetic energy of turbulence in isothermal and combustion conditions. He concluded that the turbulence levels of the axial components were very high particularly in the annular recirculation zone and the tangential velocity fluctuations were low.

Arscott *et.al.* (1980) [12] investigated the distribution of air and fuel in an oil fired boiler of 500 MW which had 32 burners on the front wall. They explained that the following factors affect the distribution of air:

1- Variations in burner loss coefficients, a proportion of the pressure drop across a burner caused by flow detachments at the air door, swirl vanes and flow splitters.

2- Variations in burner size.

3- Cross-flow in the wind box. Model measurements indicated that the variations in flow were of the order of ±3% for the particular symmetrically-fed wind box.

4- Wind box air temperature. This is the effect of temperature difference between top and bottom burners from 280 ºC to 239ºC caused a 4% variation in air flow.

5- Buoyancy forces. The density variation of the furnace gas and wind box air causes the lower burners to pass more air than the upper ones.

Then, they deduced that there was an overall standard deviation of 3.7%, which is probably quite small in comparison with the majority of boilers, but a bias between the two sides of the boiler of 3.5%.

Sislian *et.al.* (1988) [13] measured experimentally the mean velocity components, turbulent intensities, velocity probability density functions, power spectra and autocorrelation functions of axial velocity fluctuation. Spatial turbulence macroscale which were reported in a turbulent round jet flow issuing vertically into stagnant air in non-combusting and combusting situations. The density of fuel (a mixture of methane and argon) was chosen to be equal to the cold flow gas density (a mixture of air and helium) in order to minimize cold fuel/ cold gas mixture density difference effects on measured turbulence properties. A one dimensional laser Doppler velocimetery was used to obtain the measurements, and the temperature was measured by thermocouples. They concluded that turbulence in the jet diffusion flame was appreciably more anisotropic than in the corresponding cold jet in all regions of the flow. The combustion process had been found to have a marked influence

on the turbulence macroscale which was significantly smaller than in the cold jet flow in the upstream region and increased appreciably at downstream distances.

Holmborn (2003) [14] developed a lean premix prevaporised (LPP) burner for the use in Alstom Power Sweden `s industrial gas turbines. He used numerical simulation for the flow field. The proposal and the restrictions were to increase the flame stability over the operating range for both liquid and gaseous fuel operation by development of the fuel injectors. This geometry changed the internal aerodynamics of the burner and suppressed the pressure oscillations over the load range to decrease the lean blow off limit (LBO) by a factor 1.5 for the gaseous fuel operation. The risk of droplets impacting on the swirl generator vanes and burner wall was reduced. The liquid fuel operation with new injection nozzle positioned in the central body has proved to be able to supply a stable main frame operation from a normalized flame temperature 30% below the design flame temperature. This development is shown in figure (2-1):

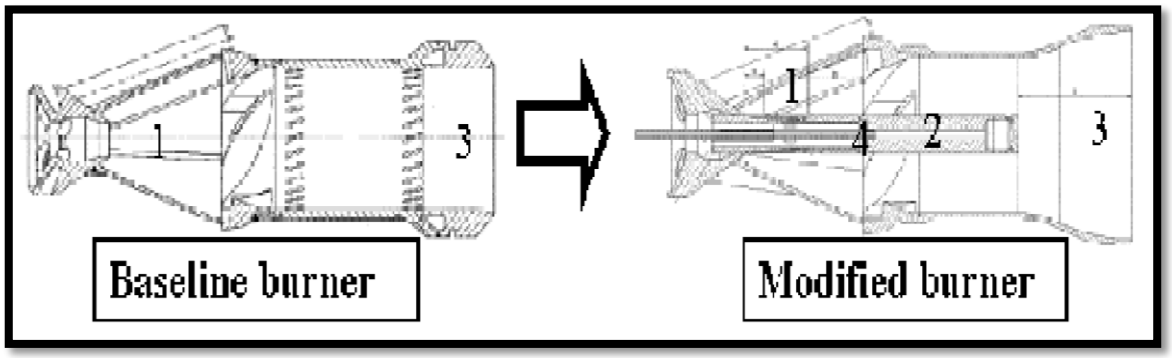

Figure (2-1) Modifications introduced to baseline burner [14].

Where 1: central body, 2: centerline of the burner, 3: concave diffuser section, 4: airblast-prefilmer injector

Bruno and Losurdo (2007) [15] presented the trapped vortex combustor (TVC) challenge to provide a new class of combustors performing at a high combustion efficiency and low emission indices with multi fuel capability (gas and liquid) and low pressure drop. This strategy was based on

mixing hot combustion products and reactants at a high rate. Turbulence occurring in a TVC combustion chamber was trapped within a cavity where reactants were injected and efficiently mixed. Since part of the combustion occurs within the recirculation zone, a typically flameless regime could be achieved, as shown in figure (2-2):

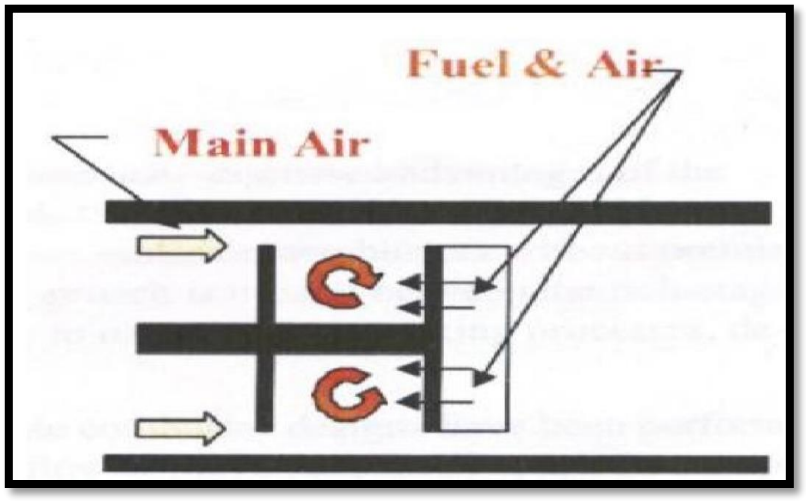

Figure (2-2) Sketch of TVC strategy [15]

Love *et.al.* (2009) [16] developed an experimental method for the rapid characterization of combustion properties, such as pollutant emission indices and flame radiation that requires only small amounts of a liquid fuel. The burner conditions were selected to make flame properties sensitive primarily to fuel chemistry. The technique was validated through a comparison of measured radiative heat release fraction and pollutant NO and CO emission indices available in literature. They concluded that all petroleum-derived fuels showed a higher radiative heat fraction than CME B100 and methanol. The CME biodiesel flames also had lower emission index of CO and higher emission index of NO compared with those of the petroleum-derived Diesel flame. The present technique can serve as a valuable tool for fuel researchers and developers to obtain quick feedback on the combustion properties of the new fuels.

2-3 The Computer Simulation on Combustion

Gruenberger (2000) [17] presented a study of incomplete combustion and thermal decomposition of natural gas using experimental and numerical studies. He found that the natural gas combustion processes produce solid carbon emissions like any other hydrocarbon fuel. And concluded (based purely on environmental aspects and considered the primary aim of reducing carbon emissions by the observed process) that the application of harnessing waste gas by producing carbon black envisaged had to be considered as not viable. If a minimum rate of carbon recovery as initially set at about 25% is not attained, then on this basis alone the process has to be considered as environmentally infeasible.

Azazi (2001) [18] presented a study to Al- Hartha power plant furnace in Iraq. This furnace has square shape (8×8×8) m, pressurized and tangential corner firing. He used a (2-D) aerodynamics and thermal aspects by using FORTRAN computer program. He concluded that the predicted pressure inside the fire-ball and in the furnace is with agreement with the design value. The furnace losses were 14.5% to get 1500 ºC inside temperature and the tangential velocity played a great role for keeping the stability of the fire ball.

Alhabbubi (2002) [19] presented a prediction of temperature distribution and heat flux along the walls of Al-Mussaib thermal power plant furnace in Iraq by using Zonal method to analyze the radiative heat transfer and the weighted sum of gray gas to determine the nongray characteristics of the confined gas mixture. He used quick BASIC software program to get the results concluding good agreement with practical results. Then, he showed that the temperature range is from 1450K to 2100 K.

Baranski (2002) [20] simulated a numerical modelling with real combustion processes for advanced industrial utility boiler by using pulverized fuel. The output thermal power of the boiler was 125 MW, which was analyzed by CFD (FLUENT) code for all flow, mixing patterns, temperature field and

species concentration. He noticed that additional air and fuel give better mixing process with uniform temperature field. The maximum difference of temperature between the measured and predicted was about 100K.

Raja Saripalli (2005) [21] made a study of combustion and flue gases in a 3-D water tube boiler working on pure methane and air. The simulations are conducted using the commercial CFD package FLUENT. The 3-D Navier-Stokes equations and five species transport equations are solved with the eddy-breakup combustion model. The simulations are conducted in three stages. In the first stage, the entire boiler is simulated without considering the steam tubes. In the second stage, a complete intensive calculation is conducted to compute the flow and heat transfer across about 496 tubes. In the third stage, the results of the saturator / superheater sections are used to calculate the thermal flow in the chimney. He found that the results provided insight into the detailed thermal-flow and combustion in the boiler and showed possible reasons for superheater tube rupture. He found that the exhaust gas temperature is consistent with the actual results from the infrared thermograph inspection so that the overall simulation was successful and provides comprehensive information of combustion and thermal flow in the studied boiler. Several ideas were formed from this study to improve boiler efficiency and minimize the thermal stress problem imposed on the super-heater tubes.

Syred (2006) [22] presented a study of occurrence of the processing vortex core (PVC) and other instabilities. Which occur in, swirl combustion systems whilst identifying mechanisms that allow coupling between the acoustics, combustion and swirling flow dynamics to occur, as shown in figure (2-3). He concluded the following:

1- Under combustion conditions, the PVC occurrence and amplitude are strong functions of mode of fuel entry, equivalence ratio and level of confinement.

2- Premixed or partially premixed combustion could produce large PVC.

3- Swirling flame was unstable and close to the burner exit.

4- Jet precession was associated with spatial shapes of nozzles.

5- Two gas turbine combustor units firing into chambers, strong PVC are developed under isothermal conditions. It is suppressed with premixing in the equivalence ratio range 0.5 – 0.75. He showed the formation of strong helical coherent structures for equivalence ratios greater than 0.75.

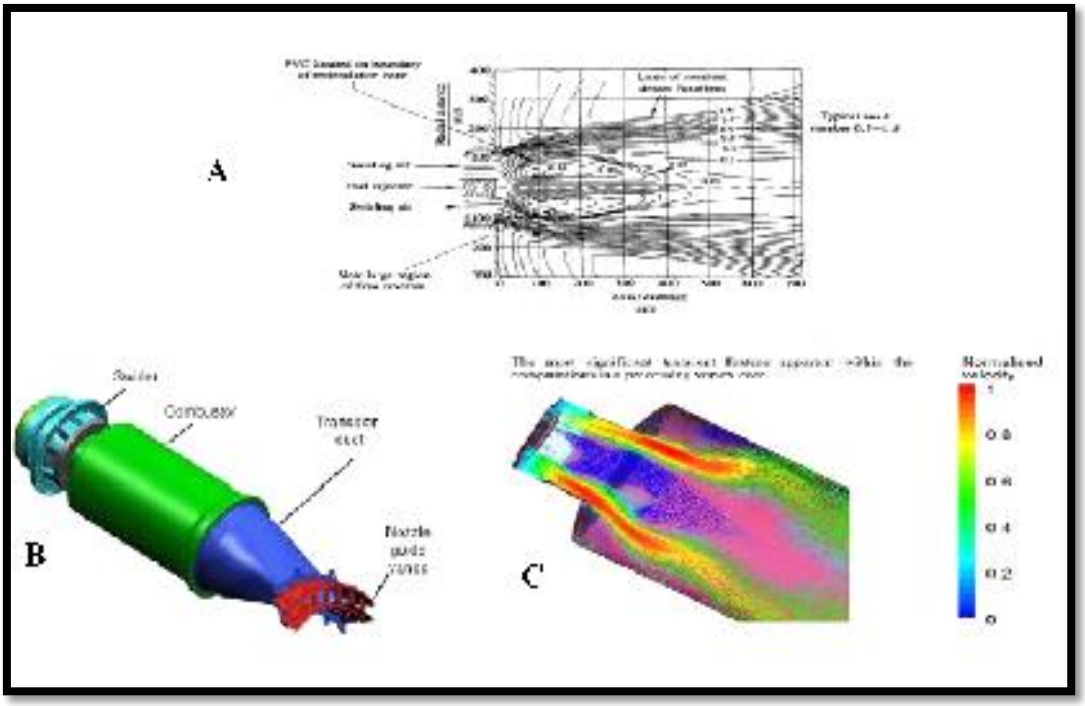

Figure (2-3) A-recirculation zone, B-computational domain geometry, C-CFD velocity vectors. [22]

Soroka (2007) [23] focused on the results achieved through the addition of previously unaccounted for processes to existing calculation procedures relevant to combustion units as a whole and low – emission boiler furnaces in particular. It is concerned with the processes accompanying the use of NOx reduction facilities.

Numerical simulations have been performed with respect to the chemical reactions of natural gas and/or methane – air mixtures and the recirculation of flue gases (combustion products). He concluded that measurements were taken to reduce NOx emissions. Soot formation is due to the fact that he involve the conversion of natural gas with steam, carbon dioxide

or a combination of the two. The dependence of the thermodynamic equilibrium soot concentration on both the controlling temperature and concentration process conditions have been determined based on the results of numerical simulations as shown in figure (2-4).

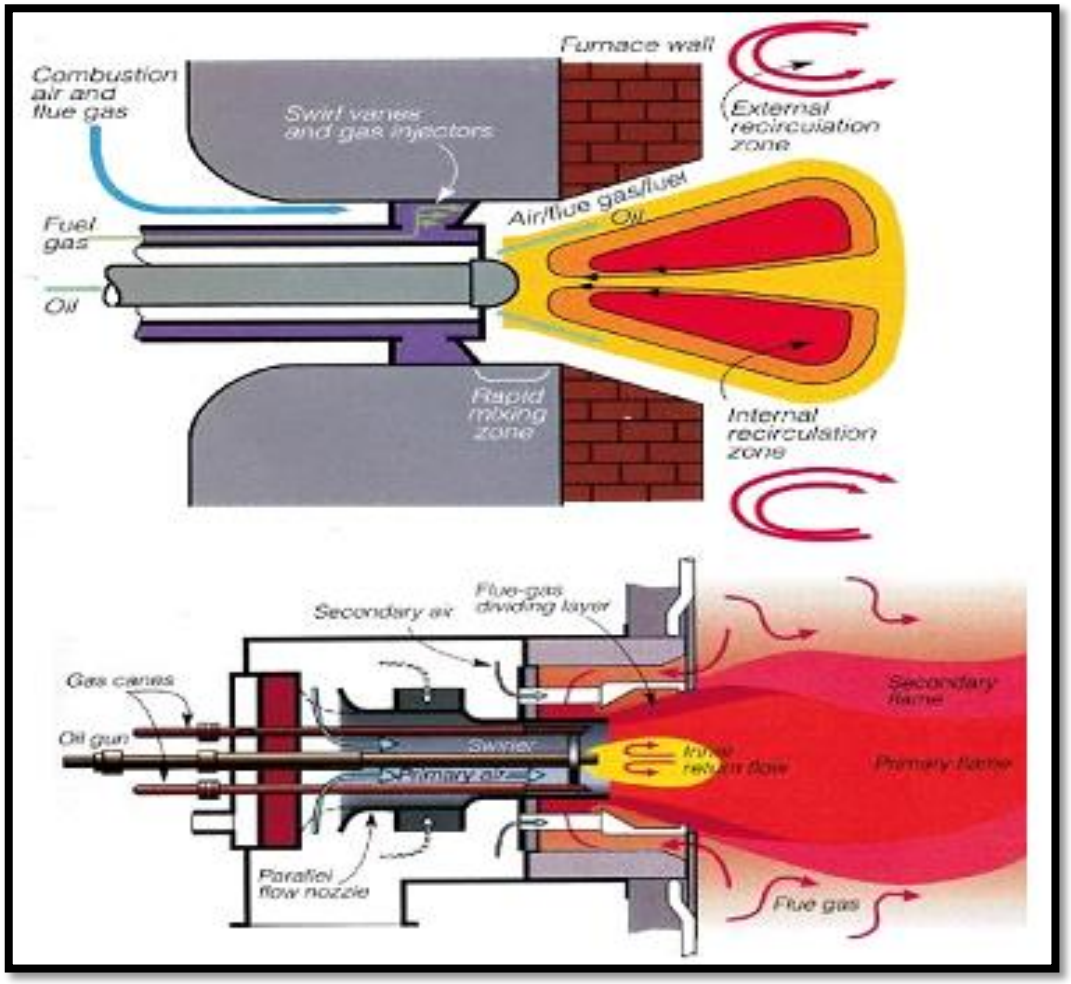

Figure (2-4) Combustion at burner outlet [23]

He found that the specifics of soot formation are determined by two basic schemes of gaseous hydrocarbons combustion, full preliminary mixing of the initial components (combustible + oxidant) or if no preliminary premixing occurs, simultaneous mixing and burning (diffusion combustion). So, he demonstrated by means of calculations of thermodynamical equilibrium within corresponding systems that the recirculation of the combustion products with the initial reactants (fuel) induced the endothermic reactions of carbon dioxide, water vapor and mixing conversion, which accompany soot formation.

Agranat *et.al.* (2007) [24] tested and developed advanced computational fluid dynamics CFD model of gas release and dispersion (GRAD) by modelling of various industrial real – life indoor and outdoor flammable gas (hydrogen, methane, etc.) release scenarios with complex geometries. This software (PHOENICS) was used for the options:

Dynamic boundary conditions, describing the transient gas release from a pressurized vessel, the calibrated outlet boundary conditions, the advanced turbulence models, the real gas law properties applied at high pressure releases, and the special output features. All these are for 3-D predictions of transient distribution of flammable gas concentrations.

Snegirev and Isaev (2007) [25] studied actual large-scale fire of combustibles in open storage where the fire growth and flame dynamics were greatly affected by the cross wind. They developed a model of computer code for studying buoyant turbulent diffusion flames and radiative heat flux, using large eddy simulation (LES) technique, probability density function, Monte Carlo for radiation adopting either the weighted sum of Gray gases (WSGG) approach or the Gray media assumption. All these were compared with experimental data.

Sigal and Dolinsky (2007) [26] presented the double role of moisture in the hydrocarbon fuel oxidizing process in Ukraine which affected the working efficiency of the boilers. They showed that:

1- The energy necessary for the evaporation of 1 kg of moisture is nearly 6000 kJ/kg. The energy of water molecule dissociation (depending on how dissociation occurs) is 114 – 122 kcal/gram. Molecule, approximately 5500 kJ/kg. In general, the energy consumed by evaporation and dissociation is nearly 25000 kJ/kg.

2- For natural gas under adiabatic conditions, the dissociation of 1.3 kg of moisture consumes over 33500 kJ/m^3. In practical conditions, it is much more difficult to estimate the energy that may be consumed by dissociation.

However, by various estimations. It forms 10-20% of the amount consumed under adiabatic conditions, i.e. 3-5 MJ/m^3 of dry gas will be enough for water dissociation. The estimation of moisture content of the primary reactants with 280 g/m^3 natural gas, 20 g/m^3 moisture content of air and α=1.3 (excess moisture content factor). The optimal moisture content in the air used for combustion has a value between 13-15 g/m^3 of dry air. The moisture must be controlled by suitable air heaters.

Sobolev *et.al.* (2008) [27] Presented numerical calculation results of Methane turbulent diffusion jet flames of rectilinear burner in the furnace of high capacity boiler by using CFD ANSYS CFX10.0 program. They used standard furnace with a height of 30m, burner diameter of 0.9 m, furnace wall temperature of 410 ºC, air inlet temperature of 297 ºC, and fuel temperature of 7 ºC. They demonstrated the influence of the swirling effect of the central jet flow of the oxidizer to the flame structure and the calculation results of NOx production. They found that the average concentration of NOx is 0.1-0.2 g/m^3. This modeling data agreed well with real measurements (0.14-0.22 g/m^3). Calculated amount of NOx production is in the range of 2.6-3g NOx/1 kg CH_4, which agreed well with literature data [28].

Anand and Jenny (2009) [29] developed a study of a unified PDF modeling framework and a new hybrid solution algorithm to simulate turbulent evaporating sprays by using Eulerian-Lagrangian-Lagrangian approach. Two-ways coupling between the droplet and gas phases was implemented and an infinite thermal conductivity (ITC) evaporation sub-model was used. Opposed to previous approaches, the decorrelation between droplet and seen gas velocities was formulated based on individual separation and correlation length scales. They concluded that to enhance the computational efficiency, a local particle time-stepping algorithm needs to be implemented and a particle time-averaging technique to be employed to reduce statistical and bias errors. This enabled the use of much fewer computational gas and droplet particles per grid cell in comparison to previous studies. The PDF algorithm was validated with

the experimental data of a turbulent evaporating Iso-propyl alcohol spray. Overall, reasonable agreement could be observed.

Stopper *et.al.* (2009) [30] analyzed lean premixed natural gas/air flames produced by an industrial gas turbine burner by using laser diagnostic methods as shown in figure (2-5). For this purpose, the burner was equipped with an optical combustion chamber and operated with preheated air at various thermal powers, equivalence ratios, and pressures up to 6 bars. For the visualization of the flame emissions, they applied OH_ chemiluminescence's imaging and measured absolute flow velocities using particle image velocimetry (PIV), and the reaction zones as well as regions of burnt gas were characterized by planar laser-induced fluorescence (PLIF) of OH. They divided the mean flow field into different regimes: the inflow, a central and an outer recirculation zone, and the outgoing exhaust flow. Single-shot PIV images demonstrated that the instantaneous flow field was composed of small and medium sized vortices, mainly located along the shear layers. The chemiluminescence images reflected the regions of heat release. From the PLIF images it was seen that the primary reactions were located in the shear layers between the inflow and the recirculation zones and that the appearance of the reaction zones changed with flame parameters.

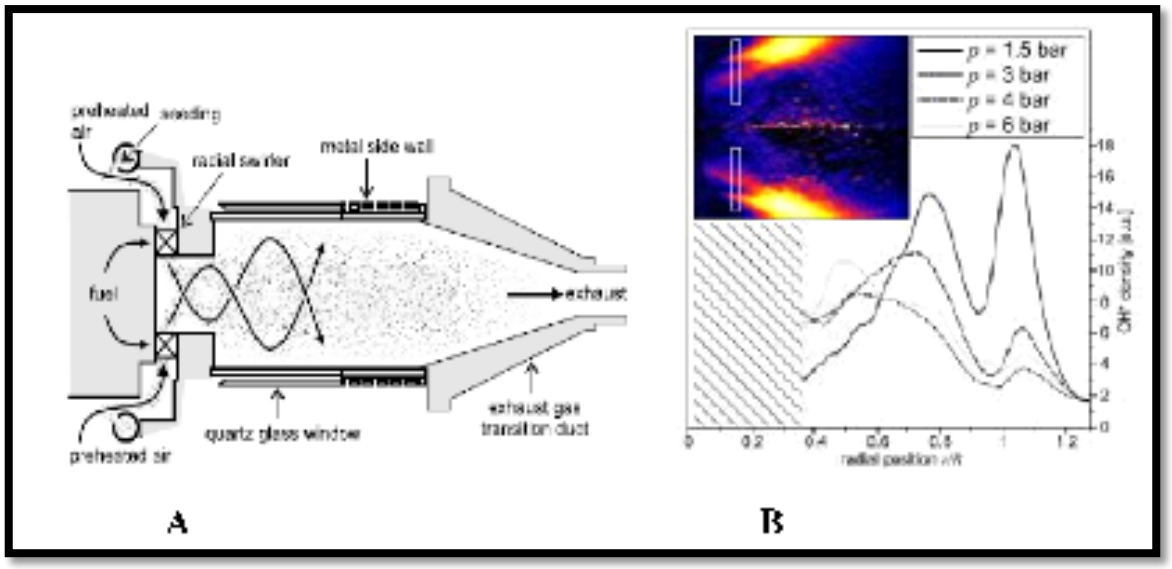

Figure (2-5) A. Combustor diagram, B. The radial OH_ distribution is influenced by the pressure [30]

2-4 Objectives of this Study

The objective of this study is to find the boiler performance using Iraqi liquid fuel (Iraqi diesel) both experimentally and numerically and other fuels (Light Diesel, Methane and Iraqi LPG) numerically to predict the following parameters:

1. Measure the rate of air-fuel consumption and the species concentration at the exhaust experimentally.
2. Applying a CFD simulation of combustion of the Iraqi Diesel by using the CFD commercial package ANSYS FLUENT to predict the temperatures and velocity distribution inside the boiler.
3. Doing a comparison among the combustion of four types of fuel (Iraqi Diesel, Light Diesel, Methane and Iraqi LPG).
4. Compare the obtained numerical and experimental results of this study with the literature results in the same field.
5. Suggest appropriate design of the burner nozzles to operate the boiler on a gaseous fuel like Iraqi LPG.

CHAPTER THREE

Experimental work

CHAPTER THREE
EXPERIMENTAL WORK

3-1 Introduction:

The experimental work in this study is very necessary to obtain the boiler performance, also to measure the actual dimensions of the system (ICI Caldaie sixen boiler) which is helpful in presenting the model of the boiler. Also to measure the rate of air–fuel consumption and measure the temperatures of inlet air, inlet fuel and walls that were used later in the CFD (ANSYS FLUENT) programs as a boundary conditions to obtain the combustion characteristics in it.

The other advantages of the experimental work are to measure the species concentration and exit flue temperature at the exhaust in order to compare it later with the exit flue temperature calculated by the CFD (FLUENT) program to ensure that the simulation is accurate.

3-2 The boiler

The boiler used is a three pass, reverse flame, wet back, horizontal fire tube boiler with flanged head welded as shown in figures (3-1) and (3-2).

The boiler body is suitable for use on liquid fuel and gaseous fuel depending on the type of the burner used [31]. The type of fuel used in this boiler is the Iraqi Diesel fuel ($C_{7.2083}H_{11.199}S_{0.072}$) .The boiler was also equipped with all the necessary accessories for regulating and safety for automatic operation. It is capable of producing high equality saturated steam, owing to its wide evaporation, which avoid water intake even with fast steam demand. It is capable of generating a pressure steam (12- 15 kg_f/cm^2).

The main parts of the boiler are :

1. Burner.
2. Combustion chamber and tubes.
3. Chimney.
4. Accessories.

Figure (3-1) ICI Caldaie Sixen boiler.

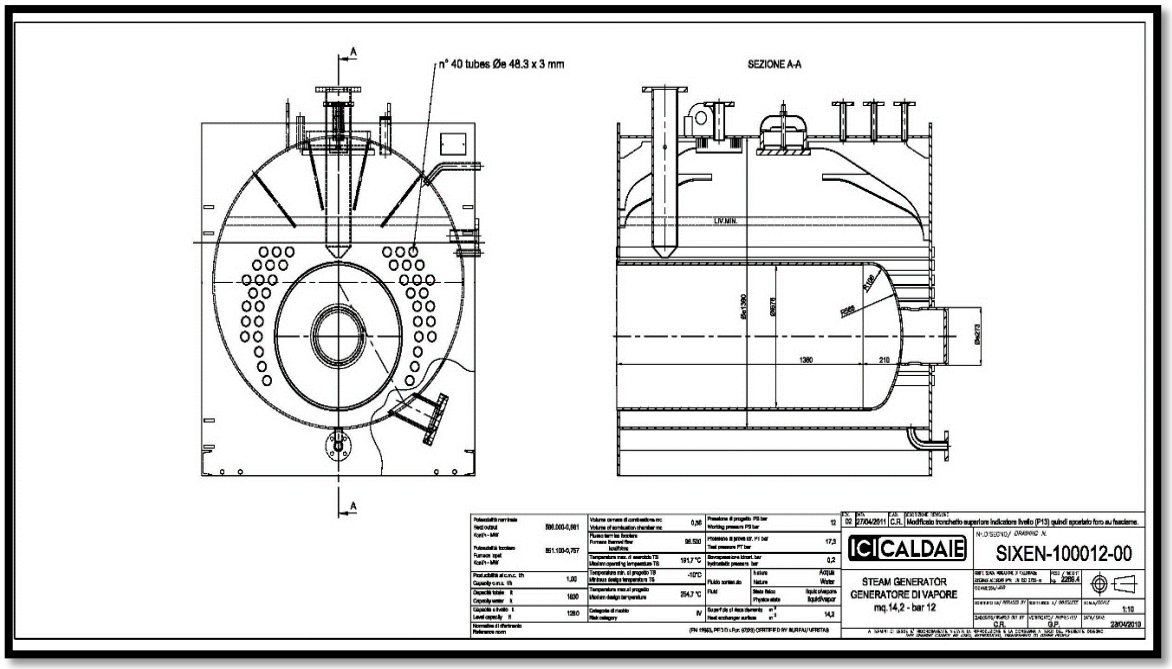

Figure (3-2) Schematic diagram of the sixen boiler [31**].**

3-2-1 The Burner

The boiler ICI sixen 1000 provided with a burner of type RL- 70 was American made, as shown in figure (3-3).

The burner had a tube of 385 mm in length penetrates the boiler to inject the tangential air and fuel inside the combustion chamber. The tube inner diameter was 156 mm and contain two identical nozzles placed in the center of tube to inject the fuel spray to the combustion chamber. The nozzles of type WDB solid cone, was American made with orifice diameter 0.65 mm. As shown in figure (3-4).

Figure (3-3) Burner RL-70.

Figure (3-4) The Nozzle.

3-2-2 Combustion chamber and tubes

The boiler has a horizontal cylindrical combustion chamber with hemispherical closed end so that the combustible gases hit the closed end and returned toward the burner side. The inner diameter of combustion chamber is 676 mm with 10 mm thickness and the length of the combustion chamber is 1570 mm.

The boiler has 40 identical horizontal tubes distributed symmetrically about the length of the boiler (Z-axis) as shown in figure (3-5).The tubes are distributed according to the experimental experience of the manufacturer Company to help transfer the maximum amount of heat from the tubes to the water [31]. The outer diameter and thickness of each tube are (48.3 mm) and (3 mm) respectively. The tubes length is (1740 mm).

Figure (3-5) Combustion chamber and tubes distribution at burner end.

3-2-3 The Chimney

The boiler has a horizontal chimney located in the backside opposite to the burner, where the flue gases are dismissed to the atmosphere after been produced by combustion in the combustion chamber and passes through the tubes to be collected by the rear plenum and then to the chimney. The chimney has an inner diameter 320 mm with 15 mm thickness, as shown in figure (3-6)

Figure (3-6) The Chimney of the boiler.

3-2-4 The Accessories

The boiler ICI Caldaie Sixen 1000 is fitted with a series of accessories that can be sub divided into [31]:-

1. Safety accessories (safety valves, water level limits, safety pressure switches).
2. Observation accessories (level gauge , pressure gauge ,flame inspection)
3. Control accessories (level and pressure switches).
4. Feed water accessories (centrifugal pump, injector or alternating steam pump).
5. Manual operation accessories (stop valves, purge valve).

Figure (3-7) shows the boiler with some accessories and components [31].

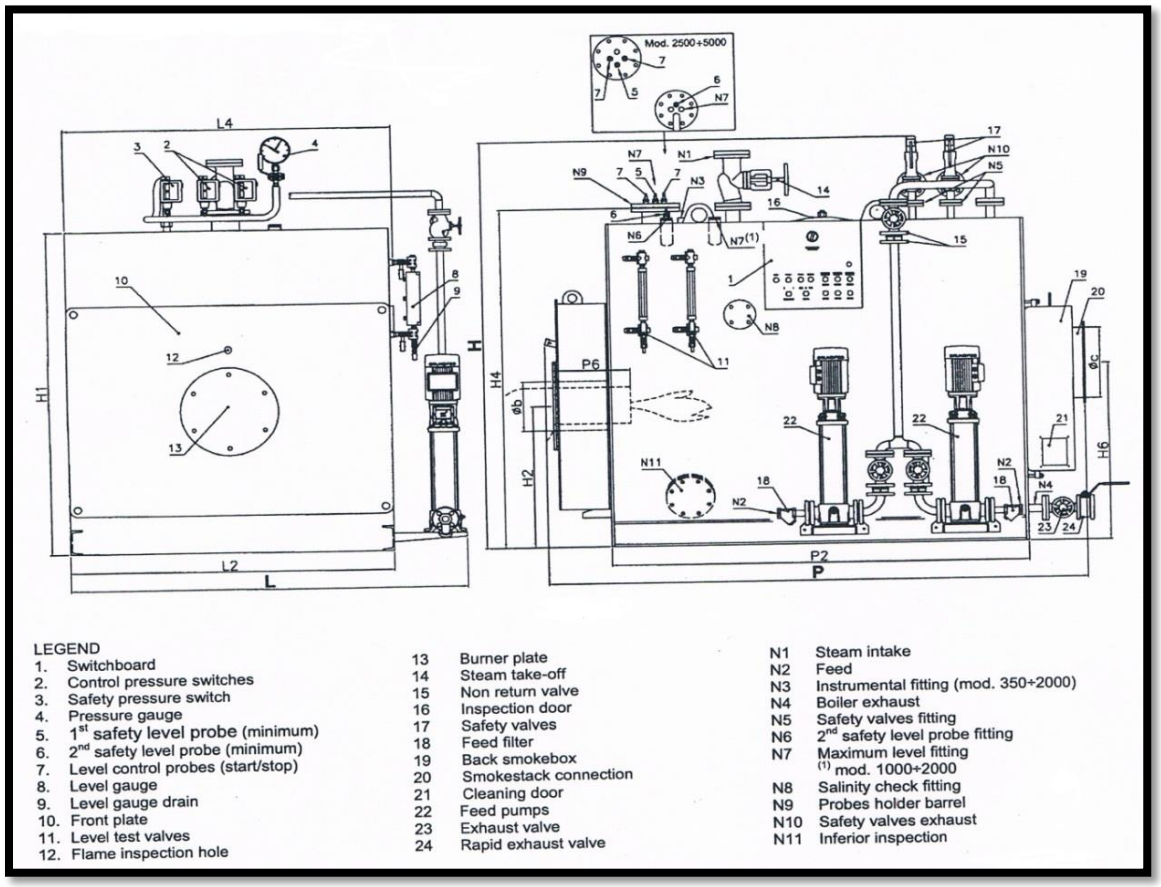

Figure (3-7) The Accessories of the boiler [31**].**

3-3 Instrumentation and Measurement Techniques

Many instruments were used to measure the parameters of the boiler that been required in the CFD program to make the simulation of combustion inside the boiler possible.

3-3-1 Measuring instrument calibration

To ensure that all the data read from the measuring devices are acceptable, all the measuring devices were calibrated.

3-3-2 Measurement of the rate of fuel consumption.

The boiler provided with a fuel tank of dimensions 760 mm length, 600 mm width and 800 mm height. The height of fuel inside the tank was measured by a transparent measurement tubes with ruler. As shown in figure (3-8).

The measurement of fuel consumption is as follows:-

- Measuring the height of fuel in the tank by the measuring tube before and after the operation of the boiler.
- Using the stop watch to calculate the time of the boiler operation
- Measuring the rate of fuel consumption from the following equations:-

The volume flow rate of fuel consumption (m^3/s) = {change of fuel volume in the tank ($\Delta\forall$)}/ time (s) (3-1)

Where the volume of fuel = area of tank × height of fuel

The rate of fuel consumption (kg/s) = (density ×$\Delta\forall$) (3-2)

After many repetitions, the rate of fuel consumption of the Iraqi Diesel fuel founded to be equal to 63.8 kg / h.

Figure (3-8) Fuel tank and gages.

3-3-3 Measurement of air flow rate

Since the area of the burner tube that provides the combustion chamber with air is constant, then it is necessary to adjust the velocity of the air to achieve the stoichiometric mass of air flow rate.

The following steps were done to measure the velocity of air:-

- Operate the burner without injection of fuel (dry run).
- Use the flow meter to measure the actual velocity of air.
- Adjust the gates that control the air provided by the burner.

According to the chemical equation of the Iraqi Diesel fuel ($C_{7.2083}H_{11.199}S_{0.072}$) at the stoichiometric equivalent ratio (Φ =1),

(Mass of air / mass of fuel) = 15.6 (3-3)

So that the flow meter used to measure and control the velocity of air to be (11.87 m / s) to achieve a stoichiometric mixture mass flow rate of air . Figure (3-9) shows the flow meter.

Figure (3-9) The Flow meter.

3-3-4 Infrared thermometer

The infrared thermometer was used to measure the temperature of the combustions chamber wall, tubes walls and all the other walls in the domain of the ICI Caldaie boiler. The temperature of the combustion chamber walls and tubes walls were measured to be 465℃ (738K).

Figure (3-10) shows the infrared thermometer that was used in temperature measurements of walls.

Figure (3-10) The infrared thermometer.

3-3-5 Thermometer

The thermometer was used to measure the temperature of the air, the temperature of fuel and the calibration of the thermocouple.

The temperature of air was equal to 27℃ (300K).
The temperature of Iraqi Diesel fuel was equal to 27℃ (300K).

3-3-6 Emission measurements

The exhaust gas analyzer type (model 488 Italy) was used to analyze the emissions of exhaust, as shown in figure (3-11).The analyzer detect the CO-CO_2-HC-O_2 contents .The gases are picked up from the boiler chimney pipe by means of a probe. They are separated from the water moisture through the condensate filter, and then they are conveyed into the measuring cell. A ray of infrared light, generated by a transmitter, is sent through the optical filters on to the measuring elements. The gases in the measuring cell absorb the ray of light at different wavelengths, according to their concentration. The H_2, N_2, and O_2 gases due to their molecular composition

(the have the same number of atoms), do not absorb the emitted ray .This prevents measuring the concentration through the infrared system .The CO, CO2 and HC gases (depend on their molecular composition), absorbs the infrared rays at specific wavelengths (absorption spectrum).However, the analyzer is equipped with a chemical kind sensor through which the oxygen percentage (O_2) is measured.

The mass fraction of CO_2, CO and UHC measured were (0.207), (0.251) and (4.83×10^{-5}) respectively at outlet.

Figure (3-11) The Exhaust gas analyzer type (model 488 Italy).

3-3-7 Thermocouple and Reader

Before using the thermocouple a calibration is done using a standard thermometer, such that the thermocouple and standard thermometer are inserted in a vessel filled with distilled water .This vessel was heated by using an electric heater with heat regulator to change the water temperature.

The water temperature was read before heating with both thermometer and thermocouple and the two readings are compared for calibration. Then the water was heated until it reached a stable temperature then reading of another water temperature was made by both the thermocouple and thermometer then compared for calibration. For a while the water was left to cool down until it reached the temperature before reheating the water again and the two readings were compared and so on the calibration table is obtained.

After doing the necessary calibration for the thermocouple, it is used to measure the exhaust flue gases temperature by means of a probe inserted in the chimney. This temperature was compared later with the temperature calculated by the CFD program (FLUENT) to make sure that the simulation is acceptable if the two temperatures are consistent. Figure (3-12) shows the thermocouple.

The exit flue gases temperature measured was 657℃ (930 K).

Figure (3-12) Thermocouple and Reader.

CHAPTER FOUR

NUMERICAL ANALYSIS

CHAPTER FOUR
NUMERICAL ANALYSIS

4-1 Introduction:

The following practical assumptions were assumed to carry out the CFD simulations using ANSYS FLUENT program:

- Steady state.
- Incompressible flow for liquid fuel.
- Compressible flow for gaseous fuel.
- Constant properties.
- Constant velocity at inlet vents of burner.
- Neglect losses at all parts of domain.

4-2 Boundary Conditions:

The general elliptic differential equation should be solved after the boundary conditions of whole domain are applied with permissible and satisfied values with the following procedure:

I. Inlet boundary conditions:

The properties of entering fluid to boiler are known, such as temperature, viscosity, density, velocity.

Input mass flow rate of fuel to the boiler =63.8 kg/h.

The burner had two identical nozzles with equal orifice areas, therefore the mass flow rate provided by each nozzle equal to one-half of the average total mass flow rate of the fuel to the boiler.

Input mass flow rate of air for the stoichiometric reaction supplied by the burner = 995.28 kg/h.

II. Symmetry line dividing the burner and the boiler in z direction:

The boundary conditions change for variables could be considered zero value at $(\frac{\partial \emptyset}{\partial \theta} = 0)$, and the maximum temperature considered equal 1986°C for Iraqi Diesel fuel.

III. Velocity:

No slip conditions and zero velocity at θ, R and Z directions (U=V=W=0) at walls of furnace chamber.

IV. Properties conditions:

The temperature of the wall is measured 465°C (T_w=738K), but the other space temperature is at room temperature. The other properties may be determined after determining the temperature with mathematical relations (density, enthalpy …etc.).

4-3 Combustion and Chemical Reactions:

A boiler requires a source of heat at a sufficient temperature to produce steam. Fossil fuel is generally burned directly in the boiler furnace to provide this heat.

Combustion is defined as the rapid chemical combination of oxygen with the combustible elements of a fuel. There are just combustible elements of significance in most fossil fuels: Carbon, Hydrogen and Sulfur. Sulfur has minor significance as a heat source, but it is a major contributor to corrosion and pollution problems. Therefore, fossil fuel may contain ash, iron, vanadium…etc., which has no effect on the heat value of fuel [32, 33].

The objective of a good combustion is to release all the energy in the fuel while minimizing losses from combustion imperfections and excess air. System requirement objectives include minimizing nitrogen oxides (NO_x), carbon monoxide (CO), and volatile organic compounds and for more difficult to burn fuels minimizing unburned carbon and furnace corrosion.

The combination of the combustible fuel elements and compounds in the fuel with all the oxygen requires temperatures high enough to ignite the constituents, mixing or turbulence to provide intimate oxygen-fuel contact, and sufficient time to complete the process [34].

The type of fuel employed in ICI Caldaie boiler is:

Iraqi Diesel fuel ($C_{7.2083}H_{11.199}S_{0.072}$) which has the following composition as analyzed by south oil Refinery Company (percentage by weight):

Specific gravity at 15.6 Cº	0.8641
Carbon (C)	86.5%
Hydrogen (H_2)	11.199%
Sulfur (S)	2.3%
Ash	0.001%
Salt Content as (NaCl) ppm	0 % (ppm: part per million)
Water and Sediment	0%

Table (4-1) shows the analysis of the combustion process.

Table (4-1) Combustion process analysis.

No	Fuel constituent	Concentration by weight %	Reaction	Theoretical O_2 required per kg of fuel	Products per kg of oxidant
1	C	0.865	$C+O_2 \longrightarrow CO_2$	$C\% \times \frac{M_{O_2}}{Mc}$	$CO_2 = C\% \times \frac{MCO_2}{Mc}$
2	H	0.11199	$2H_2+O_2 \rightarrow 2H_2O$	$H\% \times \frac{M_{O_2}}{M_{H_2}}$	$H_2O=H\% \times \frac{MH2O}{2MH}$
3	S	0.023	$S+O_2 \longrightarrow SO_2$	$S\% \times \frac{M_{O_2}}{MS}$	$SO_2 =S\% \times \frac{MSO_2}{MS}$

Neglecting the ash value because it is not entering in the reaction process of combustion, i.e. from the above table:

The total mass of oxygen required per kg of fuel:

$$m_{O_2} = C\% \times \frac{M_{O_2}}{M_c} + H\% \times \frac{M_{O_2}}{M_{H_2}} + S\% \times \frac{M_{O_2}}{M_S} \quad (4\text{-}1)$$

But the concentration of oxygen in air is 23.14% by weight, then; the exact weight of air required for combustion per kg of the fuel = $\frac{m_{O_2}}{0.2314}$ (4-2)

The Stoichiometric Air/ Fuel ratio = $\frac{m_{O_2}}{0.2314 \times m_f}$ (4-3)

Where m_f … the mass of fuel considered equal 1 kg.

N_2 associated with the air = $0.7686 \times \frac{m_{O_2}}{0.2314}$ (4-4)

Most gases involved in combustion calculations can be approximated as an ideal gases, the reacting substances can be modeled by the equation of state [35].

This simulations study dealt also with other fuels, they were: Light Diesel ($C_{10}H_{22}$), Methane (CH_4) (these fuels included in the FLUENT database) and Iraqi LPG ($C_{3.437}H_{8.874}$) (which has been added in this study to the FLUENT database).The Light Diesel and Methane had an experimental results because they already had been burned in the boiler by the manufacturer company [31], while the Iraqi LPG was solved theoretically in this study. The results obtained for these fuels would be compared with that of the Iraqi Diesel ($C_{7.2083}H_{11.199}S_{0.072}$) to study the effect of different combustion parameters like carbon to hydrogen ratios, temperature, velocity…etc.

4-4 Radiation and Heat Balance:

After combustion of fuel inside the furnace, heat must be radiated from the flame to all walls of furnace. Then by the first law of thermodynamics:

Heat released by burning fuel (Heat input) = Heat absorbed by air +Heat radiated to all inside faces of the furnace

$$Q = m_a C_P (T_f - T_a) + \varepsilon_E \sigma A_p (T_f^4 - T_w^4) \quad (4\text{-}5)$$

Where

$$Q\ (kW) = \text{mass} \times \text{calorific value of fuel} \quad (4\text{-}6)$$

4-5 Basic Principles of Solution

There are many principles for solving the present case study in FLUENT package program depends on the following:

4-5-1 Choosing Turbulence Model

There are many turbulence models used in FLUENT depending on time-average with modified equations containing additional unknown variables. Turbulence models are needed to determine these variables in terms of known quantities. It is an unfortunate fact that no single turbulence model is universally accepted as being superior for all classes of problems. The choice of turbulence model will depend on considerations such as the physics encompassed in the flow, the established practice for a specific class of problem, the level of accuracy required, the available computational resources, and the amount of time available for the simulation [10], [35].The standard k-ε model is used in this study, the assumption of this model in FLUENT is that the flow is fully turbulent, and the effects of molecular viscosity are negligible.

4-5-2 Modeling Liquid Fuel Combustion:

Liquid fuel combustion can be modeled with the discrete phase and non-premixed models. The fuel stream produced by evaporation of the liquid fuel appears within the domain as a source of the mean fuel mixture fraction.

In FLUENT, the liquid fuel discrete-phase model in the usual way is defined and the gas phase (oxidizer) flow inlet is modeled using an inlet mixture fraction of zero and the fuel droplets are introduced as discrete phase injections. The property inputs for the liquid fuel droplets are unaltered by the non-premixed model. The largest components of fuel mixture should be selected as the "evaporating species". In this study, Iraqi Diesel fuel ($C_{7.2083}H_{11.199}S_{0.072}$) is used as evaporating species.

1.Outline of Steady-State Discrete-Phase Problem:

The combustion of a liquid fuel must be solved by using discrete phase models according to the following outline:

- Solving the continuous phase flow.
- Creation of the discrete phase injections.
- Tracking the discrete phase injections by using plots or reports.

The procedure for setting up and solving the problem as in the following:

i. Enabling interaction with continuous phase in the discrete phase.

ii. Choosing the steady state treatment of liquid fuel particles.

iii. Enabling the required physical sub models for the discrete phase model. In this study, just" Particle Radiation Interaction" is needed.

iv. Setting the numeric parameters.

v. Specifying the initial conditions and particle size distributions.

vi. Defining the boundary conditions.

vii. Defining the material properties for the discrete phase.

viii. Initializing the flow field.

ix. Solving the flow.

x. Examining the results.

2.Droplet Size Distribution:

For liquid sprays a convenient representation of the droplet size distribution is the Rosin-Rammler expression [10], [35]. The complete range of sizes is divided into an adequate number of discrete intervals, each represented by a mean diameter for which trajectory calculations are performed.

In this study, the Iraqi Diesel particles (droplet) are used with mean diameter (0.00017) m, (minimum diameter is 50×10^{-6} m, maximum diameter is 330×10^{-6} m) [36], as shown in figure (4-1)

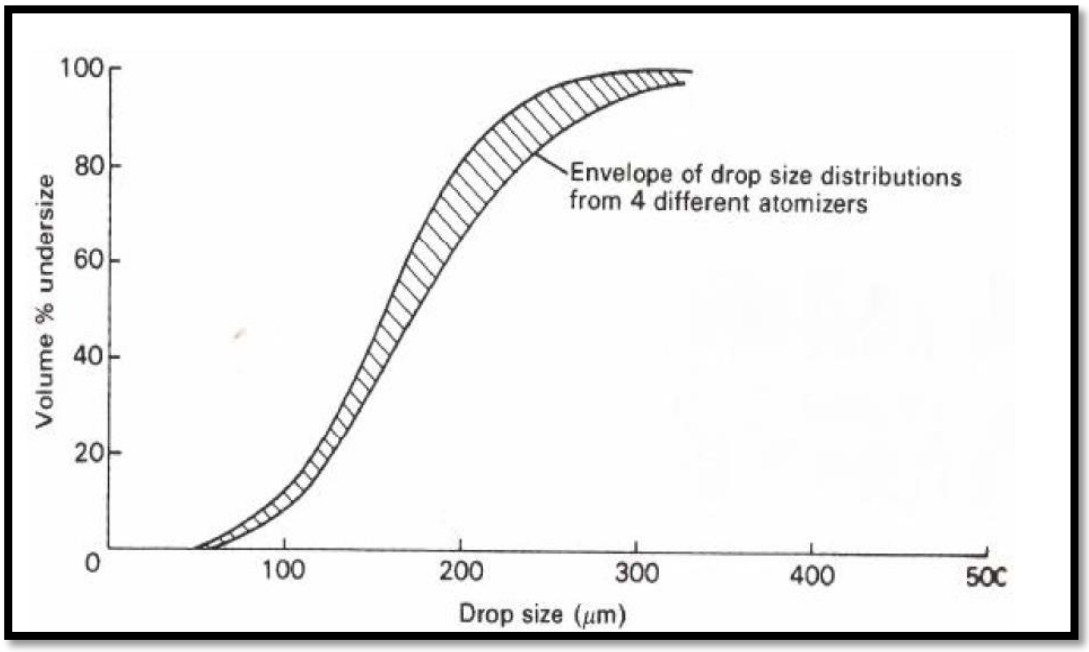

Figure (4-1) Droplet diameter for Iraqi Diesel fuel.

3. Heat and Mass Transfer of Liquid Particles:

There are six relationships (Laws) for heat and mass transfer of particles (generally) in FLUENT for discrete phase models.

4. Atomizer Models:

There are five atomizer models available in FLUENT to predict the spray characteristics from knowledge of global parameters such as nozzle type and liquid flow rate. Pressure-swirl atomizer model is used in this study.

5. Injection Types:

There are 11 types of injection in FLUENT. Choosing the injection type depends on the nozzle type used to inject the fuel in real. It's solid-cone (only in 3-D) is used in this study.

Herein, the initial conditions of solid cone have been employed instead of the particle type, which is used when choosing any type of atomizers.

4-6 Solution Procedures

The practical application of this thesis was processed with Solidworks and ANSYS package program which contains many software packages including design modeler, mesh and FLUENT.

Solidworks version 2012 was designed to help in drawing the domain while ANSYS is used to analyze and design mesh-building models for computational fluid dynamics (CFD) and other scientific applications. The following steps were considered for building the case study:

4-6-1 The Case Designed in Solidworks and ANSYS

Solidworks version 2012 was used for drawing all the parts of the domain of the boiler separately with high accuracy. It was then assembled in volumes of the body. These processes in Solidworks were complicated because of the many curved parts in the design. Forty-five models were designed for furnace and their accessories (46 volume parts for one model of domain). It required two months to have the correct applicable design. The

body was finally exported in a tense of parasolid to the ANSYS Design Modeler for further modifications.

The following steps were done on the case in ANSYS Design Modeler.

1. Fill the hollow volumes with fluid and extract those volumes. These volumes are impossible to extract in Solidworks.
2. Enhance the case by making many body operations like surface merging, slice parts, and unite ….etc.
3. Define the fluid parts and solid parts.
4. The resulted case shown in figure (4-2) was exported again to the Solidworks to make the automatic symmetry for the rig (this function is not found in ANSYS Design Modeler) as shown in figure (4-3).

After making the symmetry for the rig, the case was exported from Solidworks to the ANSYS again to make the mesh.

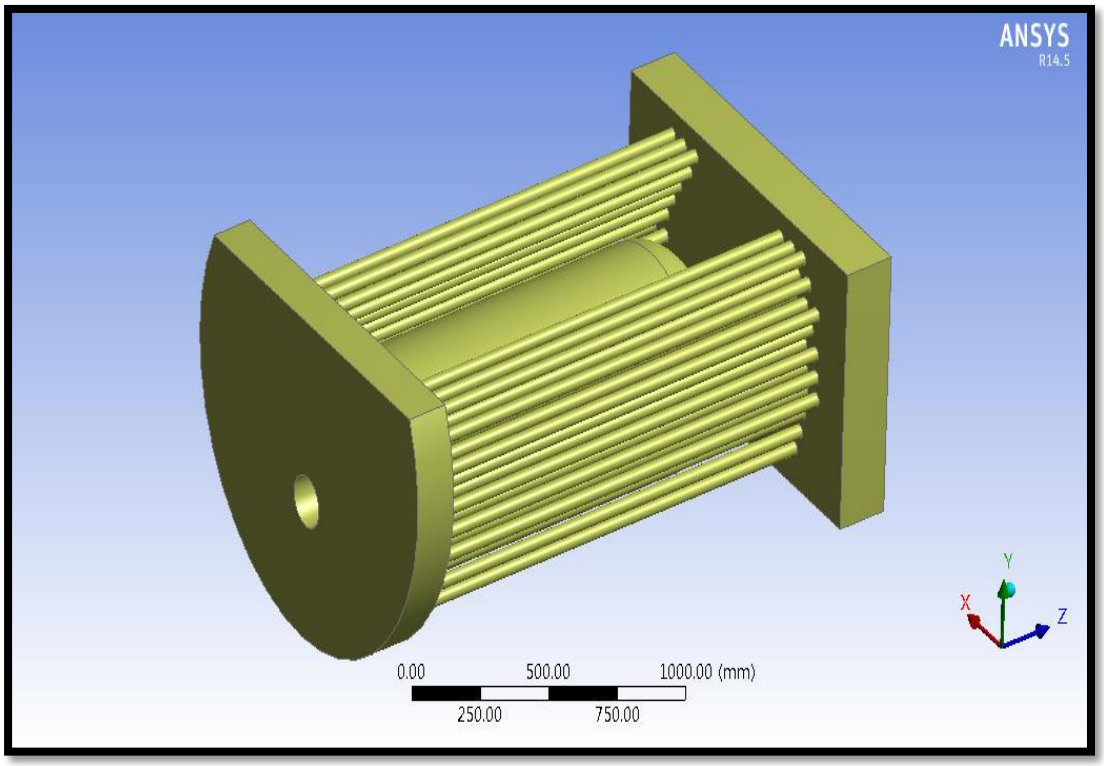

Figure (4-2) The Extracted fluid of the model.

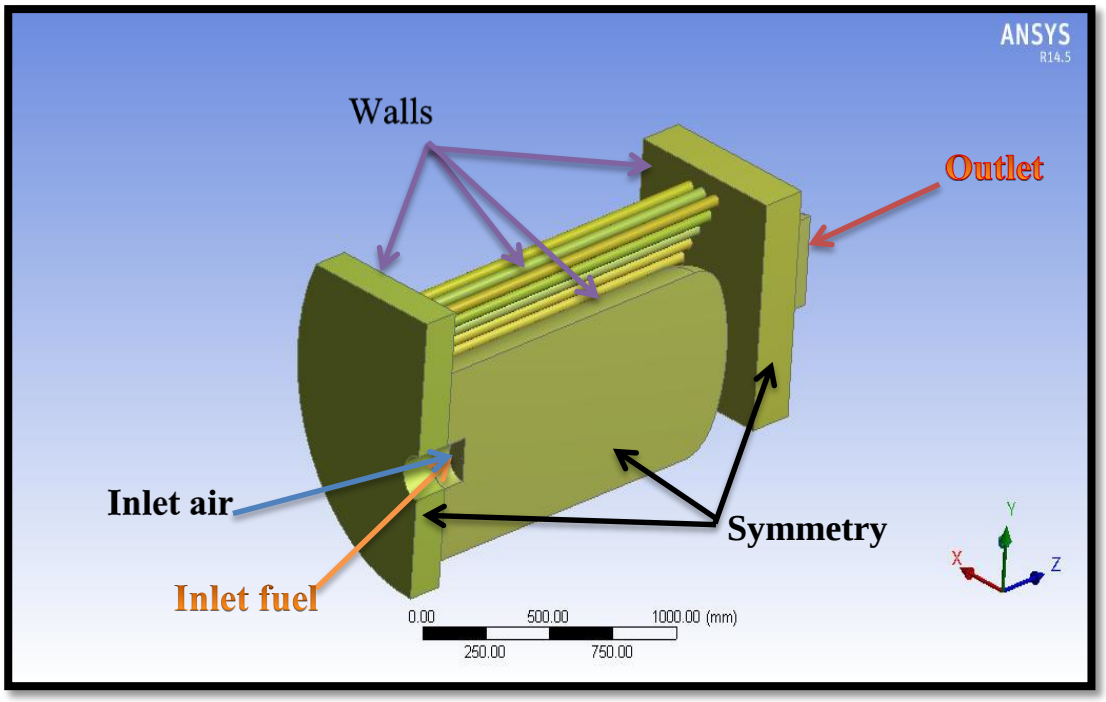

Figure (4-3) The Symmetry of the model.

4-6-2 Meshing the case

ANSYS Meshing version 14.5 was used for meshing the parts of all domains with high accuracy. Which include a grid generation, refinement of mesh specification of zone type (continuum or boundary type). The meshing was completed by using suitable meshing schemes. The following steps were considered:-

1- Choosing the tetrahedral method for all volumes in this case, because it is the best meshing method for the CFD and it is the only method applicable to complicated geometries.
2- Name all the boundaries inlets, outlets, symmetry and walls.
3- Use the size Functions for many volumes, surfaces in the domain.
4- Identify the coordinate that used later in injection.
5- Mapping many surfaces to get a structured mesh.

Using the boundary layers was to transform mesh from condensed regions that had a small meshing size to the other regions that had a larger meshing size.

Table (4-2) Meshing scheme of the boiler.

Scheme	Mesh size (mm)	Number of volumes
Tetrahedral	0.05	1
Tetrahedral	10	22
Tetrahedral	15	1
Tetrahedral	35	1
Tetrahedral	45	1

In addition to above volume mesh types, there are many types of surface mesh used for meshing some interior faces before volume meshing such as pave, triangle or map scheme. The problem of meshing was the small parts engagement with those of large parts such as nozzle orifice diameter 0.65 mm with length of boiler 2.35 m… etc. The domain has (1564014) cells, (3251539) faces and (326714) nodes, with aspect ratio less than 5/1 and skewness less than 0.75, as shown in figure (4-4) and (4-5) respectively.

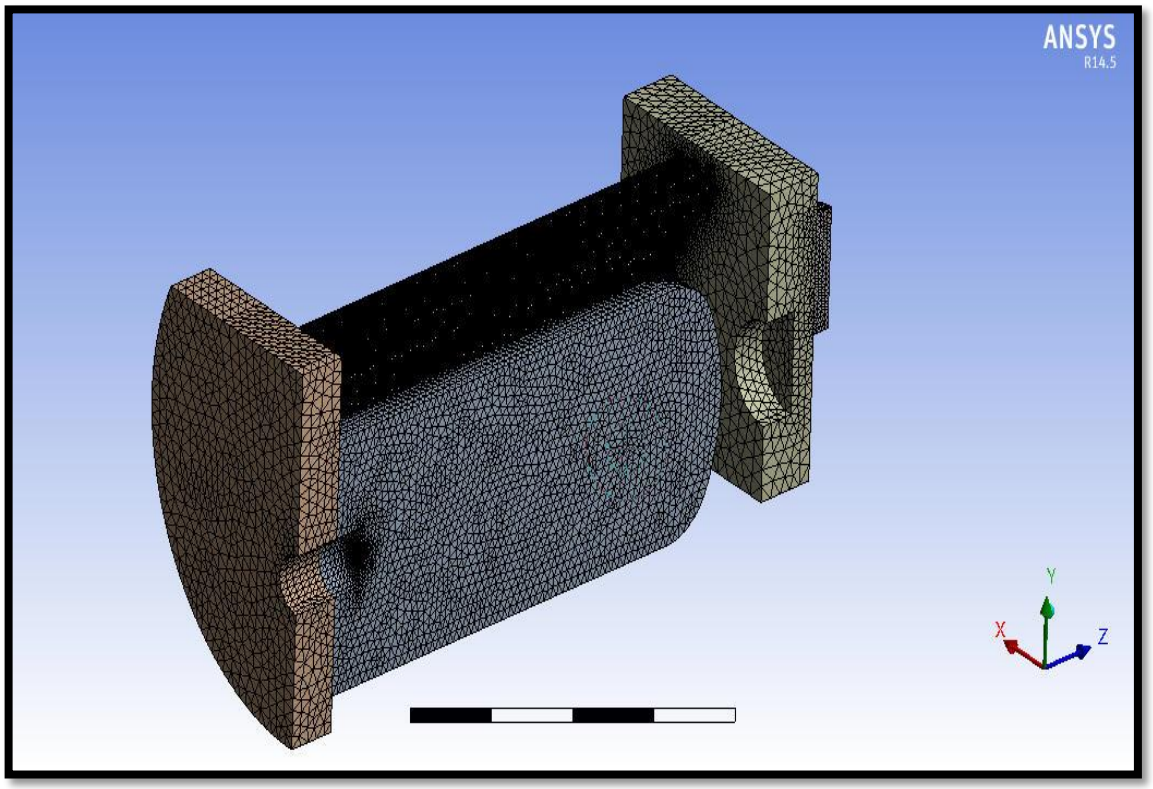

Figure (4-4) The Meshing of the boiler.

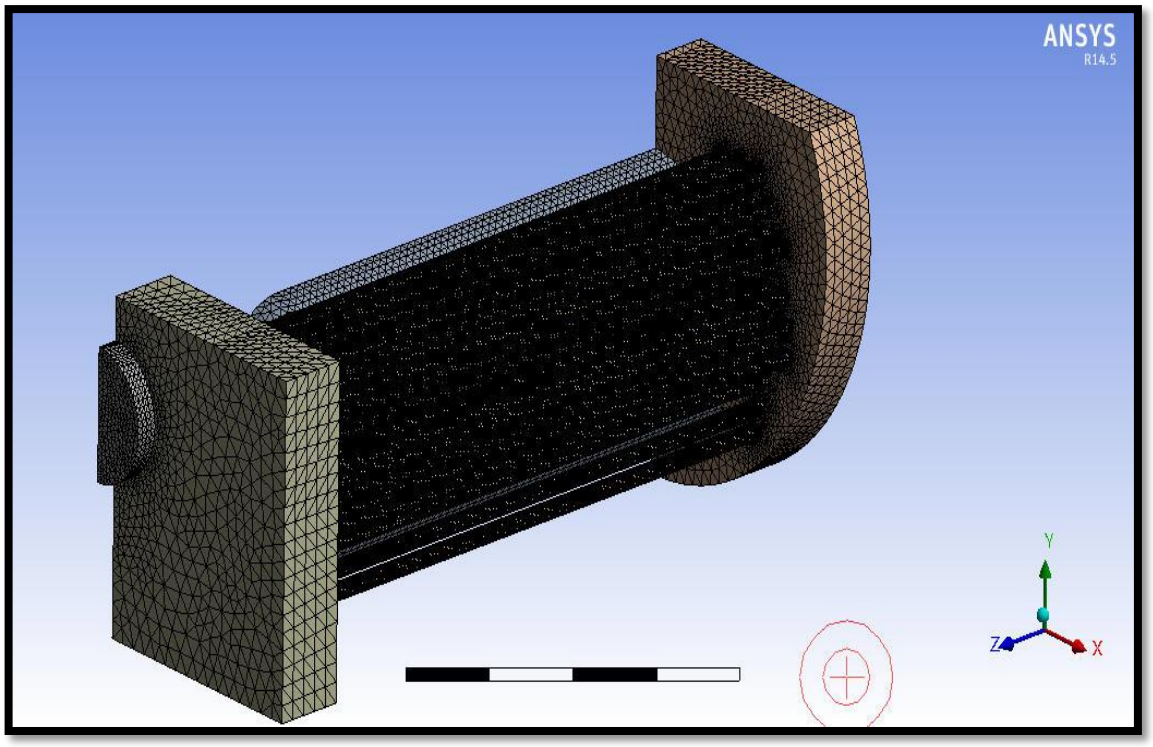

Figure (4-5) Another view for the boiler meshing.

4-6-3 Processing in FLUENT

1- Reading the mesh

Reading the mesh from the file, which was saved before**.**

2- Checking the grid

The grid checking capability in FLUENT provides domain extents, volume statistics, grid topology, periodic boundary information and verification of simplex counters. It must generally check the grid right after reading it into the solver, in order to detect any grid trouble before getting started with the problem setup. This checking is obtained by selecting the check menu item in the Grid pull-down list menu.

3- Smoothness

Truncation error is the difference between the partial derivatives in the governing equations and their discrete approximations. Rapid changes in cell volume between adjacent cells translate into larger truncation errors. FLUENT provides the capability to improve the smoothness by refining the

mesh based on the change in cell volume or the gradient of cell volume [10], [35].

4- Cell Shape

The shape of the cell (including its skewness and aspect ratio) has a significant impact on the accuracy of the numerical solution.

Skewness is defined as the difference between the shape of the cell and the shape of an equilateral cell of equivalent volume. Highly skewed cells can decrease accuracy and destabilize the solution.

Aspect ratio is a measure of the stretching of the cell. A general rule of thumb is to avoid aspect ratios in excess of 5:1.

The swap process is repeated to get zero skewness.

5 -Converting the mesh

The conversion of the mesh from tetrahedron type to polyhedral type is made to reduce the total counts of nodes, enhance the mesh quality and accelerate the solution.

6-Reordering the mesh

The mesh was reordered twice to reduce the bandwidth and that will accelerate the solution.

7-Scale

All the dimensions in this drawing of domain is in millimeters, but the other physical properties of flow measured in meters. Therefore, it is important to transform the dimensions of domain from millimeters to meters by scaling.

8-Boundary Conditions:

Boundary conditions specify the flow and thermal variables on the boundaries of model.

In this study, there were two velocity inlets one for liquid fuel and one for velocity inlet of tangential air, one outlet vent of type pressure outlet, walls of furnace, tubes, chimney and symmetry. The other interiors and walls are not needed to be put as conditions for solution.

All inlet velocities, turbulence specifications should be used as follows:

a- Turbulence Intensity:

The turbulence intensity (I) is defined as the ratio of the root-mean-square of the velocity fluctuations (u′) to the mean flow velocity (u_{avg}) [10], [35].

A turbulent intensity of 1% or less is generally considered low and turbulent intensities greater than 10% are considered high.

For internal flow, the turbulent intensity at the inlets is completely dependent on the upstream history of the flow. If the flow upstream were under-developed and undisturbed, low turbulence intensity would be used. If the flow is fully developed, the turbulence intensity may be as high as a few percent. The turbulence intensity could be estimated from the following formula derived from an empirical correlation for pipe flows [9]:

$$I = \frac{\acute{u}}{u_{avg}} = 0.16\ (Re_d\ )^{\frac{-1}{8}} \qquad (4\text{-}7)$$

Where: $\mathrm{Re}_d = \frac{\rho\, u_{avg}\, d_h}{\mu}$

The turbulent intensity for Iraqi Diesel fuel at full load of unit is calculated to be (5.29%) when Reynolds number was (7029.75).

b- Velocity Inlet Boundary Conditions:

Velocity inlet boundary conditions are used to define the flow velocity (along with all relevant scalar properties of the flow) at flow inlets. The total (or stagnation) properties of the flow are not fixed, so they will rise to whatever value necessary to provide the prescribed velocity distribution.

c- Thermal Boundary Conditions at Walls:

Thermal boundary conditions at walls are needed for solving the energy equation. There are five types of thermal conditions.

In this work, the furnace and tubes walls temperatures were measured experimentally and found equal to 738 K as in [17].

d- Radiation Boundary Conditions for Walls:

In this work, it is necessary to specify the emissivity of walls for FLUENT radiation calculations. P-1 radiation model is used because it is the suitable case, which is based on the expansion of the radiation intensity.

9- Physical materials

An important step in the setup of the model is to define the materials and their physical properties. Material properties are defined in the Materials panel. In this study, steel is used for solid materials instead of Aluminum as default material, because the boiler is made of steel.

In case of solving methane burning by FLUENT, the species transport analysis, air-methane mixture is used with default properties except changing constant specific heat to variable specific heat by using mixing law, and the other species (CH_4,N_2,O_2,H_2O) are changed to piecewise-polynomial profile.

In case of solving the Iraqi Diesel, Light Diesel and Iraqi LPG in the ANSYS FLUENT by using Non-premixed combustion model, probability density function (PDF) look up table is used for activating the mixture

properties. For this procedure, many properties must be added to complete the PDF table:

1- Chemistry state, Equilibrium state, Non-adiabatic combustion, options of fuel, in case of using Iraqi Diesel fuel and Iraqi LPG in the furnace. These fuels should be added first to the FLUENT database with all the properties of that fuel like fuel lower calorific value, fuel specific heat and molecular weight….etc.

   In case of using light Diesel, the same steps will be done except we can add that fuels from the fluent database because it is already found in that database.

2- Chemical composition of Iraqi Diesel fuel and Iraqi LPG, oxide as mole fraction.

3- Temperature of fuel and oxide in Kelvin. When using P-1 as radiation model, absorption coefficient of PDF-mixture must be changed from zero value to (WSGGM-domain-based). This should specify a composition dependent absorption coefficient, using the weighted sum of gray gases model. WSGGM-domain-based is available coefficient that uses a length scale, based on the geometry of the model.

The absorbing or emitting effects depend on the chosen radiation model [12]. If there are only absorption coefficients, then Lambert's Law of absorption applies

$$I_r = I_o \exp(-ax) \qquad (4\text{-}8)$$

Where I_r is the radiation intensity, (a) is the absorption coefficient, and (x) is the distance through the material. Along with the scattering coefficient, it describes the change in radiation intensity per unit length along the path through the fluid medium. FLUENT allows inputting a composition-dependent absorption coefficient, with local value of a function of the local mass fractions of water vapor and carbon dioxide. This modeling option is

useful for simulation of radiation in combustion applications (been applied in this study).

Therefore, FLUENT includes the effect of particles on the absorption coefficient and the effects of soot for any of the radiation models.

The scattering coefficient is set to zero assuming isotropic process.

10- Reference pressure location

The criteria for choosing a suitable operating pressure are based on the Mach number regime of the flow and the relationship that is used to determine density [10], [35]. For incompressible flow that does not involve any pressure boundaries, FLUENT adjusts the gauge pressure field (after each iteration) to keep it from floating. In this study, the reference pressure location is at the point (0, 0, 0) where the gauge pressure is zero at the reference ground of furnace.

4-6-4 Defining Injection Properties:

The injection is chosen by selecting the injection panel, as in the following:

1- Choosing "solid cone" as injection type.
2- The number of particle streams is assumed to be 2.
3- In particle type panel, "Droplet" is used [36].
4- "Iraqi Diesel" is chosen in evaporating material.
5- Rosin-Rammler was used in diameter distribution.
6- $C_{7.2083}H_{11.199}S_{0.072}$ was used as evaporating species.
7- Selecting point properties for entering the following for solid cone injection properties:

a. Position (X, Y, Z), for one injection in one burner: Injection 0 (-763.42, -366.53, 80) mm.
b. Temperature: the temperature is 300 K for the stream at inlet fuel.
c. Axis: setting the vector components, Z=1, Y=X=0 because the flow in the direction of Z only.
d. Velocity: the velocity of inlet stream is (30.9 m/s).

e. Cone angle: the angle of solid cone is 30° with Z-axis (this angle should be equal to the half of real inclination angle of the solid cone).
f. Radius: the radius of the cone is 0.325mm.
g. Mass flow rate: For Iraqi Diesel fuel is 8.861×10^{-3} kg/s.
h. The minimum diameter of droplet 50×10^{-6}m.
i. The mean diameter of droplet 170×10^{-6} m.
j. The maximum diameter of droplet 330×10^{-6} m.
k. The other parameters are not changed.

8- Enable the Discrete Random Walk Model under Stochastic Tracking and set the Number of Tries to 10.

The boundary conditions of discrete phase in this study, is used as "trap" for inlet and outlet because in this case, the entire mass of evaporating droplets instantaneously passes into the vapor phase entering the cell adjacent to the boundary.

4-7 Calculations and Inputs:

Table (4-3) demonstrates the transformation of Iraqi Diesel species from weight portions to moles:

Table (4-3) Species transformations.

Species	Weight %	Moles	Mole fraction
C	86.5	7.2083	0.39
H	11.199	11.199	0.606
S	2.3	0.072	0.004

The specific gravity of Iraqi diesel fuel is 0.8641

Tables (4-4) and (4-5) show the resulted calculations of case study:

Table (4-4) Iraqi Diesel fuel parameters input to the burner.

Higher heating value (J/kg)	Lower heating value (J/kg)	Mass flow rate of air (kg/s)	Mass flow rate of fuel (kg/s)	Velocity of fuel (m/s)	Input temperature of fuel and air (K)
4.425×10^{7}	4.1882×10^{7}	0. 2765	0.01772	30.9	300

Table (4-5) Iraqi LPG fuel parameters input to the suggested burner.

Lower heating value (J/kg)	Mass flow rate of fuel (kg/s)	Mass flow rate of air (kg/s)	Velocity of fuel (m/s)	Input temperature of fuel and air (K)
4.9602×10^{7}	0.014964	0.23179	62	300

There are other points taken into consideration:-

1- The under – relaxation factor must be taken in FLUENT with suitable values for every variable. These values may be small and then to be increased depending on convergence of equations. The equation of under relaxation factor is [37]:

$$E_{new} = E_{old} + \lambda (E_{Calculated} - E_{old}) \qquad (4\text{-}9)$$

Where

E_{new} : new value of the computed parameter.

$E_{calculated}$: newly computed value of the parameter.

λ : Under relaxation factor.

2- Number of Iterations

The number of iterations of any run in FLUENT program depends on the number of equations of variables and the volume of domain. In this thesis the number of iterations was (3000-18000) depending on gas fuel or crude oil combusted fluid which reach up to seven days (and more) of iterations to get full convergence using a high specifications of three computers (4.5 GBytes of random access memory, core I5 due, 3 GHz processor, 500 GBytes of hard disk drive memory for each one with 750 GBytes of external hard disk connected to that computers as secondary storage). These iterations should be specified by convergence factor for energy equation and radiation model (P-1) (1×10^{-6}) but for the others it was less than (1×10^{-3}).

CHAPTER FIVE

RESULTS AND DISCUSSION

CHAPTER FIVE
RESULTS AND DISCUSSIONS

5-1 Introduction:

The prediction of combustion products properties and behavior such as temperature, gases movement and gasdynamics inside a boiler, also the concentration of species and other products of combustion are studied in this chapter.

This work is carried out using both liquid and gaseous fuels. Iraqi Diesel is investigated experimentally and numerically, while Light Diesel, Methane and Iraqi LPG are studied numerically. The results of Methane and Light Diesel obtained theoretically are compared with the experimental results given by the documents introduced by the boiler manufacturers company [31].

This chapter also contains a suggested design for the burner working on the methane and Iraqi LPG or any gaseous fuel capable of producing the same energy obtained using liquid fuels.

As a test for the suggested burner design mentioned in this chapter, the methane gaseous fuel was solved theoretically and the results obtained were compared with that provided by the ICI Caldaie Company [31] and then with another study produced by Raja Saripalli [21] in the same field. That is to make sure that the suggested design of the burner is acceptable.

Results obtained for Iraqi LPG are also given in this chapter to be further used in any future experimental work to be carried out on the boiler using the suggested design.

Finally, a comparison among the liquid and gaseous fuels were made to demonstrate the differences in temperatures, pressures, velocities and turbulent kinetic energy due to the carbon to hydrogen ratios , fuel quality and type.

The packages FLUENT 6.3.26 and ANSYS FLUENT 14.5 were used to solve and display the qualitative results for the current solutions.

The programs GRAPHER10 and ANSYS CFD-POST 14.5 (after introducing some modification on the program, this modification enhanced the program ability to compare four cases and data of fuels) were used to display the quantitative results of the solutions. The original version was capable of introducing two data cases only.

5-2 Location of planes and lines in the Boiler

Many Iso-surfaces and lines are introduced in the boiler to indicate the physical and chemical parameters studied as shown in figure (5-1).

The Iso–surfaces mentioned in table (5-1) were used to display the qualitative results for the representative fuel (Iraqi Diesel),while for other fuels like Light Diesel ,Methane and Iraqi LPG are shown in (appendix A). The lines mentioned in table (5-2) are used to display the quantitative results of all the liquid and gaseous fuels.

Table (5-1) Iso-surfaces.

Name	Plane	Location (m)	Description of Position
X1	YZ	-0.76342	This plane divides the nozzle and combustion chamber vertically.
X2	YZ	-0.93017	This is a vertical plane 20 mm from the combustion chamber wall.
X3	YZ	-1.195	This plane passes through the centerline of one tube and intersects other tubes at different locations.
Y1 (Master Plane)	XZ	-0.36653	This is the most important plane in the domain because it has demonstrates all the parts of the boiler. It is pass through the centerline of the nozzle and combustion chamber in an axial direction horizontally.
Y2	XZ	-0.04303	This plane located 10 mm from the upper wall of combustion chamber.
Y3	XZ	-0.53328	This plane located in the middle of combustion chamber radius under plane Y1.
Z1	XY	-0.10005	This plane located in the middle thickness of the front plenum in side plane.
Z2	XY	0.08	This plane located at the nozzle and air inlets in the axial direction Z.

Table (5-1) Continued.

Name	Plane	Location (m)	Description of Position
Z3	XY	0.377	This plane located 0.297 m from Z2 plane in the axial direction Z.
Z4	XY	0.674	This plane located 0.594 m from Z2 in the axial direction Z.
Z5	XY	0.971	This plane is located 0.891 m from Z2 plane on axial length.
Z6	XY	1.268	This plane located 1.188 m from Z2 plane on axial direction.
Z7	XY	1.565	This plane located outside the combustion chamber and intersect the tubes only 1.485 m from Z1 plane in axial direction.
Z8	XY	1.8633	This plane located at the middle of the rear plenum thickness 1.7833 m from Z1 plane in axial direction.

Table (5-2) The Lines.

Name	Location (m)			Direction	Description of position
	X	Y	Z		
Line1 (L_{cc})	-0.76342	-0.36653	0.08	Z	This line start from the center of the nozzle to the end of combustion chamber wall.
	-0.76342	-0.36653	1.55		
Line2	-0.76342	-0.04303	1.41	-Z	This line located 25 mm from the upper wall of combustion chamber and start from the end of combustion chamber to the burner side in opposite direction.
	-0.76342	-0.04303	-0.02		
Line3	-1.195	-0.36962	-0.02	Z	This line passes through the center of one tube shown in Y1 plane till the end of tube.
	-1.195	-0.36962	1.74		
Line4	-0.82942	-0.36653	-0.10005	-X	This line passes through the middle of the front plenum thickness parallel to Z1plane.
	-1.379	-0.36653	-0.10005		
Line5	-0.75641	-0.1633	1.8633	-X	This line passes through the middle of the rear plenum thickness parallel to Z8 plane.
	-1.43	-0.1633	1.8633		

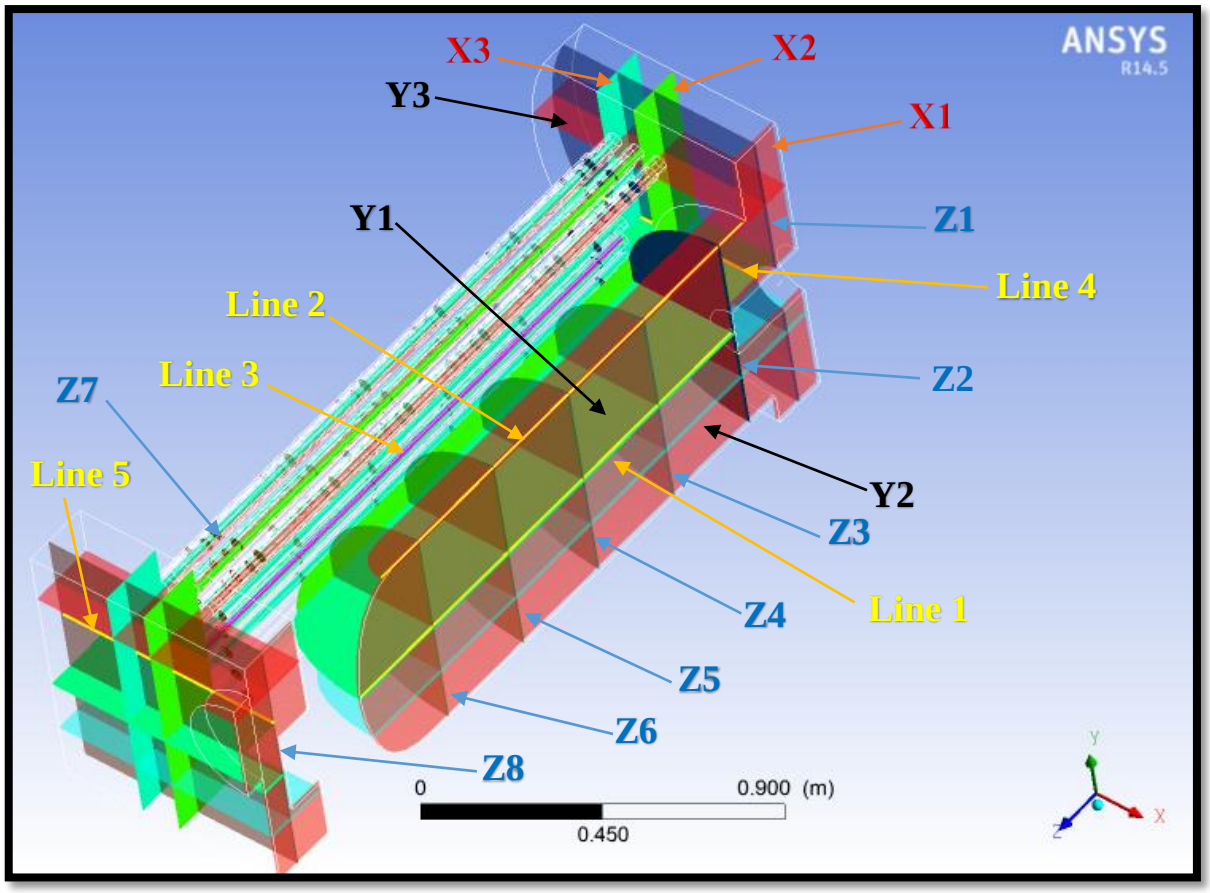

Figure (5-1) Location of planes and Lines in the Boiler.

5-3 Experimental work

The Iraqi Diesel fuel ($C_{7.2083}H_{11.199}S_{0.072}$) was burned in the combustion chamber of the boiler and the measurement shown in table (5-3) were recorded during boiler operation. The experimental tests were carried out on the rig and repeated many times for consistency.

Table (5-3) Experimental results of Iraqi Diesel fuel

Parameter	Value
Temperature of inlet fuel (K)	300
Temperature of inlet air (K)	300
Temperature of walls (K)	738
Mass flow rate of fuel (kg/h)	63.8

Parameter	Value
Mass flow rate of air (kg/h)	994.6
Temperature of exhaust gases (K)	930
Mass fraction of CO_2 at outlet	0.207
Mass fraction of CO at outlet	0.251
Mass fraction of UHC at outlet	4.83×10^{-5}

The boiler was already tested experimentally by the manufacturer company of the boiler. Their results are presented in table (5-4). They use the Light Diesel as a liquid fuel and Methane as a gaseous fuel and gave these results for their experimental works [31].

Table (5-4) Experimental results of Light Diesel and Methane [31].

Parameter	Light Diesel	Methane
Temperature of inlet fuel (K)	300	300
Temperature of inlet air (K)	300	300
Temperature of walls (K)	745	526.68
Maximum temperature in the boiler (K)	1955	1631
Mass flow rate of fuel (kg/h)	64	53.6
Mass flow rate of air (kg/h)	941	920
Temperature of exhaust gases (K)	948	564
Mass fraction of CO_2 at outlet	0.177	0.111

5-4 Numerical results

5-4-1 Iraqi Diesel fuel

The Iraqi Diesel fuel is used as a representative fuel for the presentation of the results in this study. The following CFD analysis of combustion is used to understand and predict the temperatures, velocities, species concentrations and other parameters in the boiler. Their detail results are given below.

5-4-1-1Temperatures distribution

The Iraqi Diesel fuel peak temperature predicted theoretically in the domain shown in figure (5-2) reached a value of 1986.007 K. It is approximately equal to that found experimentally by the manufacturer company of the boiler for a Heavy Diesel (gasoil) that reach 1990 K [31].This is an acceptable theoretical prediction for this study.

The shape of combustion temperature profile in the splitting section of the boiler as shown in figure (5-2) in the three axis coordinates (X, Y and Z).It demonstrates the shape of flame and the peak temperature location in the domain considered at the central section in the boiler combustion chamber.

Figure (5-3A) demonstrates the temperature distribution in the boiler at different side planes in the X-axis direction. They show clearly the effect of gravity on the shape of fuel burned plum in the combustion chamber. It shows a larger area of high temperatures at the lower part.

Figure (5-3B) ,in the X1 plane, showed a peak temperature in the domain of a value of (1986 K).It's clearly located at the center of the combustion chamber above and below the centerline in the middle of flame stream. It showed also the effect of gravity on flame shape and temperature distribution.

The X1 plane demonstrates that the nozzle had two streams the lower one is longer than the upper one due to the high density of the Iraqi diesel.

Figure (5-3C) , in the X3 plane, showed a uniform temperature distribution in the tubes .The peak temperature in this plane was 1600 K, and the temperature reduced continuously along the tubes due to the heat exchange between the walls of the tubes and the water surrounding it.

Figure (5-4A) demonstrates the temperature distribution in the horizontal (longitudinal) planes in Y direction for different levels in the boiler.

Figure (5-4B),in the Y1 plane, indicates the shape of the flame in the axial direction .The peak temperature in this plane is 1940 K. and the flame highest temperature region ends at about half of combustion chamber where the temperature start to reduce and reached to around 1200 K at the end of combustion chamber .

At the closed end of the combustion chamber, the hot gases turned back 180^{o} in the direction of the front plenum side (burner side). The product gases enter the front plenum where they enter the tubes at the burner side and exit the tubes into the rear plenum, and discharge to the outside through the chimney inlet port.

The Y1 plane also indicates that there is a continuation of combustion in the front plenum and also in about 20% of the tubes length too. The temperature showed a reduction in value to 1200 K due to water heating.

Figure (5-5A) demonstrates the shape of flame propagation and temperature distribution in sections along the combustion chamber, front and rear plenums along the Z-axis.

Figure (5-5B), in the Z1 plane, denotes the temperature distribution in the front plenum. The peak predicted temperature in this plane is 1760 K.

Figure (5-5C), in the Z8 plane, demonstrates the temperature distribution in the rear plenum. The peak temperature in this plane is 958 K as it reached the chimney inlet port.

5-4-1-2 Boiler gasdynamics

Figure (5-6A) indicates the velocity vectors and magnitude at the inlet air and fuel inlet. The peak velocity is 32.3 m/s. It is the fuel inlet velocity.

Figure (5-6B) indicates the velocity vectors and magnitude at the pressure outlet. The peak velocity at outlet is 14.4 m/s. It is the chimney inlet velocity.

Figure (5-7A) demonstrates the velocity vectors and magnitudes in the side planes in -x direction.

Figure (5-7B), in the X1 plane, demonstrates the peak velocity of fuel (34.2 m/s) in the boiler. This plane also denotes that the velocity vectors and magnitude reduced as it moves away from the burner until it comes near zero at the wall of combustion chamber. Due to the closed end of combustion chamber it trapped, and turned the gases around 180º toward the burner side. They take a path close to the combustion chamber wall while the inlet fuel and air take a path in the centerline of combustion chamber.

Figure (5-7C), in the X3 plane, demonstrates the velocity vectors and magnitudes in the tubes, inlet and outlet plenums. The velocity reduced in the front plenum due to it is expanded size and then the velocity increased rapidly as the product gases enter to the tubes due to the tubes entrance section area. The peak velocity in tubes is 30.2 m/s due to the tube entrance area contraction.

Figure (5-8A) demonstrates the velocity vectors and magnitude in the horizontal planes in Y direction.

Figure (5-8B), in the Y1 plane, (master plane) demonstrates that the peak velocity is close to the nozzle. This velocity reduced gradually as the fast-vaporized fuel mix with the slower incoming air. Far from the inlet after combustion, the trapped products reached the closed end of combustion chamber and the velocity become close to zero at the walls in the Z- direction.

As soon as the gases hit the closed end turned around 180^{o} and move toward the front plenum in opposite direction of inlet mixture producing a ring shaped path close to the wall of combustion chamber.

At the inlets side there were two big vortices on both sides appeared between the burner inlet and the wall of combustion chamber close to the front plenum inlet gases .The vortices produced were in the reverse direction to that of the returned gases causing to reverse the direction of the inlet fuel and the air that leave the combustion chamber and enter the front plenum due to combustion and trapped situation of product gases.

The Y1 plane also shows the velocity vectors at the front plenum and the tubes. It is clearly noted that the velocity reduced in the front plenum and then increased as it entered the tubes.

The plane Y1 also demonstrates that there were two vortices in the rear plenum appeared in the counterclockwise direction in the area between the tubes and the sidewall of plenum on both sides. The velocity of the product gases in rear plenum reduced again as it entered the large size of plenum.

Figure (5-8C) demonstrates the velocity contour in the Y1 plane. The velocity magnitude is clearly shown in this contour. The peak velocity is shown close to the nozzle and at the tubes inlets, and reduced near the walls and between opposite flow fluids.

Figure (5-9A) denote the velocity vectors distributions along the axial direction in the Z-axis, in the major sections of the boiler.

Figure (5-9B), in the Z1 plane, demonstrates the velocity vectors and magnitudes in the front plenum. The peak velocity in this plane is 7.3 m/s.

Figure (5-9C), in the Z3 plane, clarify the velocity vectors at about the half-length of the combustion chamber. It has clearly shown that the flame vectors in the middle of combustion chamber in the Z direction while the

returned gases appear close to the wall of combustion chamber in opposite direction to the incoming mixture (in Z- axis).

Figure (5-9D), in the Z8 plane, demonstrates the velocity vectors and magnitude in the rear plenum, it has clearly shown that there are many eddies in this plane due to the distribution of tubes in the geometry. The difference in the gases velocities magnitudes and directions of the incoming products in the tubes are clearly shown. The peak velocity in this plane was 7.52 m/s.

5-4-1-3 Species in the combustion products

Figure (5-10A) demonstrates the contour of CO_2 mass fraction in the Y1 plane. It is clearly shown that the mass fraction of CO_2 is very small in the flame path stream at centerline and then increased with proceeding of combustion process until it reached a maximum value at the outlet. The peak value of CO_2 in this plane is 0.2 while the peak value at the outlet is 0.208.

Figure (5-10B) demonstrates the mass fraction of CO_2 in the X3 plane .This plane indicates the increase of CO_2 in tubes because of continued combustion process and oxidation continuous in this section.

Figure (5-11A) denote the mass fraction of CO in the Y1 plane. It has clearly shown that the peak value of CO mass fraction in the flame path stream at centerline .Where rich mixture appears and decreased gradually with proceeding of combustion at lean mixture. It gets the minimum value at the outlet where, the most oxidation occurs. The peak value of CO mass fraction in this plane is 0.31.

Figure (5-11B) clarify the mass fraction of CO in the X3 plane .This plane indicates the decreasing of CO mass fraction because of continued combustion in tubes. The peak value of mass fraction in tubes is 0.0496.

Figure (5-12) clarify the mass fraction of Iraqi Diesel in the X3 plane .It's clearly shown that there is an unburnt mass of fuel in the front plenum and the combustion continued in front plenum and also in tubes. This does not mean a complete combustion as the fuel decomposed to C, H and S. They remain in the products gases and continue oxidation as a reduction of CO and an increase in CO_2 appeared.

5-4-1-4 Pressure

It has clearly shown that the boiler is working on constant pressure combustion.

Figure (5-13A) demonstrates the pressure variation in the Y1 plane. The peak increase in pressure in this plane is 342 Pa.

Figure (5-13B) demonstrates the pressure variation in the X3 plane in tubes. The peak increase in this plane is 168 Pa. This reduction in pressure was due to increased combustion products velocity.

5-4-1-5 Turbulent kinetic energy

Figure (5-14A) demonstrates the turbulent kinetic energy variation in the Y1 plane. The peak value of turbulent kinetic energy in this plane is 93.5 m^2/s^2.

Figure (5-14B) clarify the turbulent kinetic energy in X3 plane in tubes. The peak value (110 m^2/s^2) is at the tubes inlets. This indicates that the maximum velocity was in that region.

5-4-1-6 Radiation

Figure (5-15A) demonstrates the rate of incident radiation in the Y1 plane. The peak value of incident radiation in this plane is 2.03×10^5 w/m^2.

Figure (5-15B) denotes the rate of incident radiation in X3 plane in tubes. The peak value of incident radiation in this plane is 1.7×10^5 w/m^2.

5-4-1-7 Summary

The simulation was succeed and all the prediction parameters given by the ANSYS FLUENT 6.3.26 are acceptable for the following reasons:-

1. The ANSYS FLUENT prediction temperature is 930.746 K for the exhaust gases at the outlet of the boiler. This coincides with that measured experimentally by using the thermocouple that had a value of (930 K) at the outlet.
2. The ANSYS FLUENT give a prediction of the mass fraction of CO_2 (0.2070814) at the outlet. This value coincides with that measured experimentally (0.207) by using the gas analyzer.

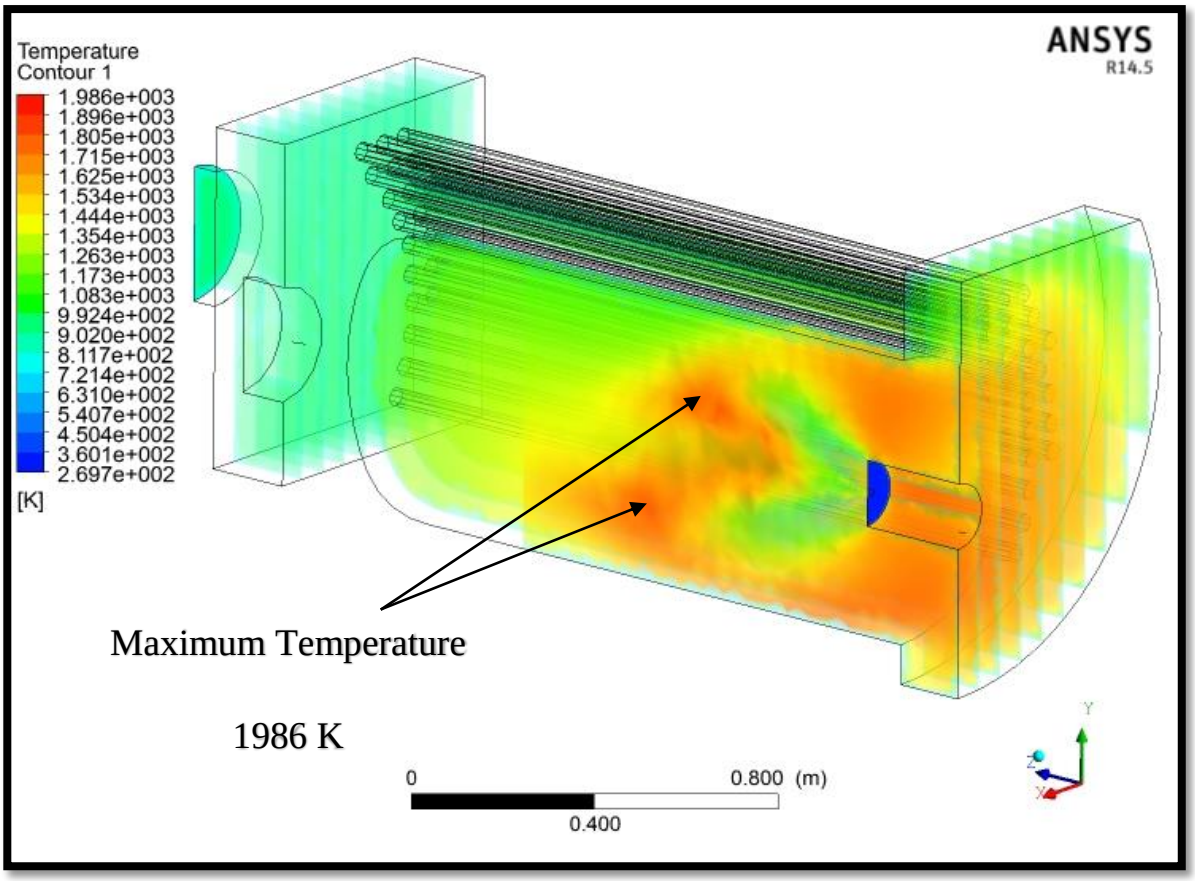

Figure (5-2) Temperature distribution of Iraqi Diesel at the whole domain.

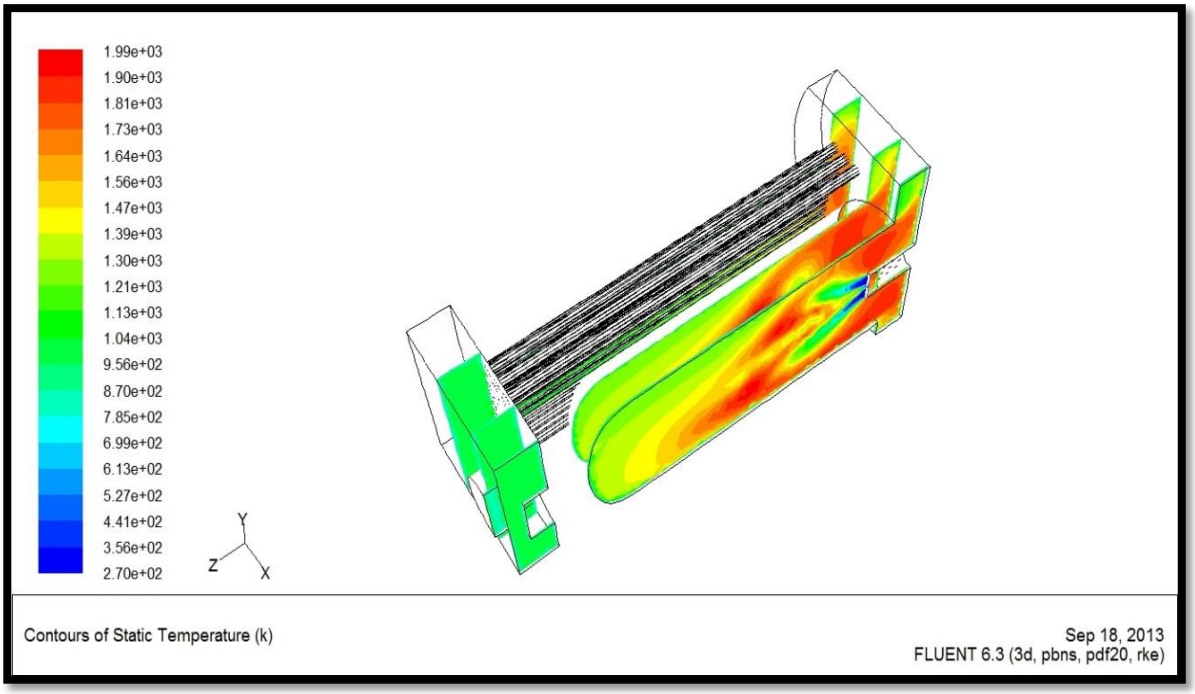

Figure (5-3A) Contours of Temperature in X planes.

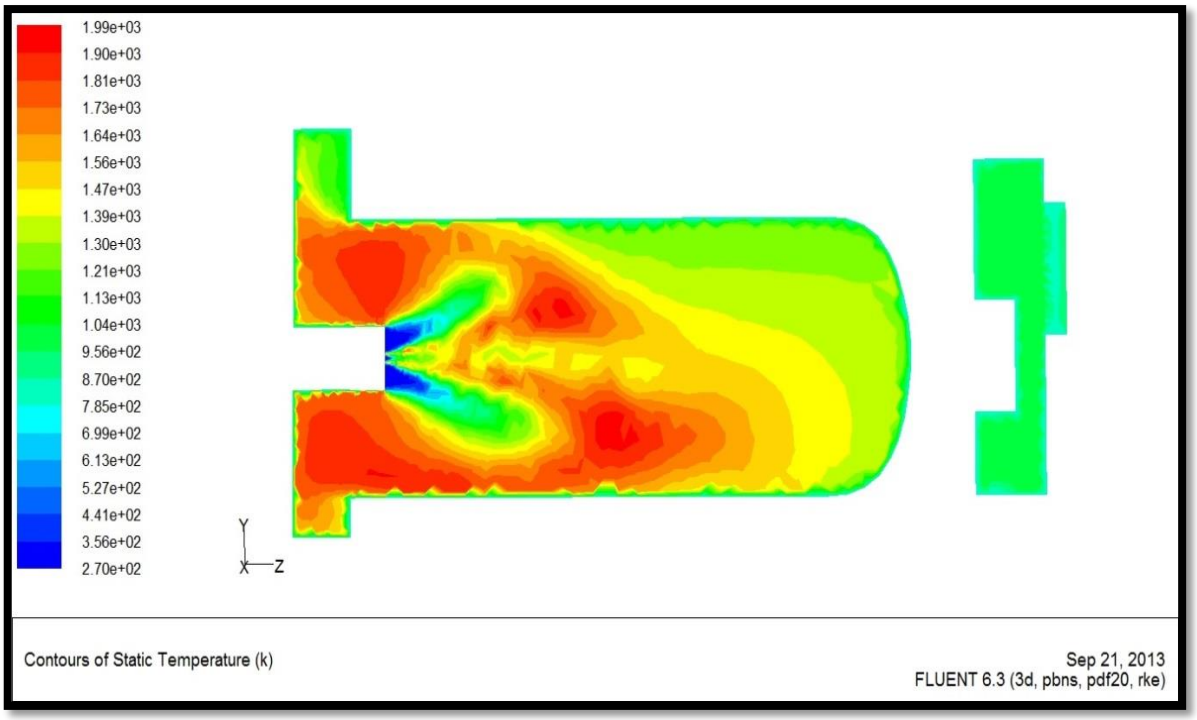

Figure (5-3B) Contours of Temperature in X1 plane.

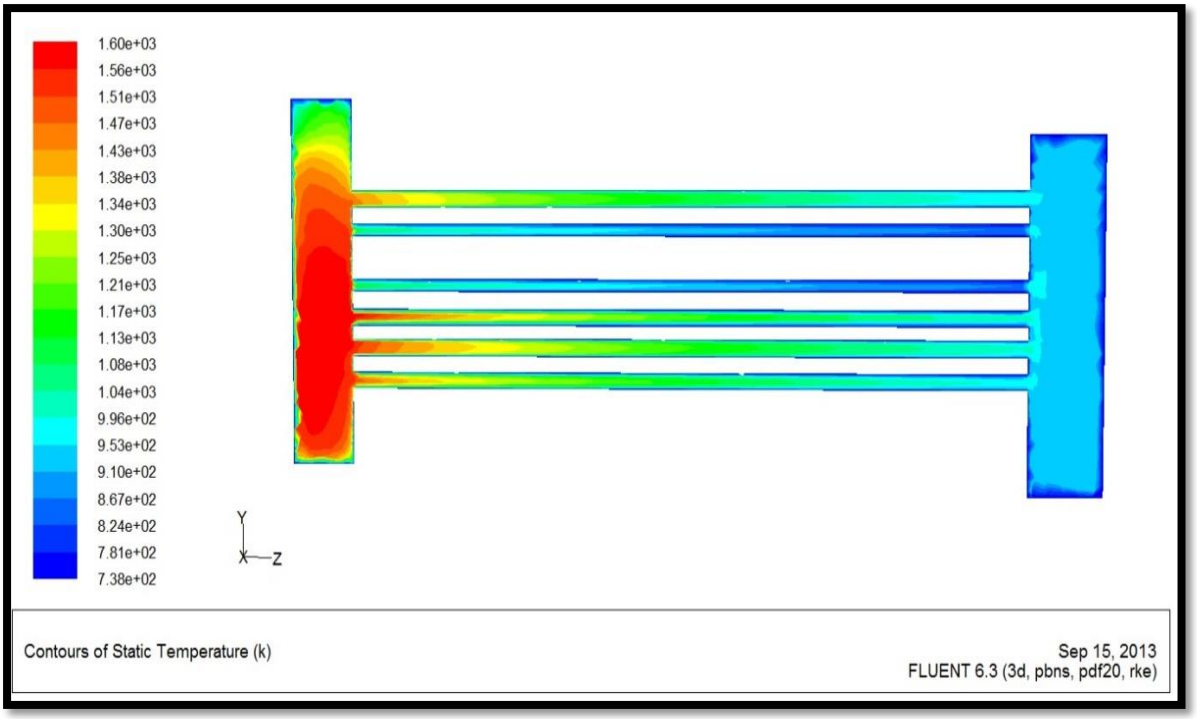

Figure (5-3C) Contours of Temperature in X3 plane.

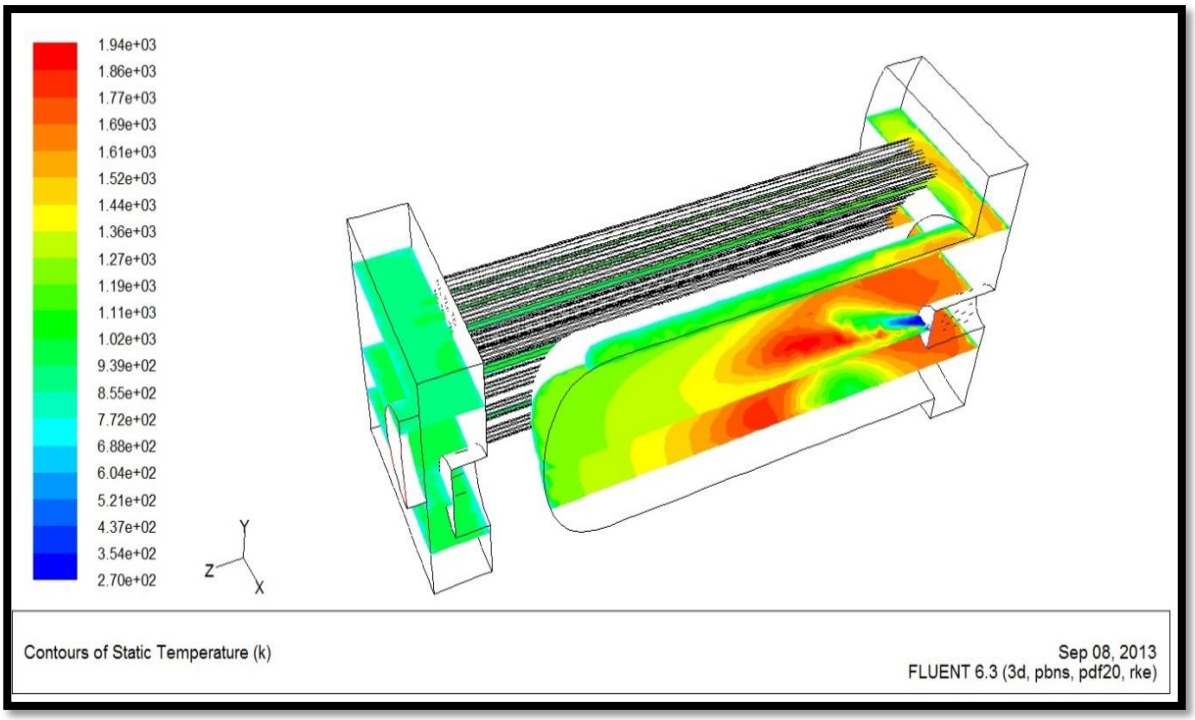

Figure (5-4A) Contours of Temperature in Y planes.

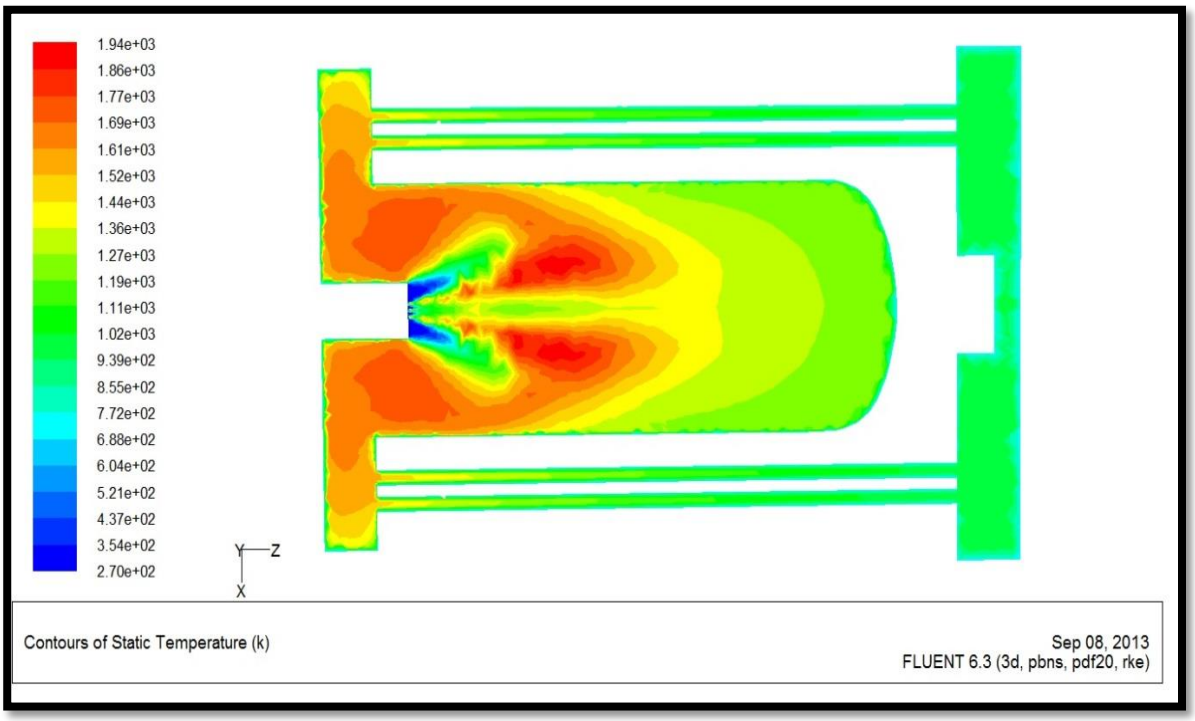

Figure (5-4B) Contours of Temperature in Y1 plane.

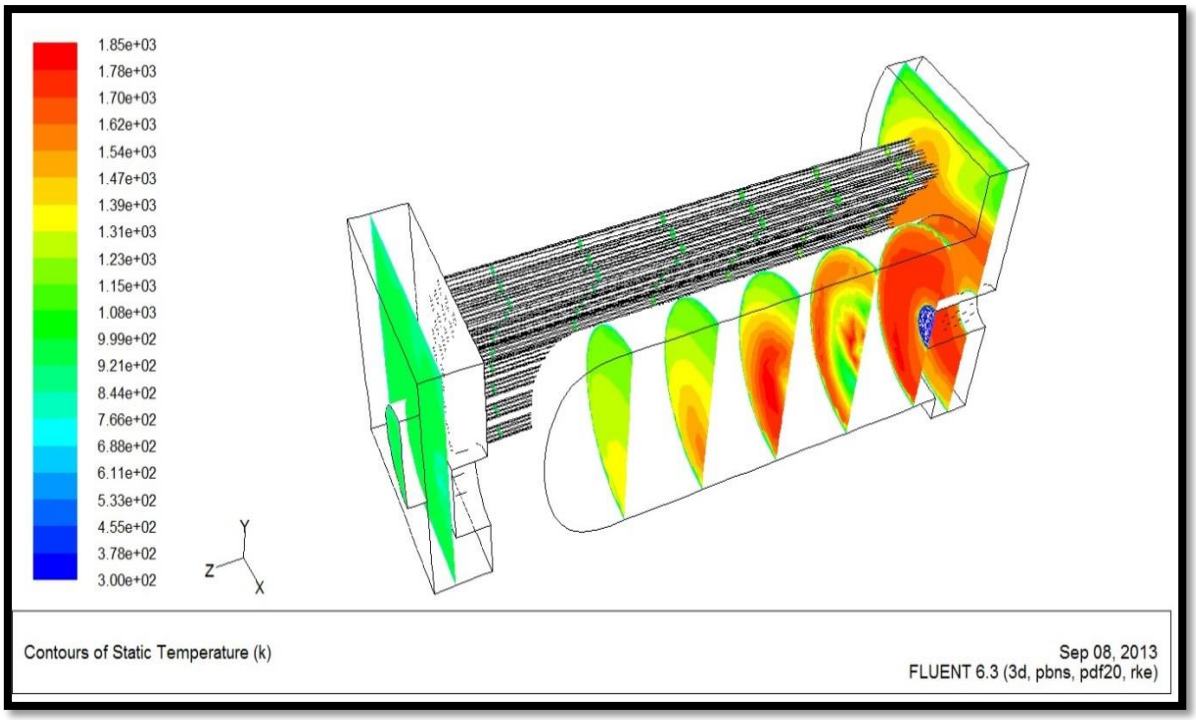

Figure (5-5A) Contours of Temperature in Z planes.

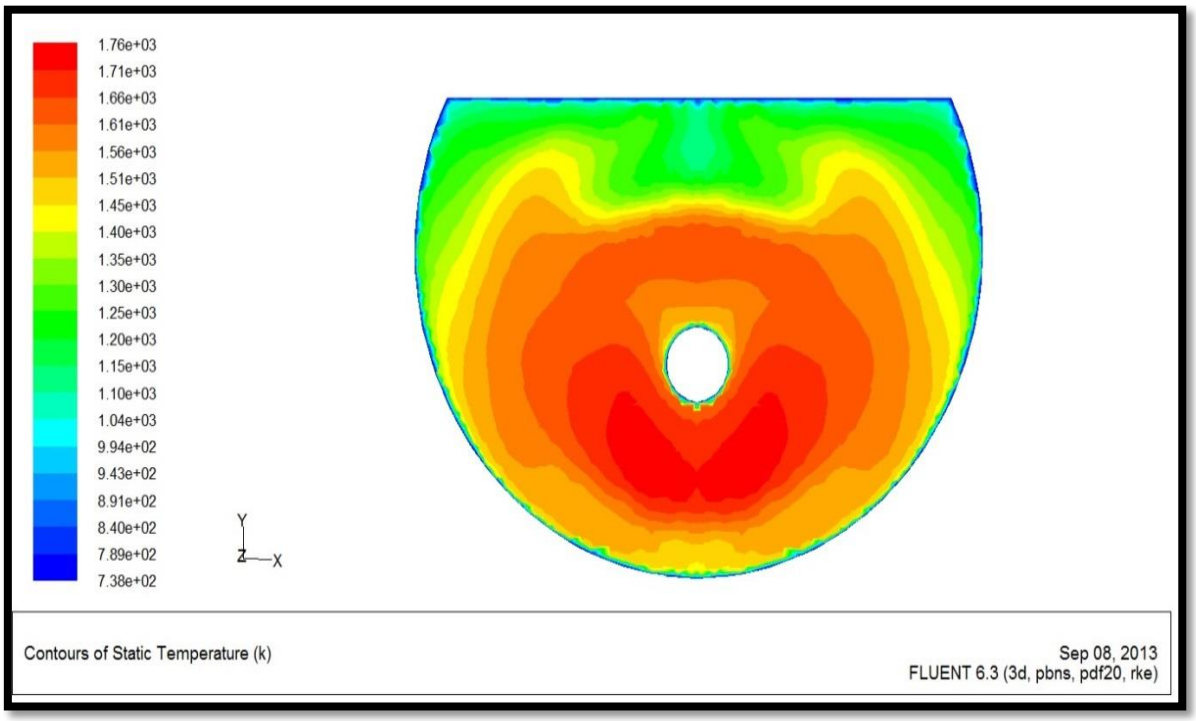

Figure (5-5B) Contours of Temperature in Z1 plane.

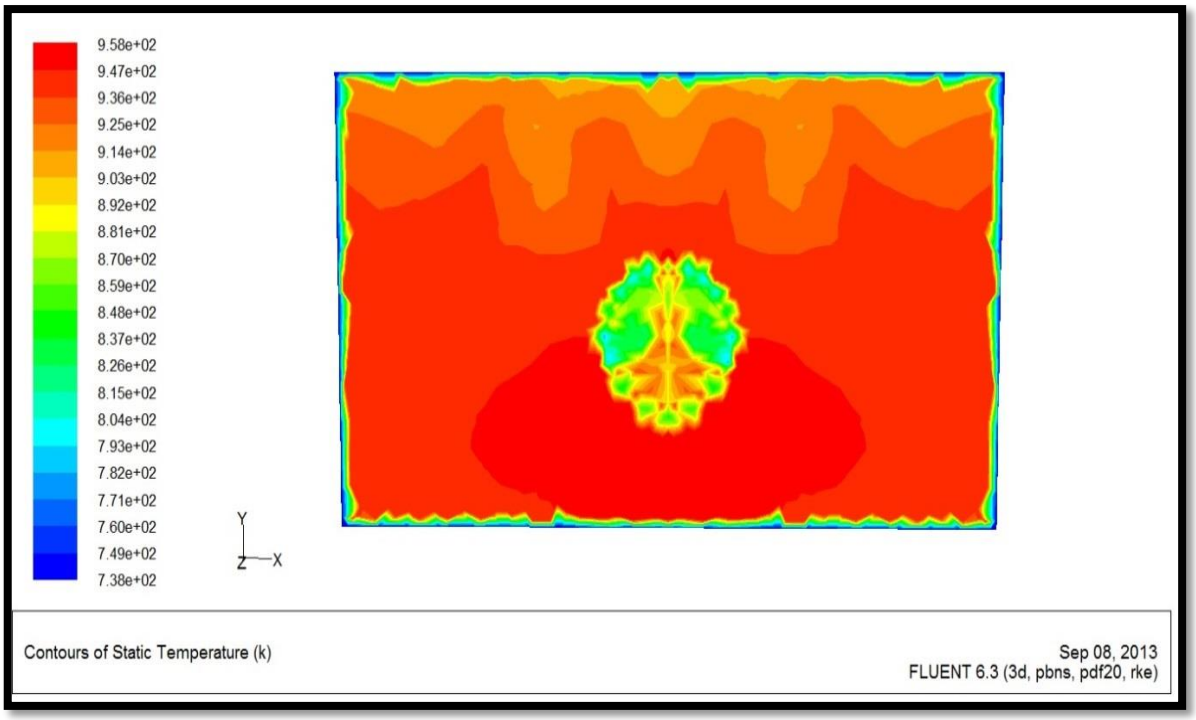

Figure (5-5C) Contours of temperature in Z8 plane.

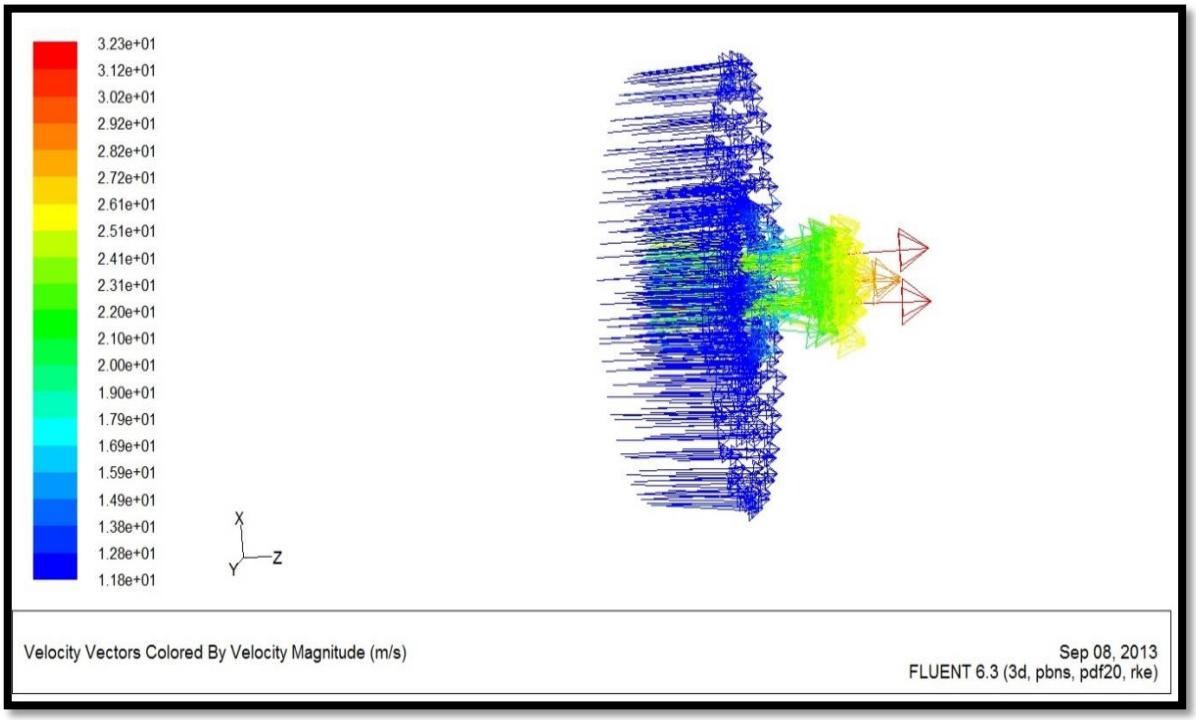

Figure (5-6A) Velocity vectors at inlet.

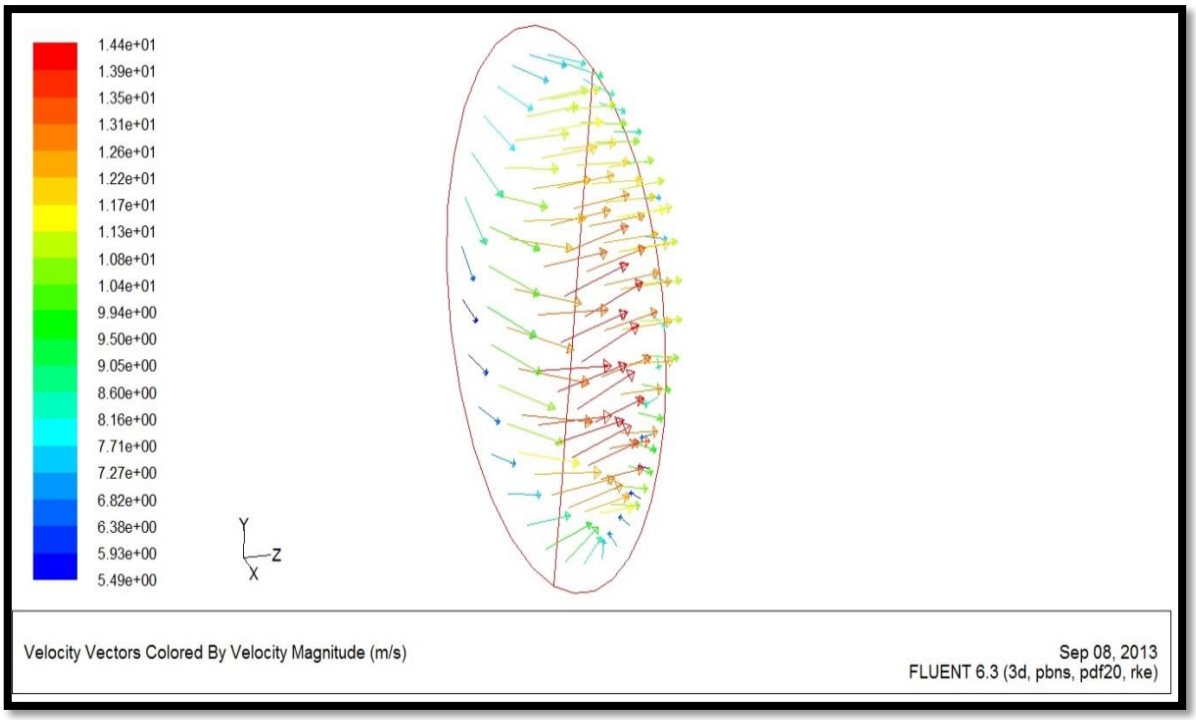

Figure (5-6B) Velocity vectors at outlet.

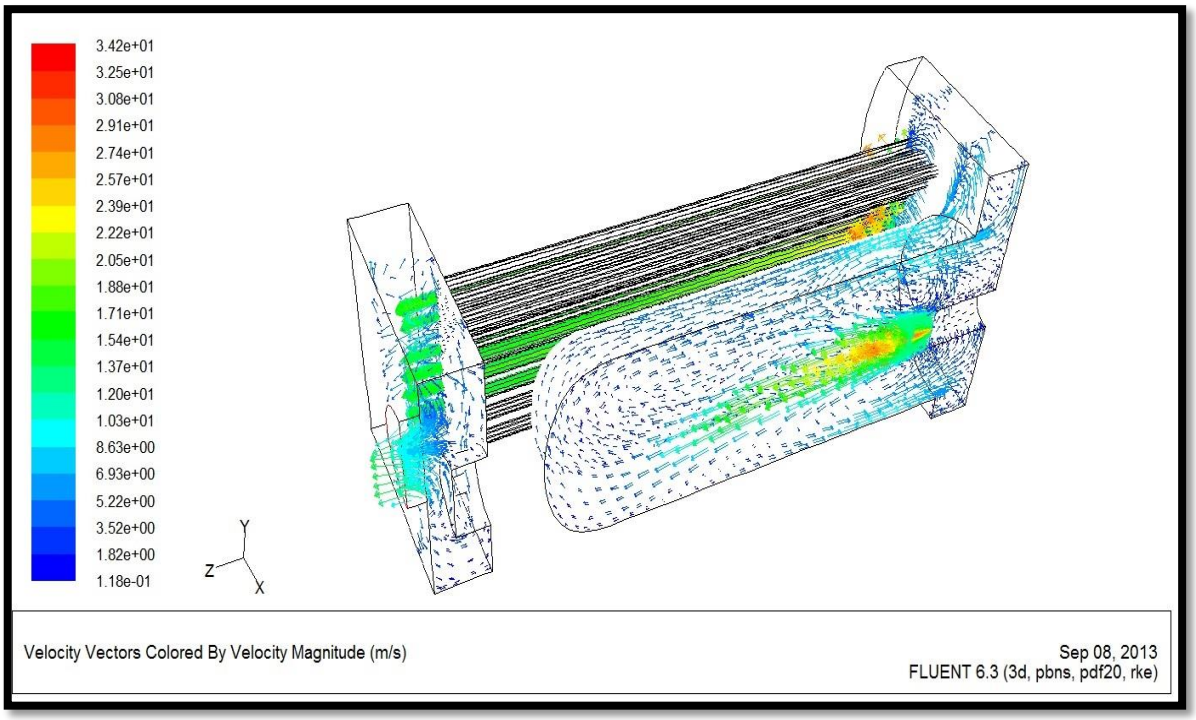

Figure (5-7A) Velocity vectors in X planes.

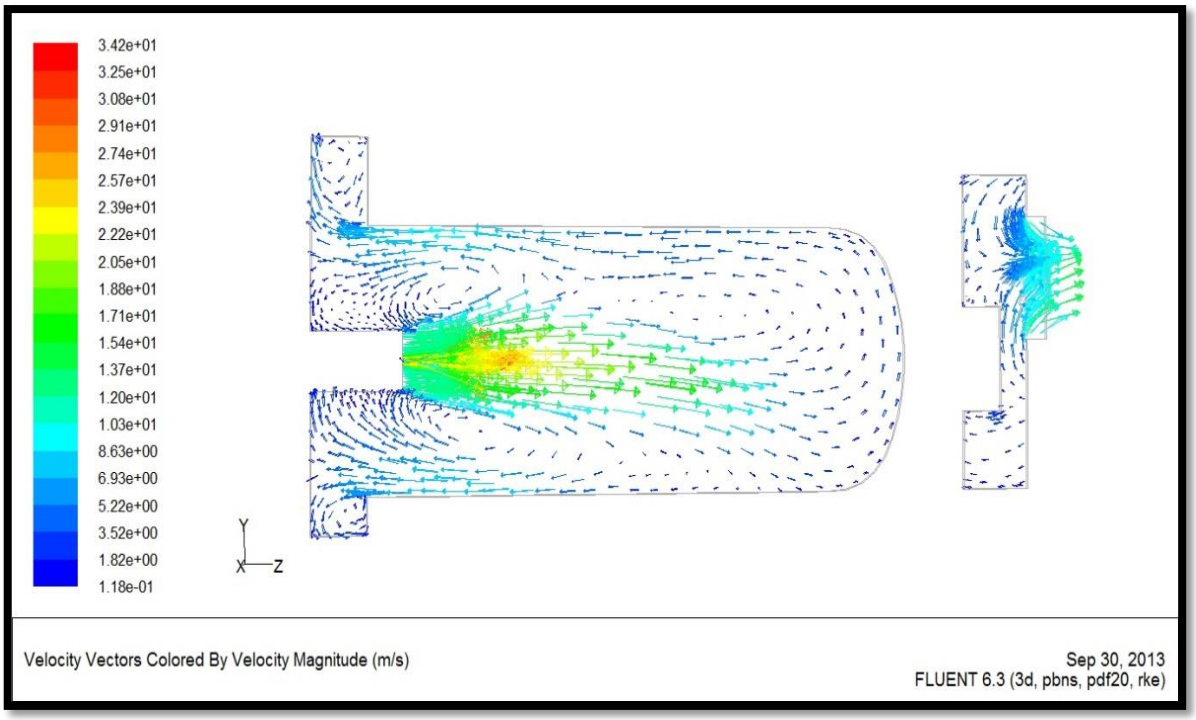

Figure (5-7B) Velocity vectors in X1 plane.

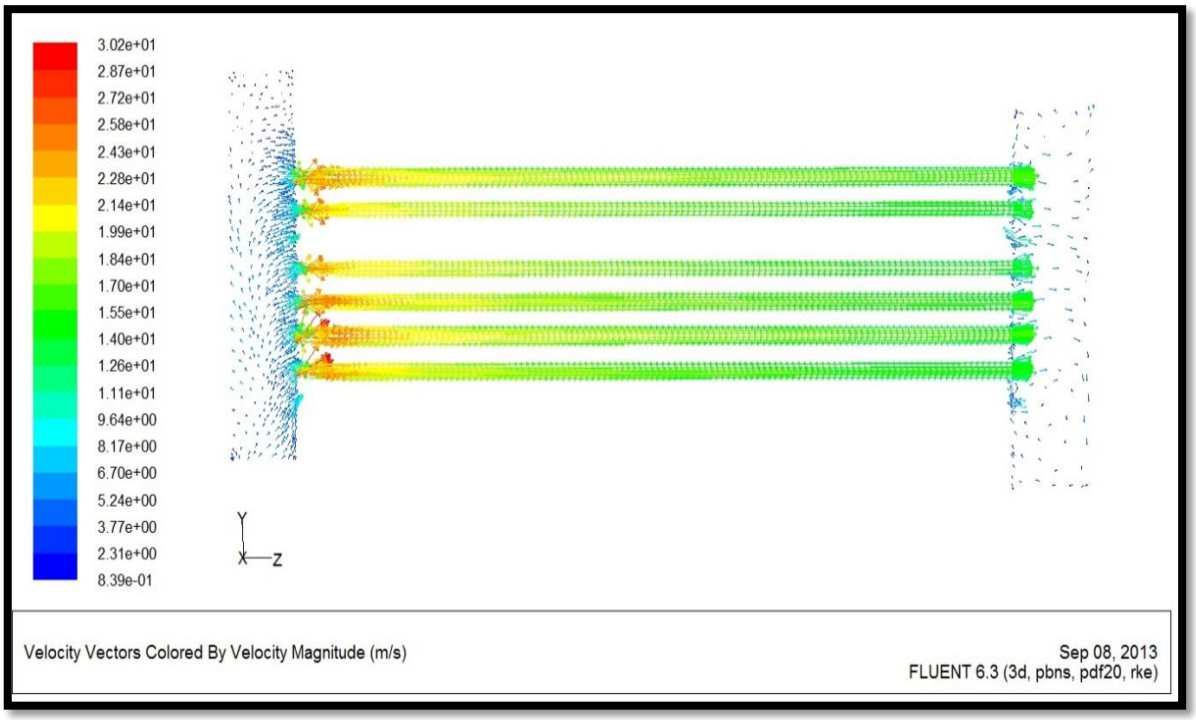

Figure (5-7C) Velocity vectors in X3 plane.

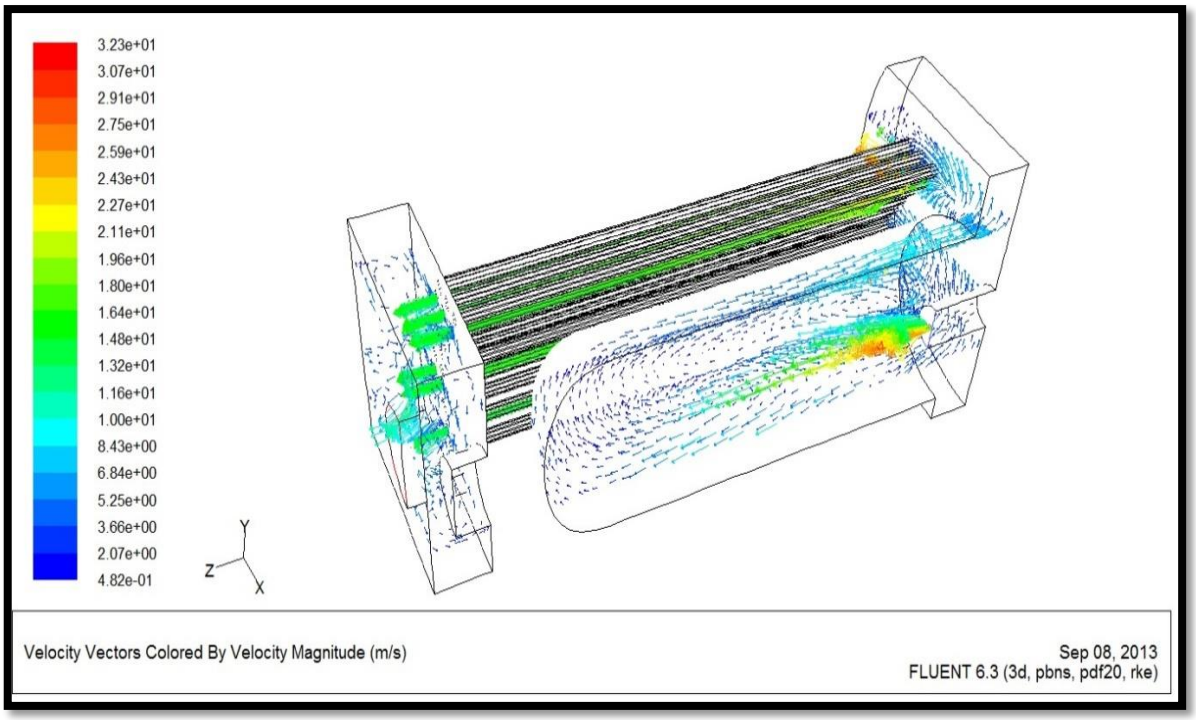

Figure (5-8A) Velocity vectors in Y planes.

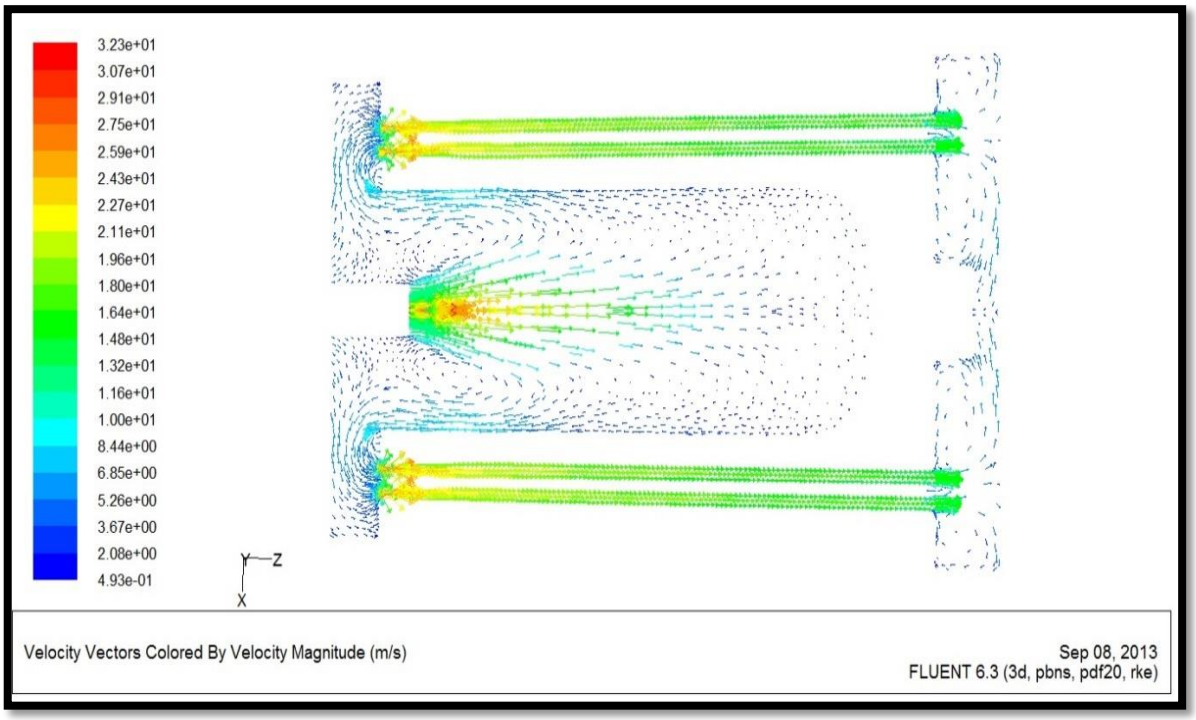

Figure (5-8B) Velocity vectors in Y1 plane.

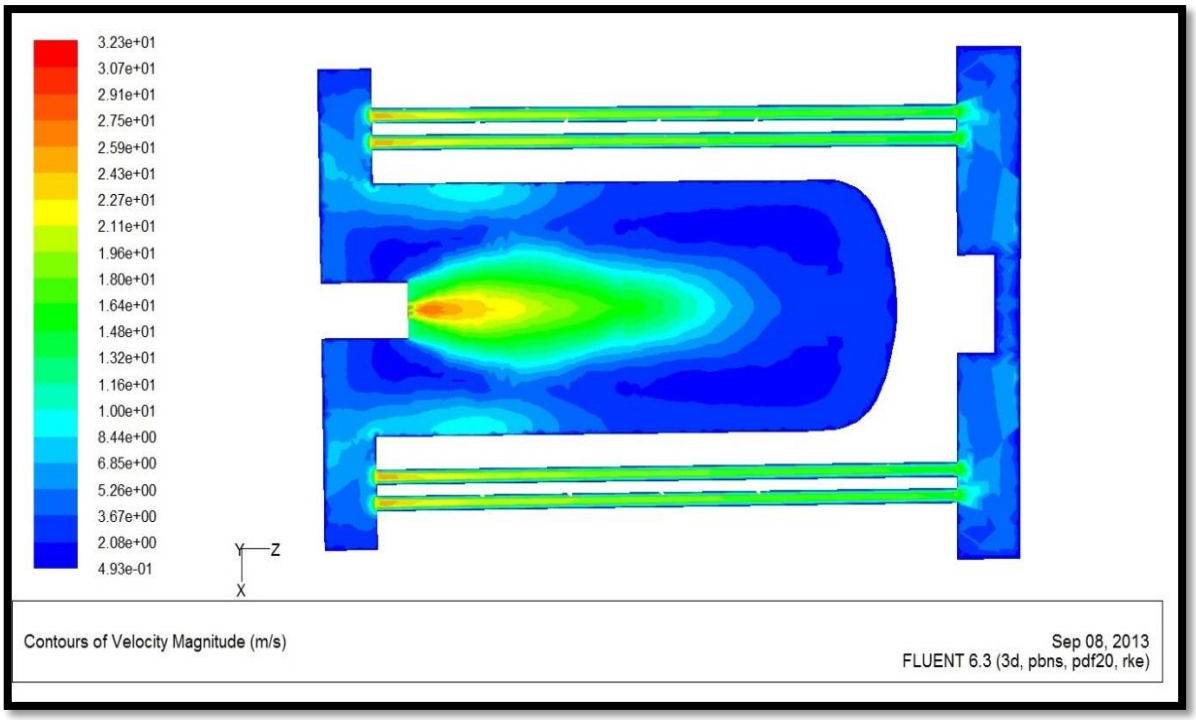

Figure (5-8C) Contours of Velocity Magnitude in Y1 plane.

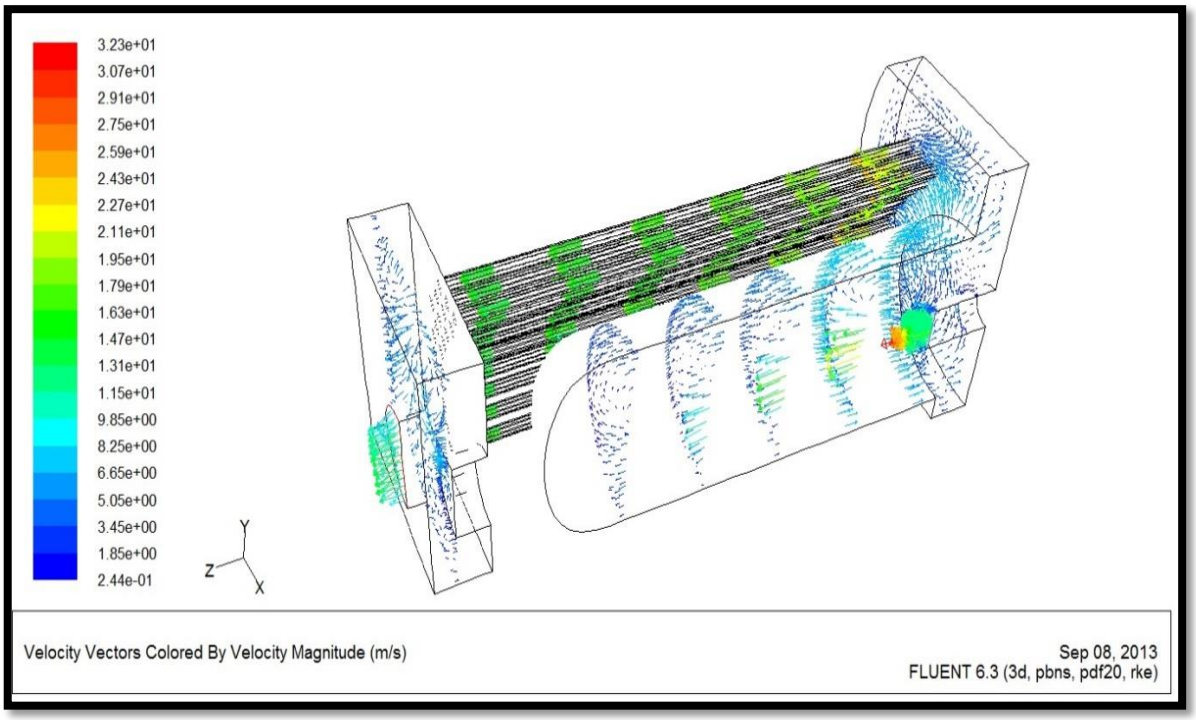

Figure (5-9A) Velocity vectors in Z planes.

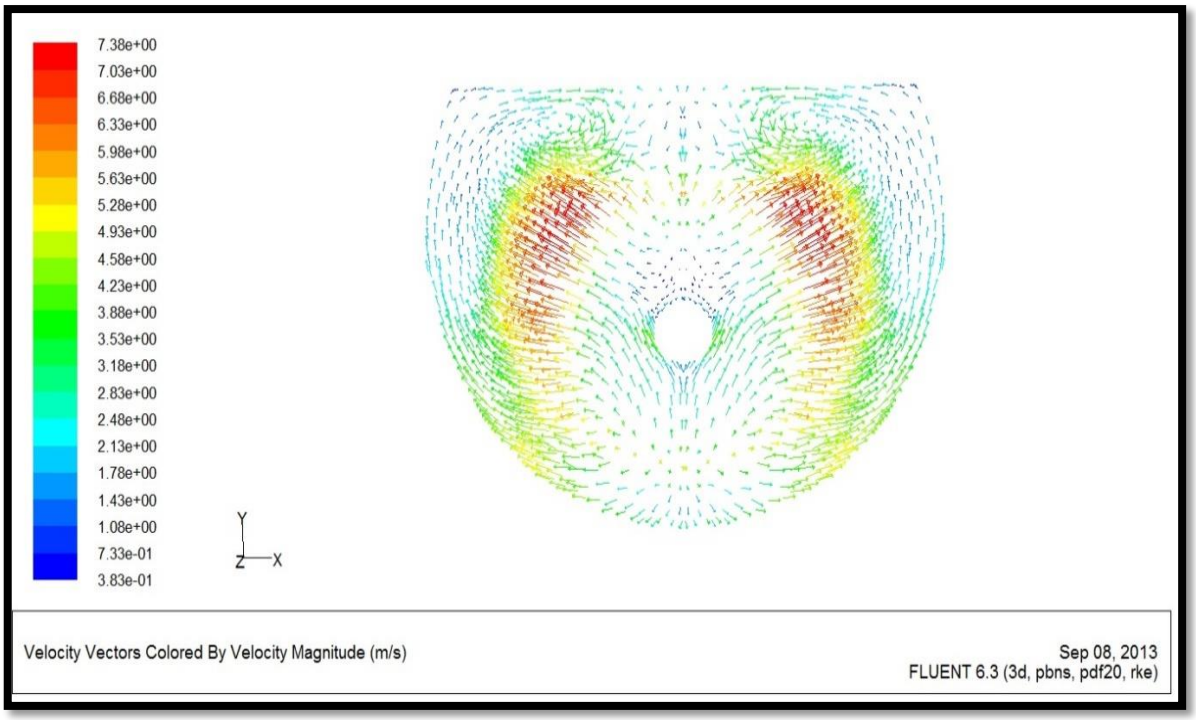

Figure (5-9B) Velocity vectors in Z1 plane.

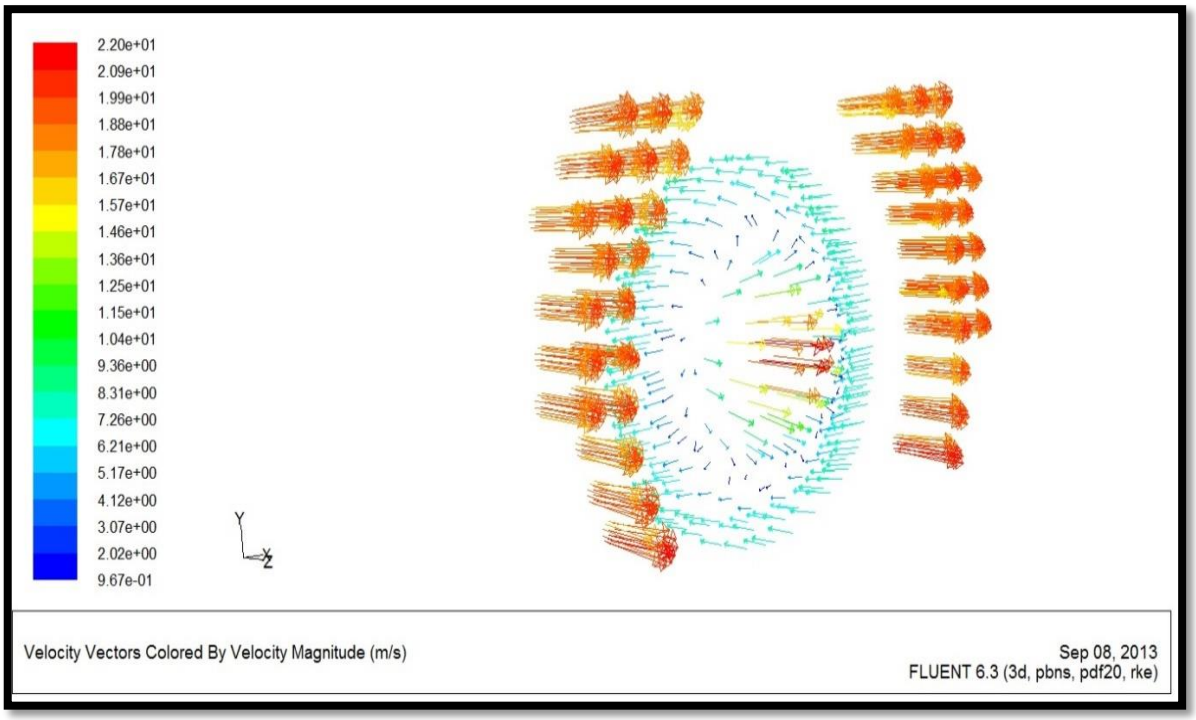

Figure (5-9C) Velocity vectors in Z3 plane.

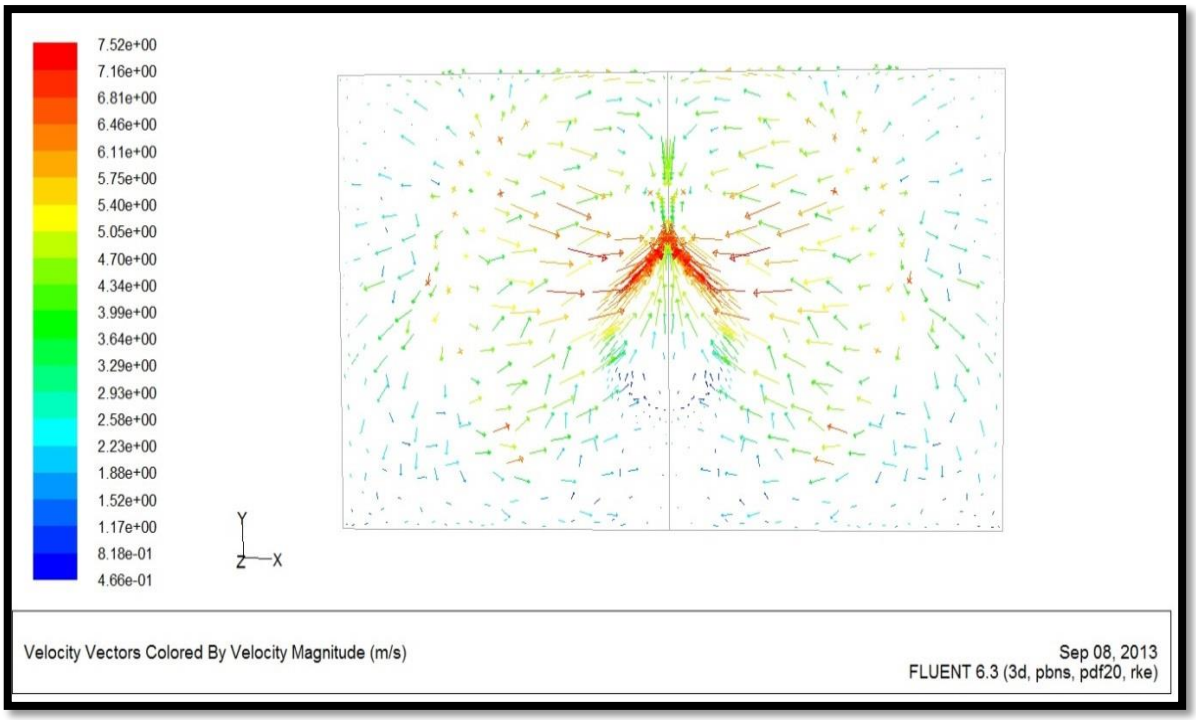

Figure (5-9D) Velocity vectors in Z8 plane.

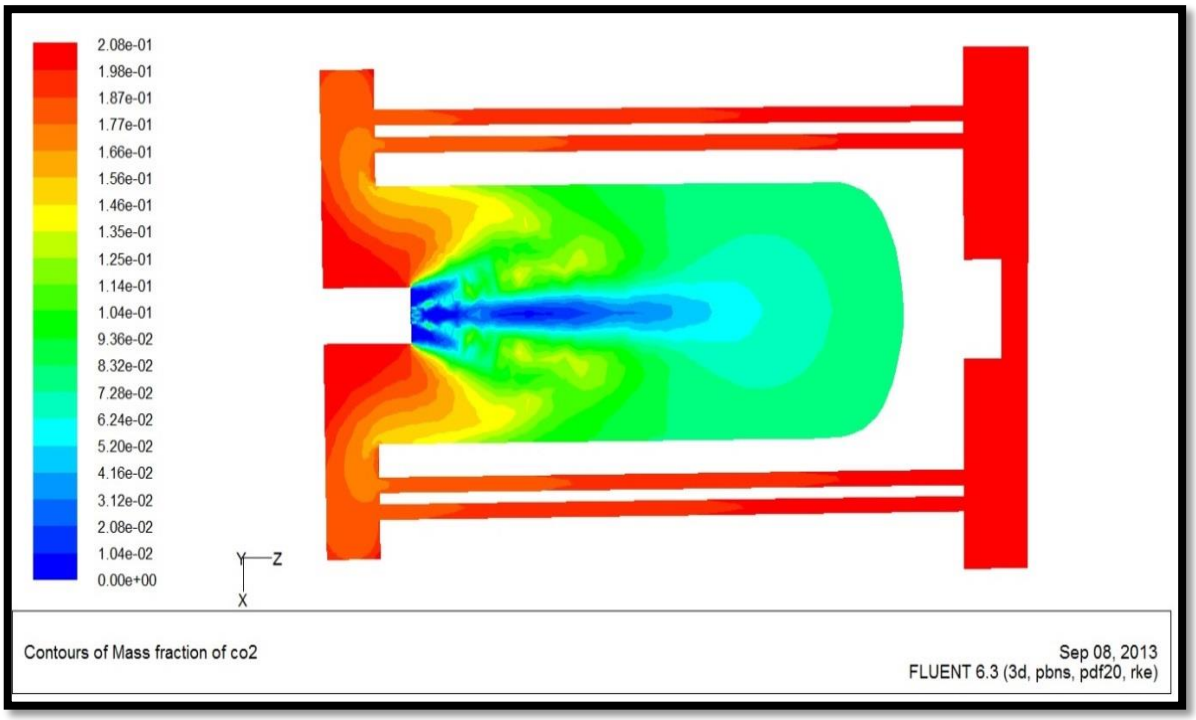

Figure (5-10A) Contours of mass fraction of CO_2 in Y1 plane.

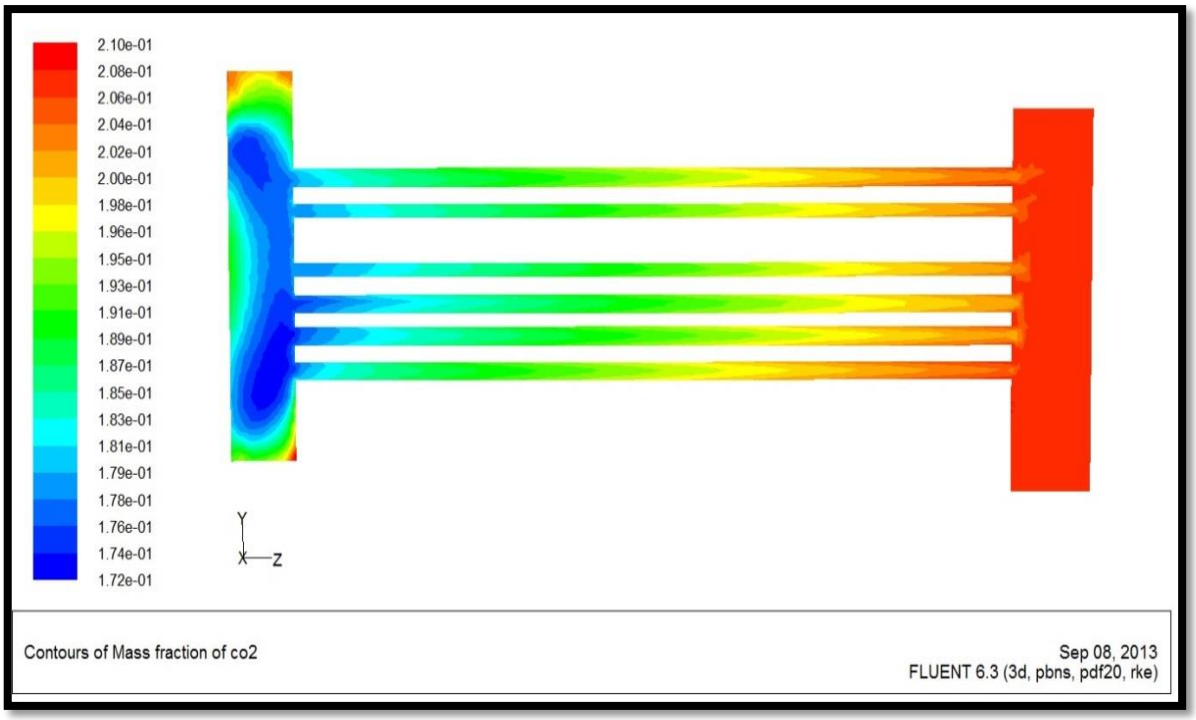

Figure (5-10B) Contours of mass fraction of CO_2 in X3 plane.

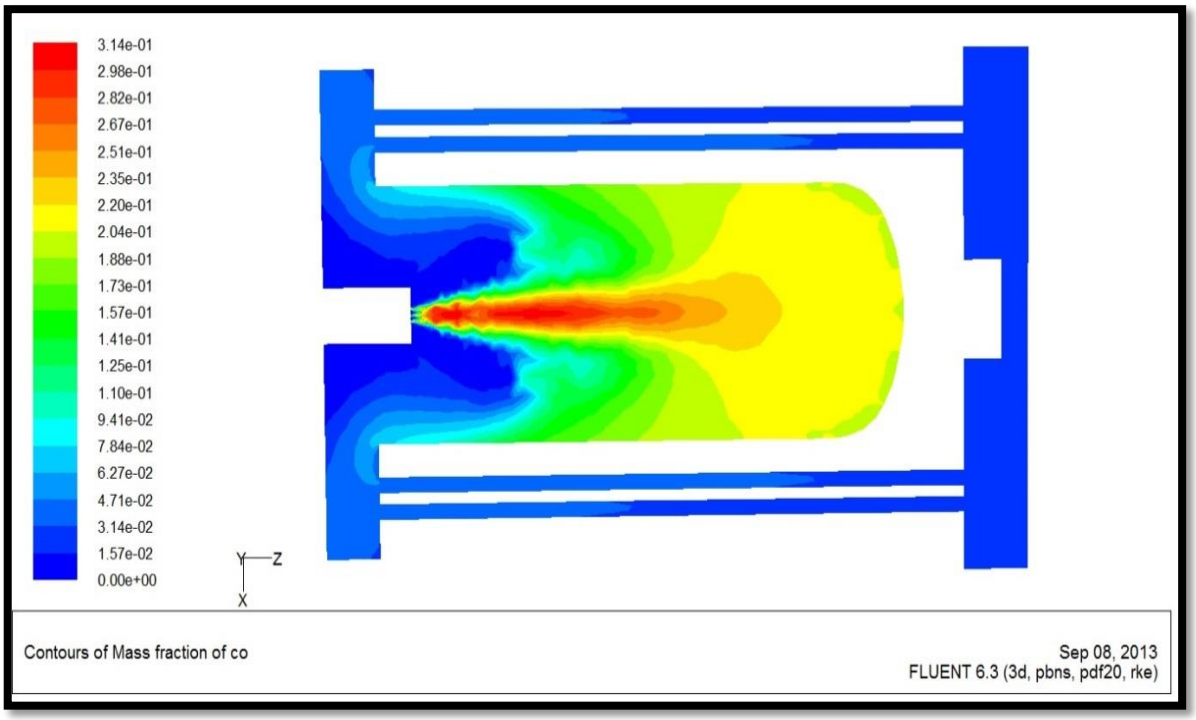

Figure (5-11A) Contours of mass fraction of CO in Y1 plane.

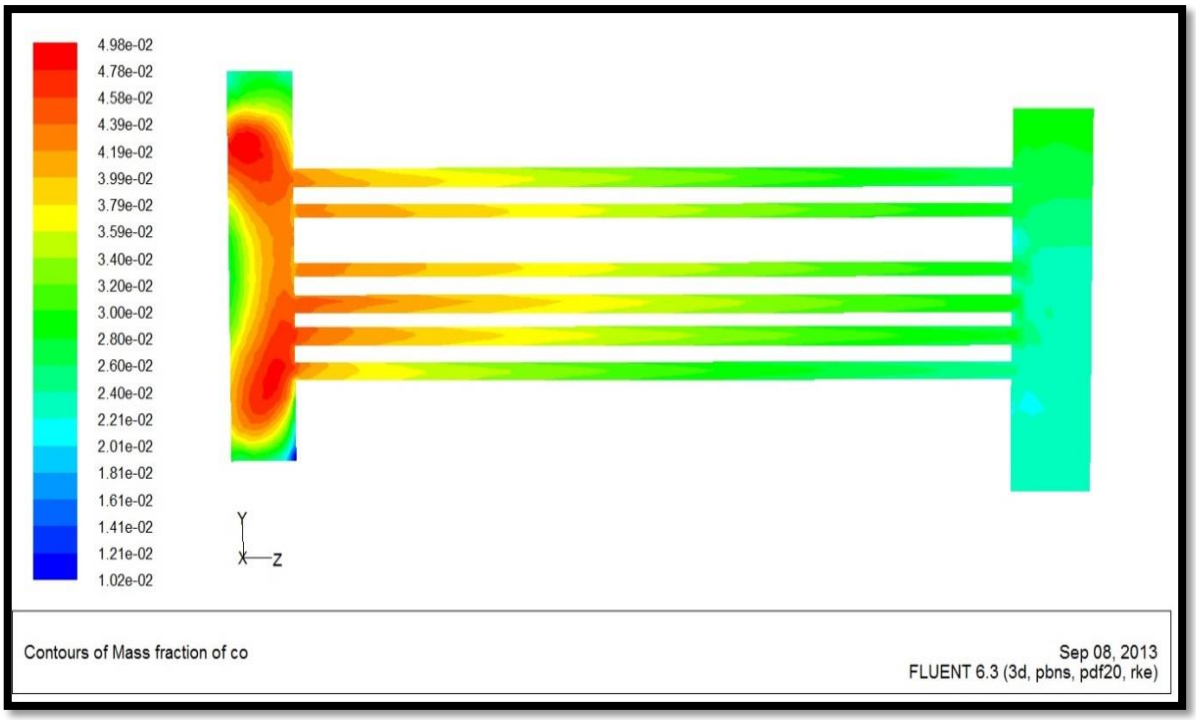

Figure (5-11B) Contours of mass fraction of CO in X3 plane.

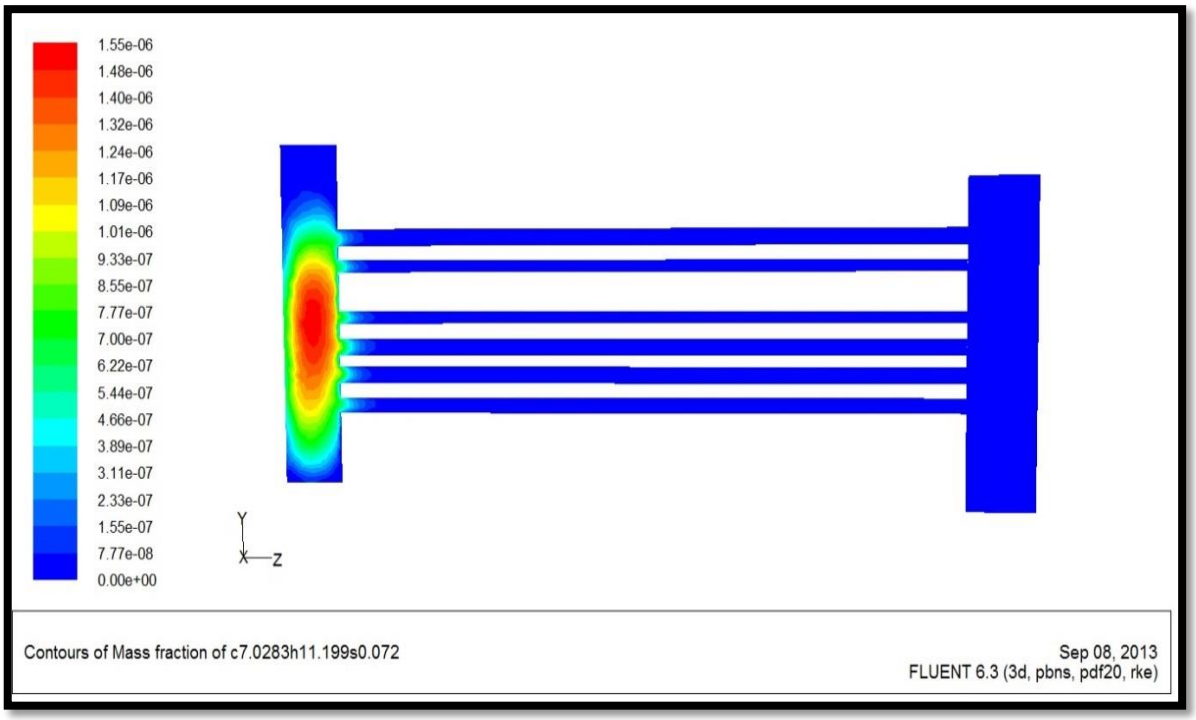

Figure (5-12) Contours of Mass fraction of Iraqi Diesel fuel in X3 plane.

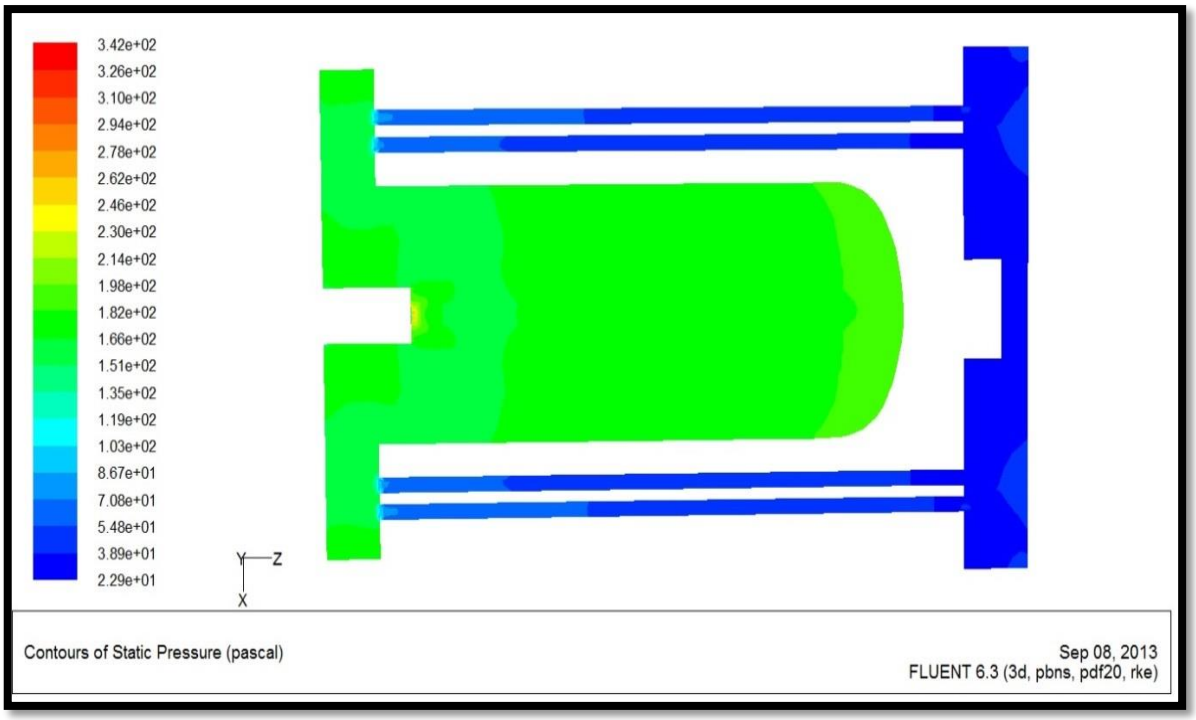

Figure (5-13A) Contours of Pressure in Y1 plane.

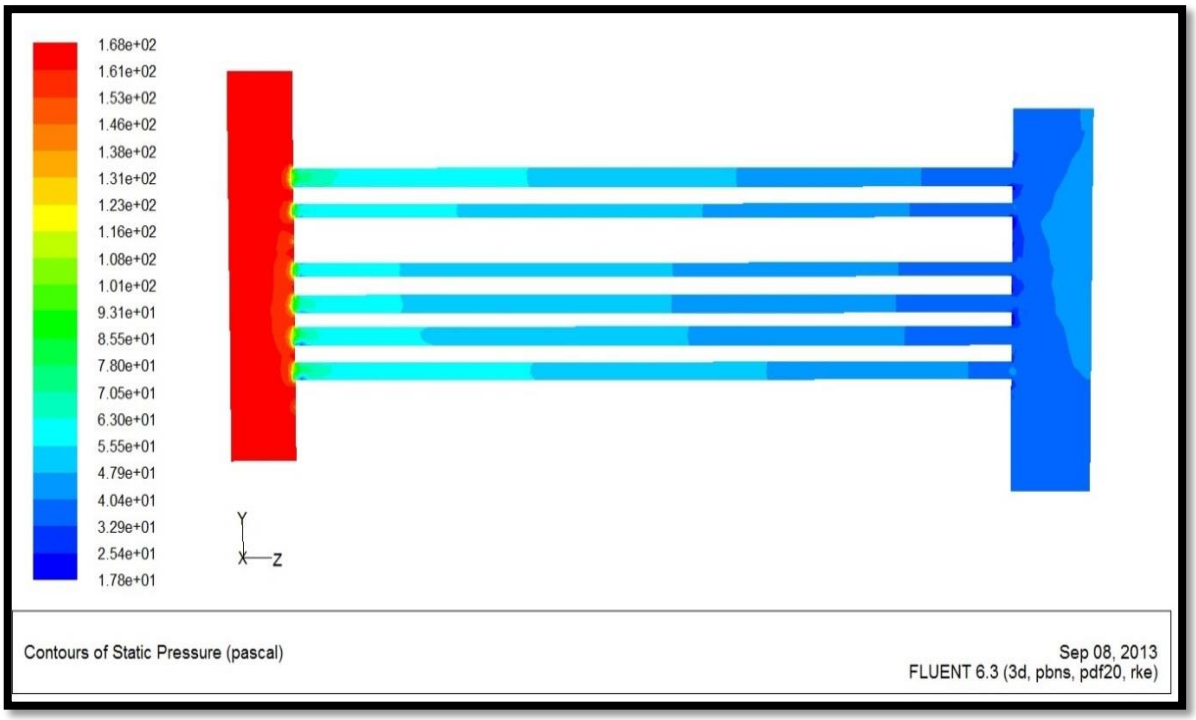

Figure (5-13B) Contours of Pressure in X3 plane.

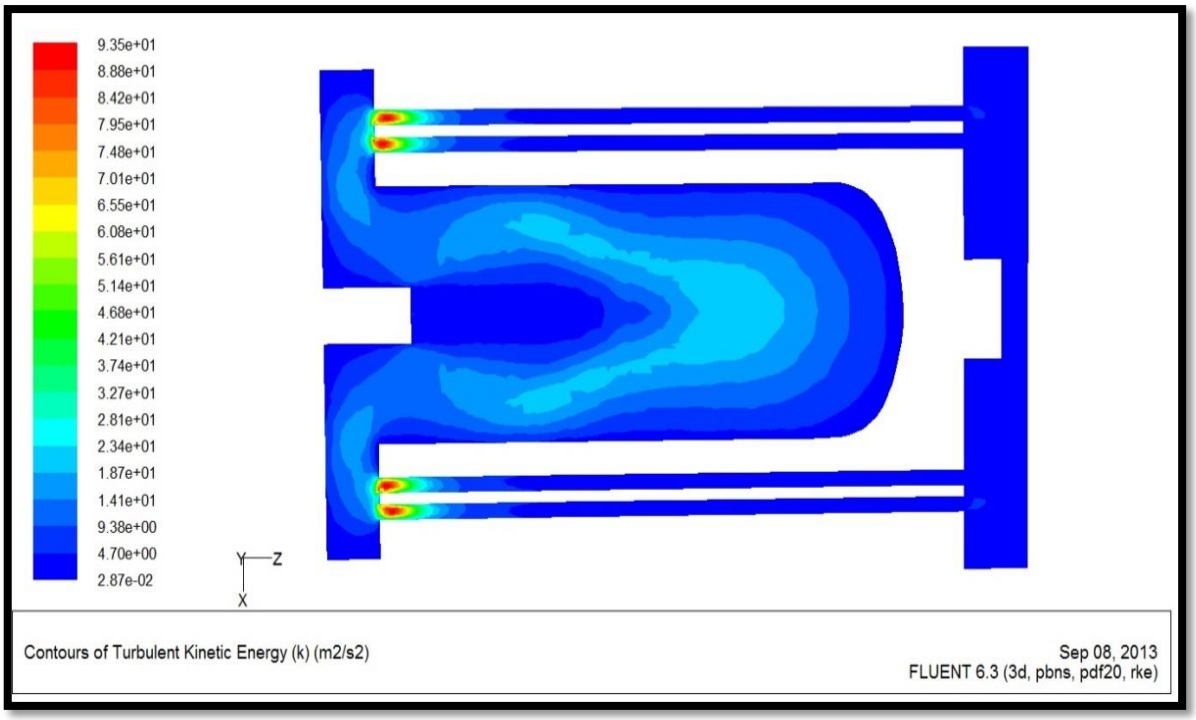

Figure (5-14A) Contours of Turbulence Kinetic Energy in Y1 plane.

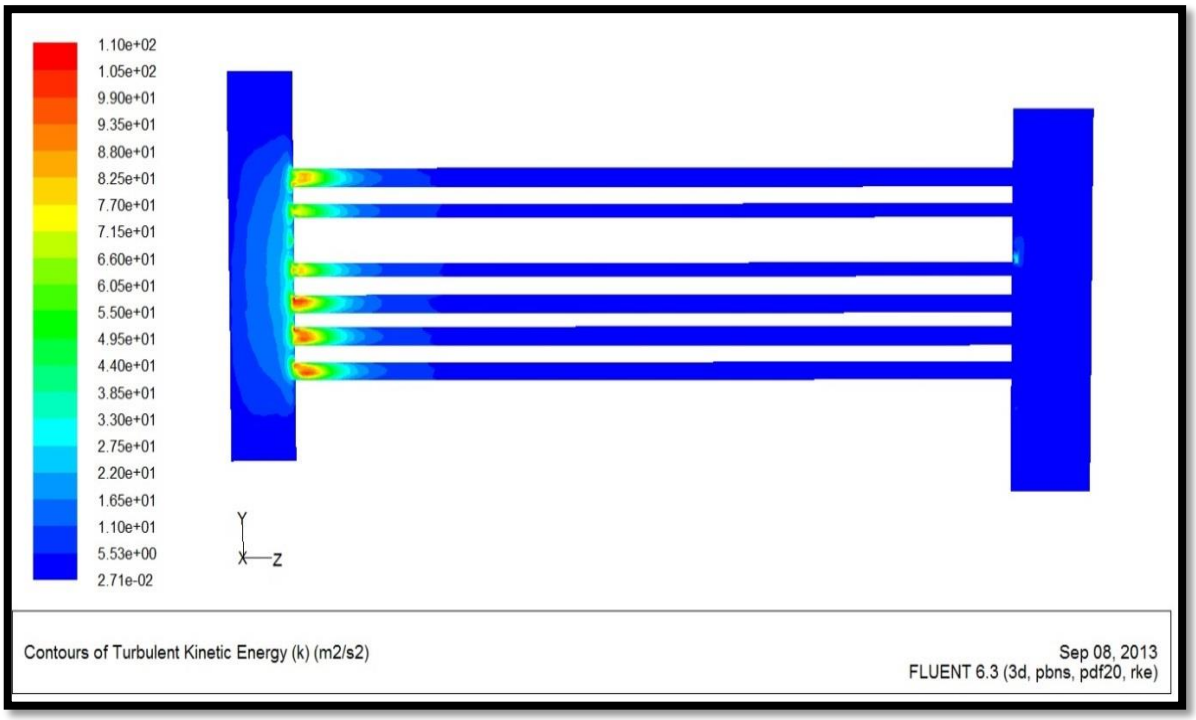

Figure (5-14B) Contours of Turbulence Kinetic Energy in X3 plane.

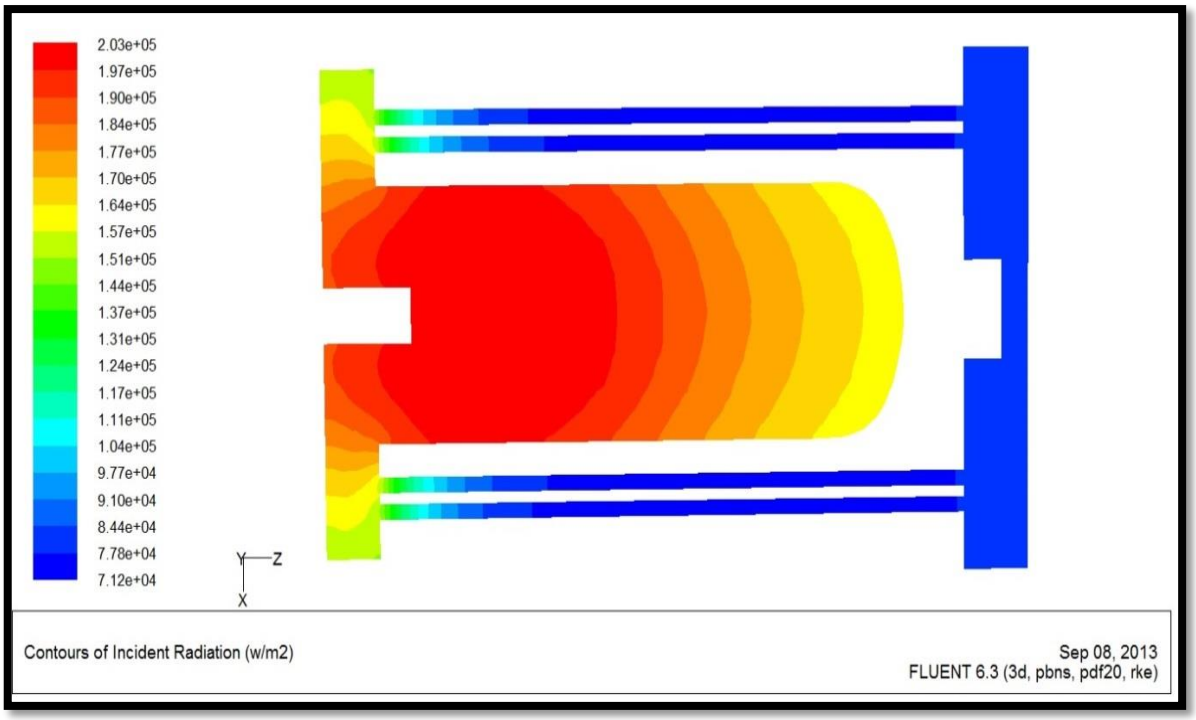

Figure (5-15A) Contours of Incident Radiation in Y1 plane.

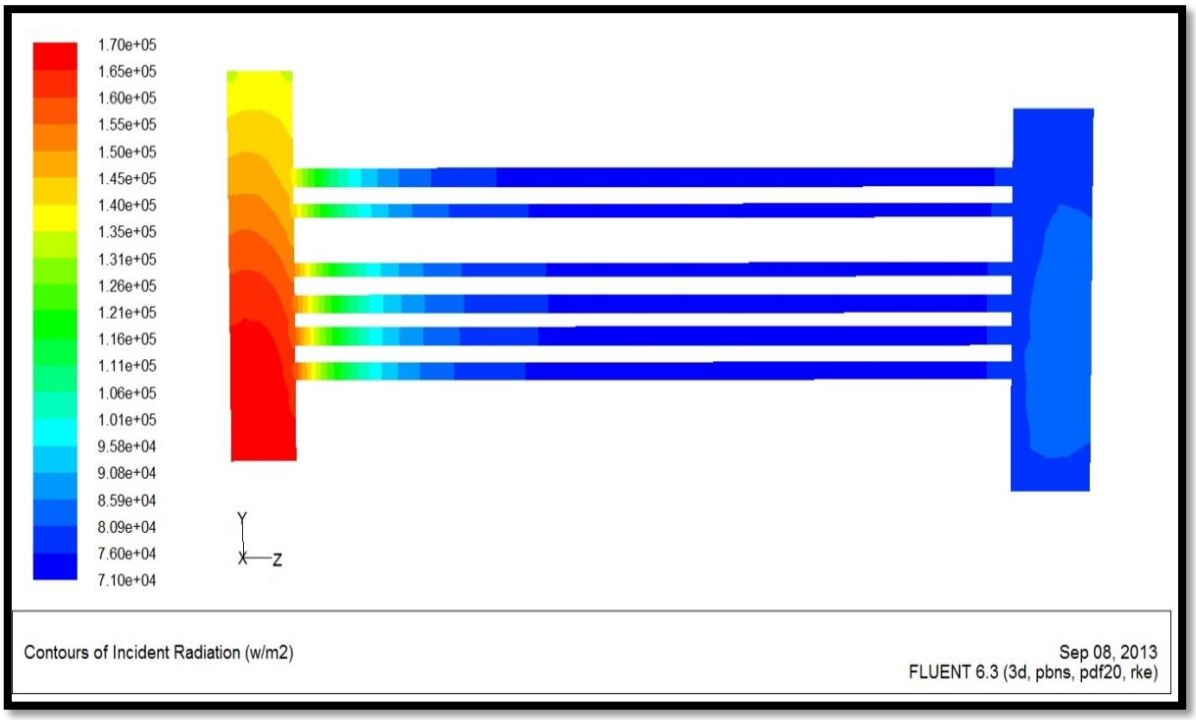

Figure (5-15B) Contours of Incident Radiation in X3 plane.

5-4-2 Light Diesel fuel

The manufacturer company of the boiler had tested the boiler on Light Diesel ($C_{10}H_{20}$) and gave their experimental results mentioned earlier [31].The light diesel combustion was theoretically examined, (their results are given in appendix A).The same initial and boundary conditions given by the company was applied to make sure that the model, mesh and procedure of solution of liquid fuel combustion employing the FLUENT program in the boiler was applicable and could simulate the liquid fuel combustion process.

Moreover, these results are compared with the results of Iraqi Diesel combustion.

The model, mesh and procedure of solution of ANSYS FLUENT are found to be applicable. The simulation of Light Diesel gave acceptable results and all the parameters given by ANSYS FLUENT14.5 were acceptable for the following reasons:-

1. The theoretical exhaust gas temperature predicted in this study by ANSYS FLUENT at the outlet (948.4695 K) coincide with the experimental exhaust gas temperature (948K) obtained experimentally by the manufacturer company of the boiler.
2. The theoretical peak temperature in the domain predicted in this study by the ANSYS FLUENT was (1955.405 K) matched with that peak temperature (1955K) that was measured experimentally by the manufacturer company [31].
3. The theoretical mass fraction of CO_2 predicted in this study by the ANSYS FLUENT at the outlet is (0.1778614) coincide with that (0.1778) which obtained experimentally by the manufacturer company of the boiler [31].

5-4-3 Methane gaseous fuel

5-4-3-1 Numerical Methane analysis

The Methane gas fuel (CH_4) was burned theoretically (Its results are given in appendix A). The reasons of selecting this fuel are:-

1. The boiler was tested experimentally using Methane gaseous fuel by the manufacturer company that gave its experimental results [31].
2. To compare the theoretical combustion results with the experimental results to make sure that the model, mesh and procedure of gas fuel combustion in FLUENT program applicable and then the simulation could be applied to other gaseous fuels.
3. Since there is a lack of simulation researches on liquid fuel combustion, the Methane simulation was compared with other simulation study using ANSYS FLUENT of Methane in a boiler produced by Raja Saripalli [21] to make sure that the results obtained in this study coincide with that obtained by other researches.

The following points were considered in this study to aid the comparison:-

1) In order to compare the results obtained by this study with the results obtained by the manufacturer company, the same initial and boundary conditions were used experimentally by the company were applied in this study numerically.
2) To compare the results of this study with the results produced by Raja Saripalli [21] in a larger water tube boiler, the same procedure assumptions of solution of ANSYS FLUENT used by Raja Saripalli [21] is used also in this study.
3) To operate the boiler on the methane or any other gaseous fuel , a suggested design and modification should be made for the burner as following :-

a. Retain the system of the air injection (centrifugal fan, diameter of air inlet, length of tube and pressure of air).
b. Adjust the mass flow rate of air to produce a stoichiometric mixture.
c. Substitute the liquid fuel pump with a gas fuel pump with a suitable pressure to achieve the required inlet mass flow rate (53.6 kg/h) and velocity.
d. Replace the nozzles that inject the liquid fuel and substitute it with nozzles of (15 mm) diameter to inject the gas fuel.

After applying the above-suggested design for the burner, the simulation, model and mesh of the boiler gave reasonable results. All the predicted parameter given by the ANSYS FLUENT 14.5 for the methane fuel were accepted for the following reasons:-

1. The theoretical exhaust gas temperature predicted in this study by ANSYS FLUENT was (564.5367 K) matched with that measured experimentally by the manufacturer company [31] of boiler that equal (564 K).
2. The theoretical peak temperature predicted in this study by ANSYS Fluent in the domain is (1631.43K) coincide with the peak temperature measured by the manufacturer experimentally(1631K) in the boiler [31] , and also coincide with the peak temperature calculated (1630K) by Raja Saripalli [21].
3. The theoretical mass fraction of CO_2 predicted in this study by the ANSYS Fluent at outlet is (0.111283) coincide with that (0.1112) which was measured experimentally by the manufacturer company [31] ,and also coincide with the mass fraction of CO_2 (0.11129) that calculated by Raja Saripalli [21] at chimney inlet.

5-4-3-2 Comparison of Methane results

The combustion chamber length of the boiler in this study was (1.65 m) while the combustion chamber length for Raja Saripalli study [21] was (12 m). Since they had different lengths, a dimensionless length parameter was employed which is a ratio of the length (L) at any point to the actual length of combustion chamber {characteristics length (Lcc)} were used to compare the quantitative results of the two studies .

For Raja Saripalli study [21], all the parameters were drawn on a line extended along the length of combustion chamber (12 m) and passes through the centerline of the nozzle until the end wall of combustion chamber in the axial direction. This line corresponds to the line1 (L_{cc}) in this study.

Figure (5-16) shows the temperature variation along the dimensionless length. It is clearly observable that in both curves the temperature increased due to the combustion process. In this study the temperature increased from (300 K) until it reached (1390 K) at (8%) of the length. While for Raja Saripalli study [21] at (9 %) of the length, the temperature reached at this point a value of (1388 K).

The peak temperature of both studies were equal to (1450 K) and appear to be at (35%) of the dimensionless length of combustion chambers, and then the temperature decreased along the dimensionless length until it approached (1110 K) for both studies close to the combustion chamber end wall.

Figure (5-17) demonstrates the pressure variation of both studies along the dimensionless length. It has clearly shown that the peak pressure is at the nozzle and then decreased and reached a constant value due to the combustion process for both studies. In this study the pressure remained constant at (5%) of the dimensionless length while in Raja Saripalli study [21] the pressure remained constant after (8%) of the dimensionless length.

Figure (5-18) demonstrates the velocity variation of the two studies along the dimensionless length. The inlet velocity of Raja Saripalli study [21] was (57 m/s).While in this study the inlet velocity was (36 m/s). For both studies, the velocity increased rapidly due to combustion. For Raja Saripalli [21] the peak velocity was (119 m/s) appeared at (12%) of dimensionless length. While in this study the peak velocity was (115 m/s) appeared at (8%) of dimensionless length. In both studies, the velocity reduced gradually away from the inlet until it reached close to zero at the end wall of combustion chamber.

Figure (5-19) demonstrates the decrease of the mass fraction of Methane (CH_4) due to the combustion process in both studies. For Raja Saripalli study [21] there was a rapid decrease of fuel (CH_4) mass fraction due to the swirl in air inlet. While in this study, the decrease of the fuel (CH_4) mass fraction was slower than that of Raja Saripalli study [21] because there was no swirl air at inlet. Where the fuel needed more time and distance to mix completely with air.

For both studies the Methane burned completely at (70%) of the dimensionless length, while the oxidation of C, H and CO remains further.

Figure (5-20) demonstrates the increasing of CO_2 mass fraction for this study and Raja Saripalli study [21] along the dimensionless length. The two studies show that there was a very small portion of CO_2 in the flame path. At (13%) of the dimensionless length the mass fraction of CO_2 increased rapidly till it get the peak value due to the combustion progress. For Raja Saripalli study [21], the peak value of CO_2 mass fraction was (0.13) at (53%) of the dimensionless length. While in this study the peak value of CO_2 mass fraction was (0.133) at (60%) of the dimensionless length. Finally, the two studies had the same value at (75%) of the dimensionless length until the end of the line.

Figure (5-21) demonstrates the variation of the O_2 mass fraction for this study and Raja Saipalli study [21]. For the latter O_2 mass fraction increased

rapidly to get the peak value of (0.199) at (20%) of the dimensionless length. While in this study the peak value of O_2 mass fraction was (0.19) at (9%) of the dimensionless length. The difference could be due to the induced turbulence in the air with swirl.

In both studies, the mass fraction of O_2 decreased rapidly due to the combustion progress and reacted O_2 produced CO_2, until the mass fraction of O_2 for the two studies get the same minimum value (0.01) at (55%) of the dimensionless length. Then it increased due to the effect of induced turbulence and eddies that bring a mass of O_2 to the line zone. Finally, the two studies had the same value of O_2 mass fraction at (75%) of the dimensionless length until the end of the length.

It may concluded from the results comparison between this study and Raja Saripalli study [21] that the two studies gave a similar behavior, and all the curves and results were nearly coincide.

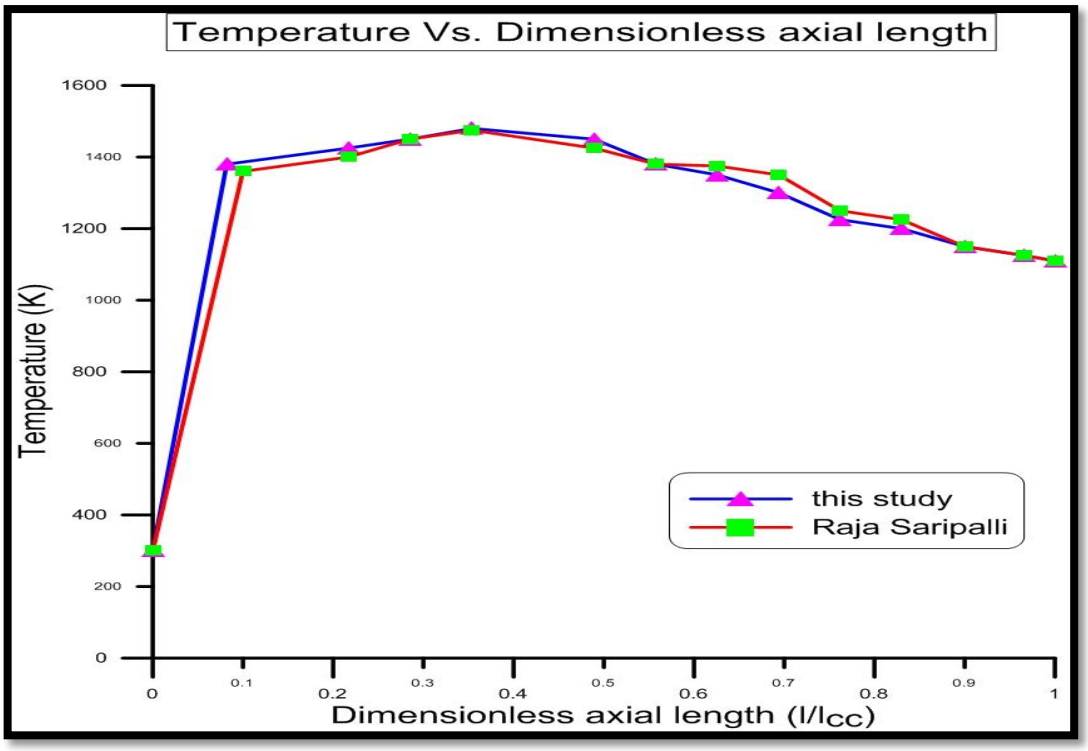

Figure (5-16) Temperature variation along dimensionless length.

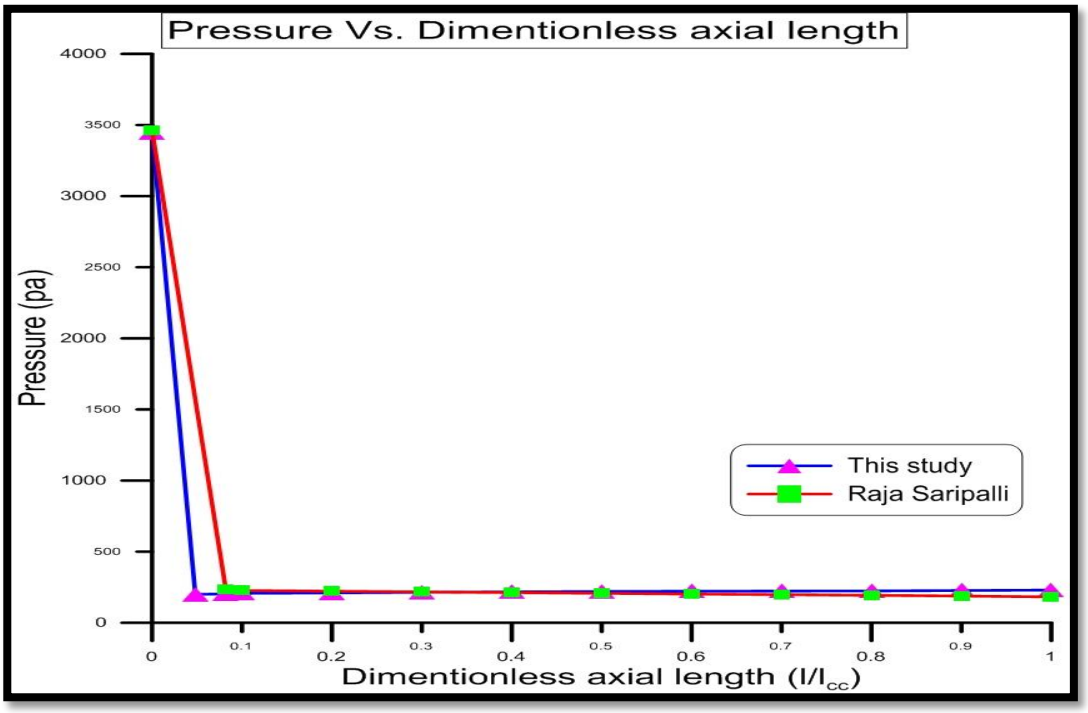

Figure (5-17) Pressure variation along dimensionless axial length.

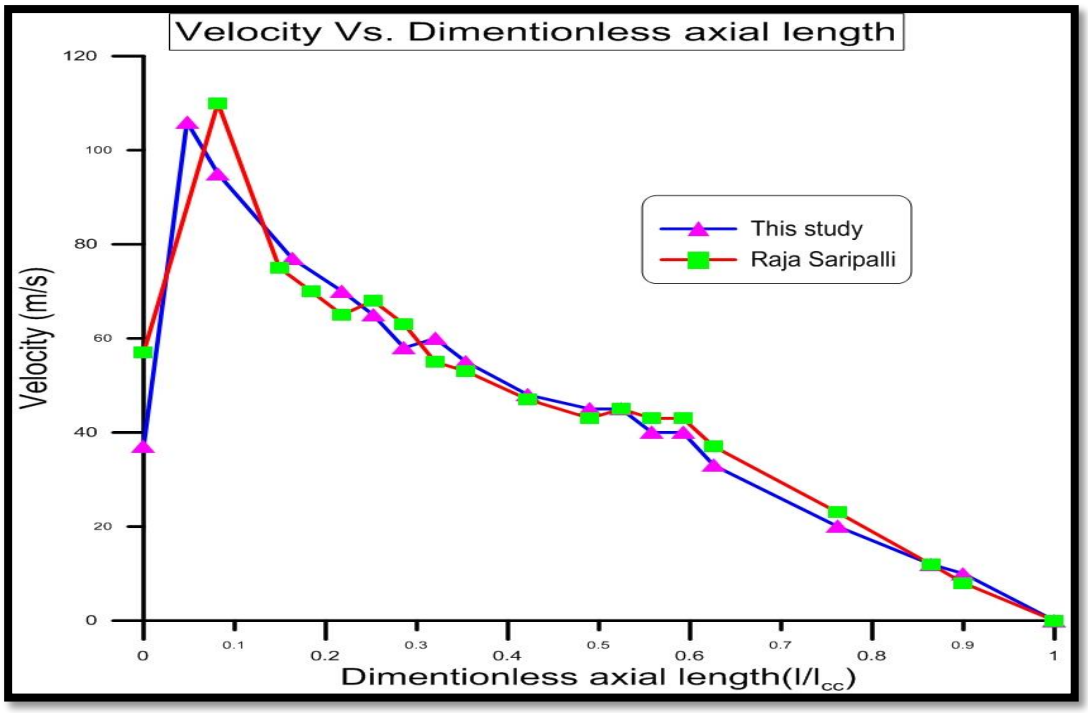

Figure (5-18) Velocity variation along dimensionless axial length.

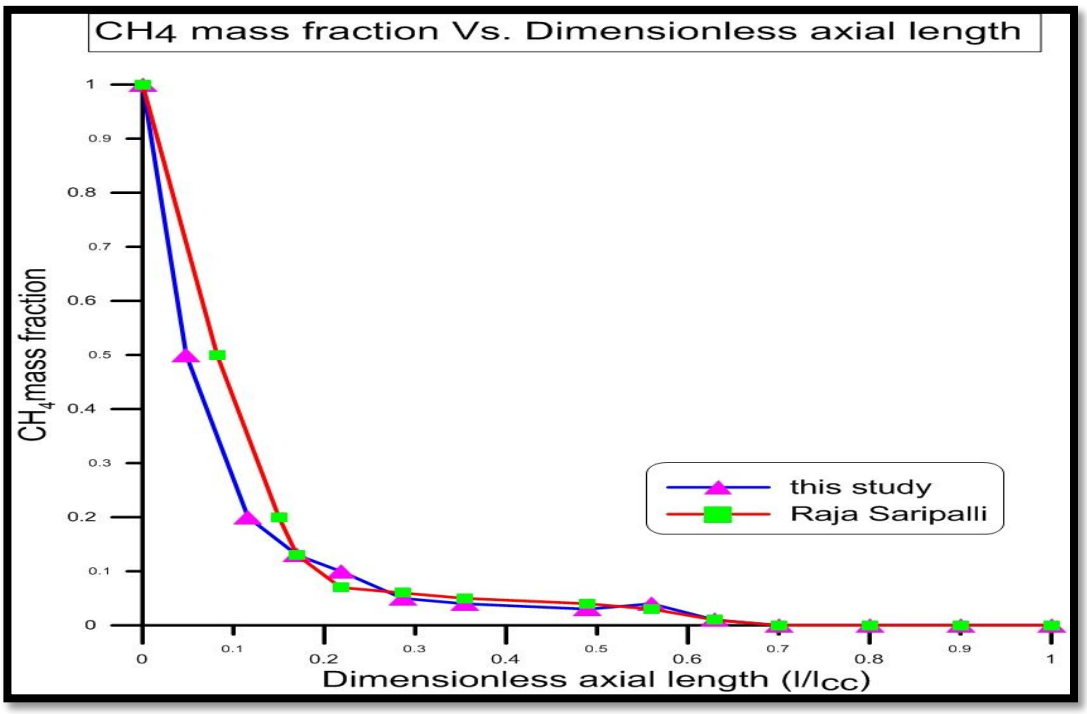

Figure (5-19) CH_4 mass fraction variation along dimensionless axial length.

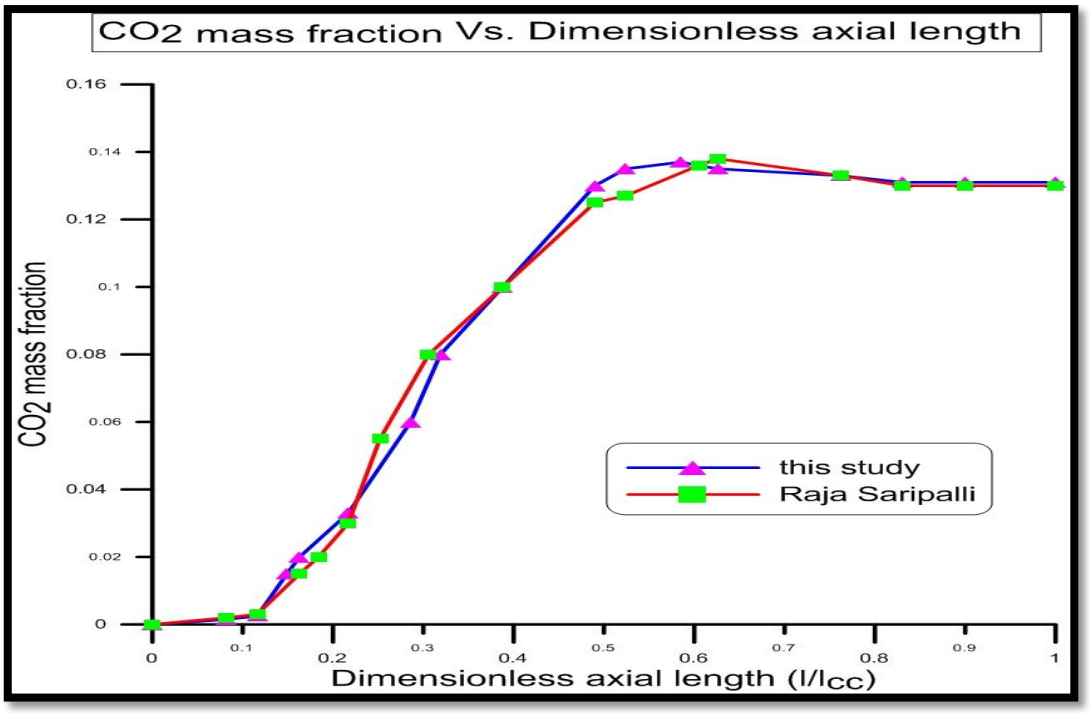

Figure (5-20) CO_2 mass fraction variation along dimensionless axial length.

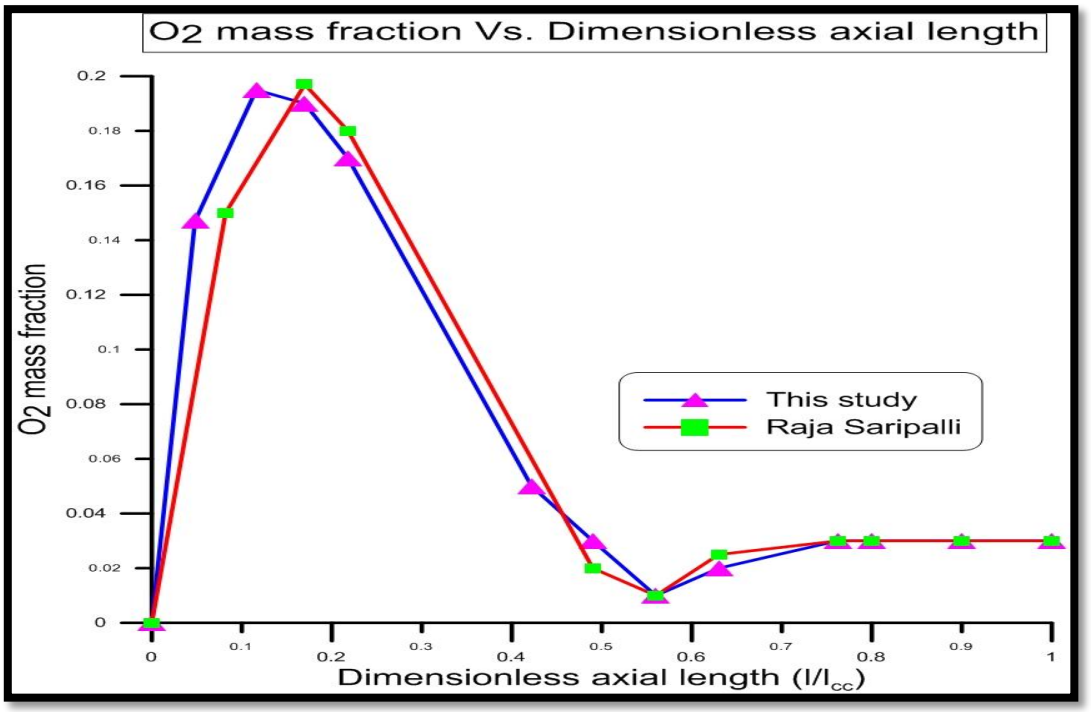

Figure (5-21) O_2 mass fraction variation along dimensionless axial length.

5-4-4 Iraqi LPG fuel

The suggested design of the burner was accepted since the numerical results of this study of Methane agree reasonably with the experimental results provided by the manufacturer company of the boiler [31], also with the results of Raja Saripalli study [21]. It is acceptable to suggest a numerical solution for Iraqi LPG ($C_{3.437}$ $H_{8.874}$) stoichiometric combustion (its results are given in appendix A). The analysis had the same heat input, heat output and boiler's efficiency as if the boiler operated on the Iraqi Diesel fuel. These results were compared with other results in this study, for future experimental work.

5-5 Results of Comparison

In this section, a comparison among the theoretical quantitative results of four types of fuel, two liquid fuels Iraqi Diesel and Light Diesel and two gaseous fuels that are Methane and Iraqi LPG is presented. These comparisons demonstrates the (C/H) effect, fuels types and properties on the fuels behavior.

Four-output parameter are compared among the above fuels these are temperature, pressure, velocity and turbulence kinetic energy in five sections in the boiler.

5-5-1 Temperature

Figure (5-22) demonstrates the temperature variation along line1.It's clearly shown the ranking of high range temperature due to high calorific value are Light Diesel, Methane ,Iraqi Diesel and Iraqi LPG,

The peak temperature of Iraqi Diesel was less than that of Light Diesel by (25.9%) and Methane by (7.2%) but higher than that of Iraqi LPG by (13.7%).

The peak temperature of Iraqi LPG was less than that of Methane by (24.2%).

Figure (5-23) demonstrates the temperature variation of the fuels along the line 2. It is clearly shows that the maximum temperature of Iraqi Diesel was less than that of Light Diesel by (6.9%) but higher than that of Methane by (44.8%) and Iraqi LPG by (48%).

The maximum temperature of Iraqi LPG was less than that of Methane by (6.3%). This could be due to the other components in the Iraqi LPG.

Figure (5-24) demonstrates the temperature variation along the line3 in one of tubes. It is clearly shows that the temperatures of the products dropped due to the heat exchange between the wall of tube and the water outside the tube.

The maximum temperature of Iraqi Diesel was higher than that of Methane by (32%) and that of Iraqi LPG by (27.9%), and equal to that of Light Diesel but the range of Iraqi Diesel temperatures along the tube was less than that of Light Diesel.

The maximum temperature of Iraqi LPG was higher than that of Methane by (5.8%)

Figure (5-25) denotes the temperature variation along the line4 in front plenum. It is clearly shows that the peak temperature of Iraqi Diesel equal that of Light Diesel but higher than that of Methane by (28.4%) and Iraqi LPG by (29.8%).

The maximum temperature of Iraqi LPG was less than that of Methane by (2.1%) only.

Figure (5-26) clarify the temperature variation along the line5 in rear plenum. The maximum temperature of the Iraqi Diesel was less than that of Light Diesel by (10.6%) but it is higher than that of Methane by (38.8%) and Iraqi LPG by (21.3%).

The Iraqi LPG maximum temperature was higher than that of Methane by (22.3%).

The results also demonstrates the effect of cooling the wall due to the water surrounding the wall at the end of the line that express the sharp drop in the temperature at the end of the line.

5-5-2 Pressure

Figure (5-27) demonstrates the pressure variation for the fuels along line1.It clearly shows that all the fuels have the maximum pressure at the inlet and the pressure dropped rapidly due to the combustion and then stayed constant at (0.175 m) on the line1, proofing constant pressure combustion.

Figure (5-28) demonstrates the pressure variation for the fuels along the line2. It clearly shows that the liquid fuels had a similar behavior but the gaseous fuels had different behavior.

The maximum pressure of the Iraqi Diesel fuel was less than that of Light Diesel by (4.9%), the Methane by (43.7%) and the Iraqi LPG by (54.1%). There are differences in pressure values for the fuels because the flames plum shapes are different from one to another that affect products movement towards the front plenum.

The maximum pressure of Iraqi LPG was higher than that of Methane by (6.7%) due to the difference in fuel components.

Figure (5-29) demonstrates the pressure variation among the fuels along the line3 in one of the tubes. It clearly shows that the maximum pressure for all fuels was at the inlet of the tube caused by the entrance region. Then the pressure decreased gradually along the line in the tube as the flow developed and pressure decrease further due to friction.

The Iraqi Diesel, Light Diesel and Iraqi LPG had a similar behavior, but the Methane had a different behavior at the entrance of tube because the drop

of pressure of Methane was higher than other fuels and then Methane behaved later as the other fuels. That was because the Methane is a more radical than the other fuels.

The maximum pressure of the Iraqi Diesel equals that of the Light Diesel and Methane but less than that of Iraqi LPG by (59.8%).

The maximum pressure of Iraqi LPG was higher than that of Methane by (37.4%), the difference might be due to the components of Iraqi LPG in continuous combustion.

Figure (5-30) demonstrates the pressure variation of the fuels along the line4 in the front plenum. The curves demonstrate that there is a similar behavior of all the fuels.

The maximum pressure of Iraqi Diesel fuel was less than that of Light Diesel by (4.8%), the methane by (12.6%) and the Iraqi LPG by (50.3%).

The maximum pressure of the Iraqi LPG was higher than that of Methane by (25.1%).

Figure (5-31) demonstrates the pressure variation of the fuels along the line5 in the rear plenum. It clearly shows that all the fuels have a similar behavior.

The maximum pressure of Iraqi Diesel is less than that of Light Diesel by (26.1%), Methane by (6.6%) and Iraqi LPG by (49.3%).

The maximum pressure of the Iraqi LPG was higher than that of Methane by (28.6%).

5-5-3 Velocity

Figure (5-32) demonstrates the velocity variation for the fuels along the line1 in the combustion chamber. This chart denotes that all the fuels had a

similar behavior but vary quantitatively as they were under similar environment.

The maximum velocity of Iraqi Diesel is less than that of Light Diesel by (15.6%), Methane by (231%) and the Iraqi LPG by (93.7%).The maximum velocity of the Iraqi LPG was less than that of Methane by (71%).

Figure (5-33) clarify the velocity variation of the fuels along the line2. The maximum velocity of the Iraqi Diesel is less than that of the Light Diesel by (12.3%), Methane by (38.3%) and the Iraqi LPG by (7.4%) The maximum velocity of the Iraqi LPG was higher than that of Methane by (33.3%).

Figure (5-34) demonstrates the velocity variation of the fuels along the line3 in one of the tubes. The curves show that all the fuels have a similar behavior of velocity in tube and all the fuels have their maximum velocity at tube inlet (about 5% of the tube length).

The maximum velocity of Iraqi Diesel was less than that of Light Diesel by (6.6%) and Iraqi LPG by (11.4%) but it was higher than that of Methane by (3.3%).The maximum velocity of Iraqi LPG higher than that of Methane by (13.2%).

Figure (5-35) denotes the velocity variation of the fuels along the line4 in the front plenum. It clearly shows that all the fuels have a similar behavior qualitatively. However, the maximum velocity of Iraqi Diesel is less than that of Light Diesel by (9%), Methane by (3.3%) and Iraqi LPG by (7.9%). In addition, the maximum velocity of Iraqi LPG was higher than that of Methane by (5.8%).

Figure (5-36) demonstrates the velocity variation of the fuels along the line5 in the rear plenum.

The maximum velocity of Iraqi Diesel was less than that of Light Diesel and Iraqi LPG by (9%) but it was higher than that of Methane by (20%).Also the maximum velocity of Iraqi LPG was higher than that of Methane by (26.6%).

5-5-4 Turbulent Kinetic Energy

Figure (5-37) demonstrates the variation of turbulent kinetic energy of the fuels along the line1 in the combustion chamber. It is clearly shows that the Iraqi Diesel, Light Diesel and Iraqi LPG have a similar behavior qualitatively but the Methane had a maximum increase in the turbulence due to Methane radical behavior. This increased the turbulent kinetic energy, which caused the fluctuations in the velocity profile on this line.

The maximum turbulent kinetic energy of the Iraqi Diesel was higher than that of Light diesel by (28.6%) but it is less than that of Methane by (495.2%) and Iraqi LPG by (81%). In addition, the maximum turbulent kinetic energy of the Iraqi LPG was less than that of Methane by (289%).

Figure (5-38) demonstrates the variation of turbulent kinetic energy of the fuels along the line2. The curves denote that the liquid fuels had similar behaviors and the methane had the maximum value. The maximum turbulence kinetic energy of the Iraqi Diesel was higher than that of Light Diesel by (12.5%) but it was less than that of Methane by (437.5%) and Iraqi LPG by (31.3%). In addition, the maximum turbulent kinetic energy of the Iraqi LPG was less than that of Methane by (309.5%).

Figure (5-39) clarify the variation of turbulent kinetic energy of the fuels along the line3 in one of the tubes. It clearly shows that all the fuels have similar behaviors and the turbulent kinetic energy reduced when the hot gases enter the tubes to reach the same value of (2 J/kg) for all the fuels at (0.5 m) of the line length and continue to do so until the end of line in the tube.

Figure (5-40) clarify the variation of turbulent kinetic energy of the fuels along the line4 in the front plenum. It clearly shows that all the fuels have a similar behavior. The maximum turbulent kinetic energy of the Iraqi Diesel was less than that of Light Diesel by (11.7%). However, it was higher than that of Methane by (30.8%) and that of Iraqi LPG by (37%). In addition, the maximum turbulent kinetic energy of the Iraqi LPG was less than that of Methane by (8.9%).

Figure (5-41) demonstrates the variation of turbulent kinetic energy of the fuels along the line5 in the rear plenum. This chart denotes that all the fuels have a similar behavior. The maximum turbulent kinetic energy of the Iraqi Diesel was higher than that of Light Diesel by (58.9%), Methane by (79.4%) and Iraqi LPG by (60.3%). In addition, the maximum turbulent kinetic energy of the Iraqi LPG was higher than that of Methane by (48.3%).

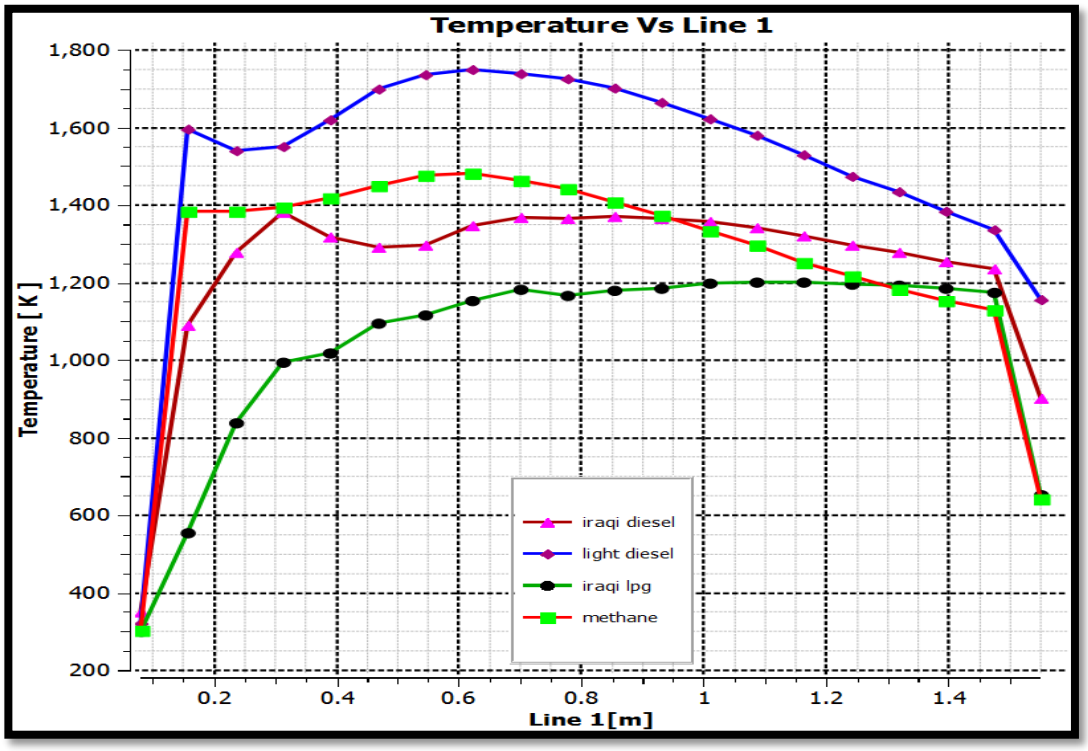

Figure (5-22) Temperature variation along line1.

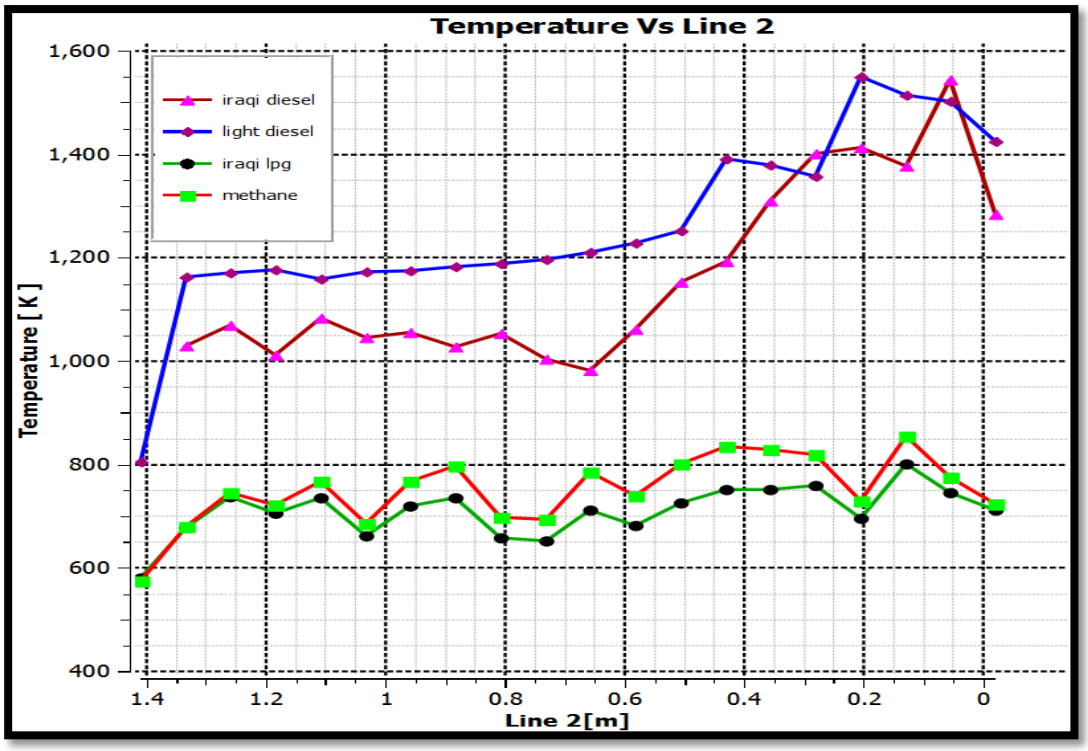

Figure (5-23) Temperature variation along line2.

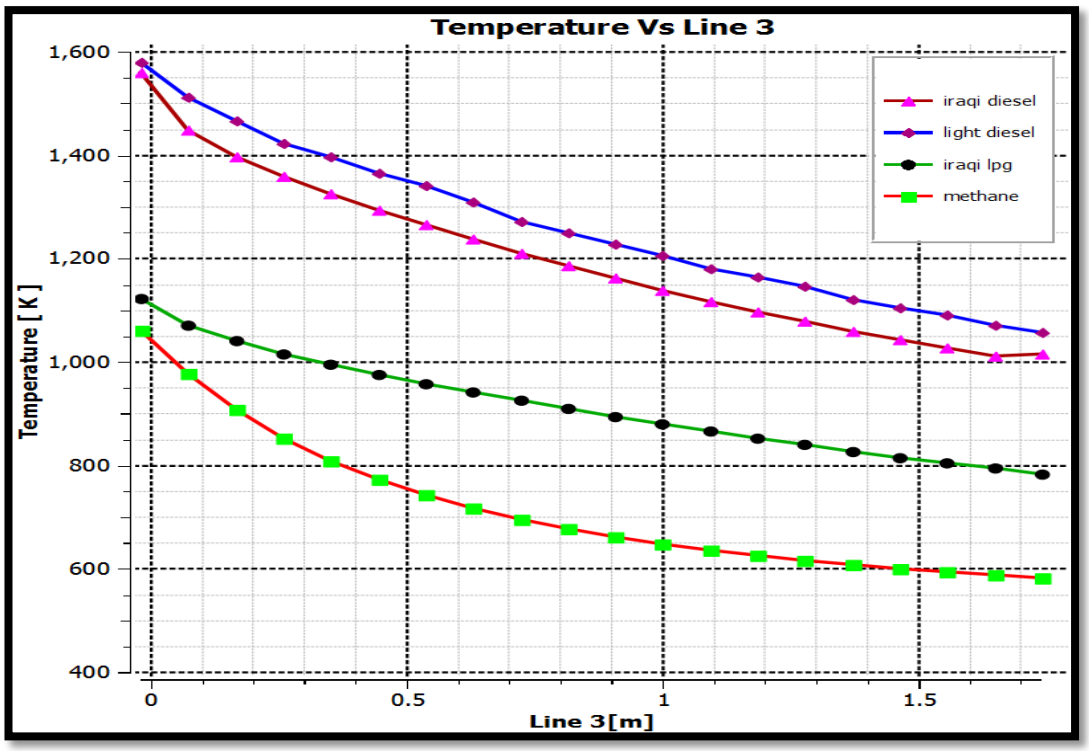

Figure (5-24) Temperature variation along line3.

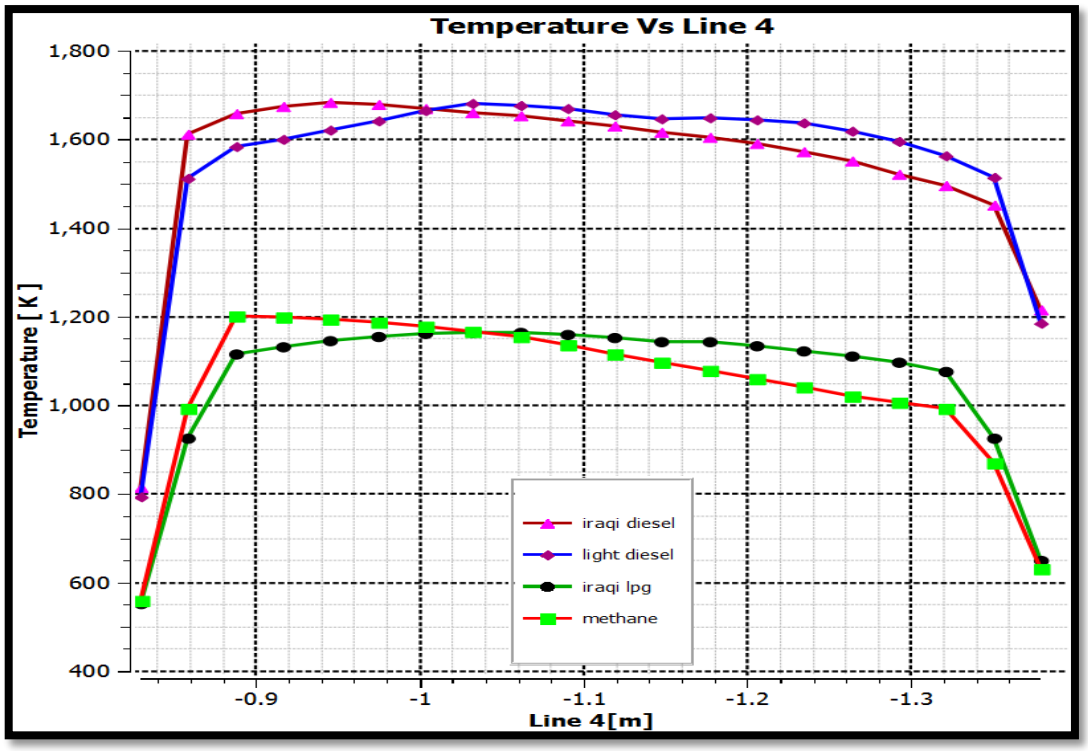

Figure (5-25) Temperature variation along line4.

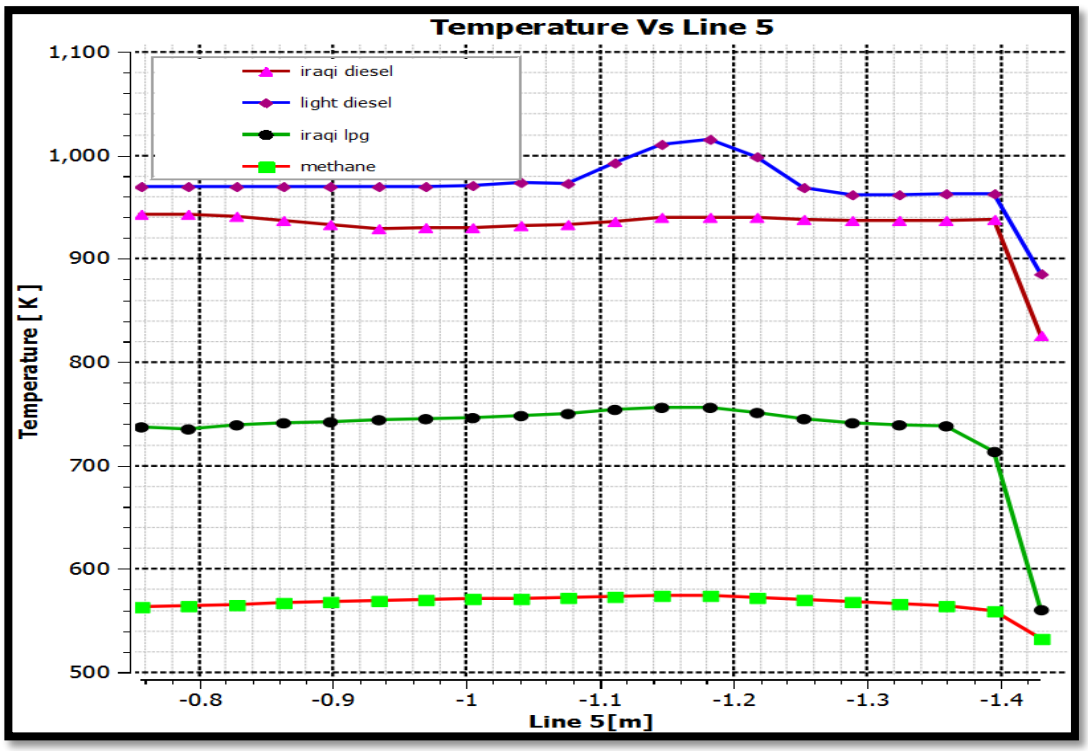

Figure (5-26) Temperature variation along line5.

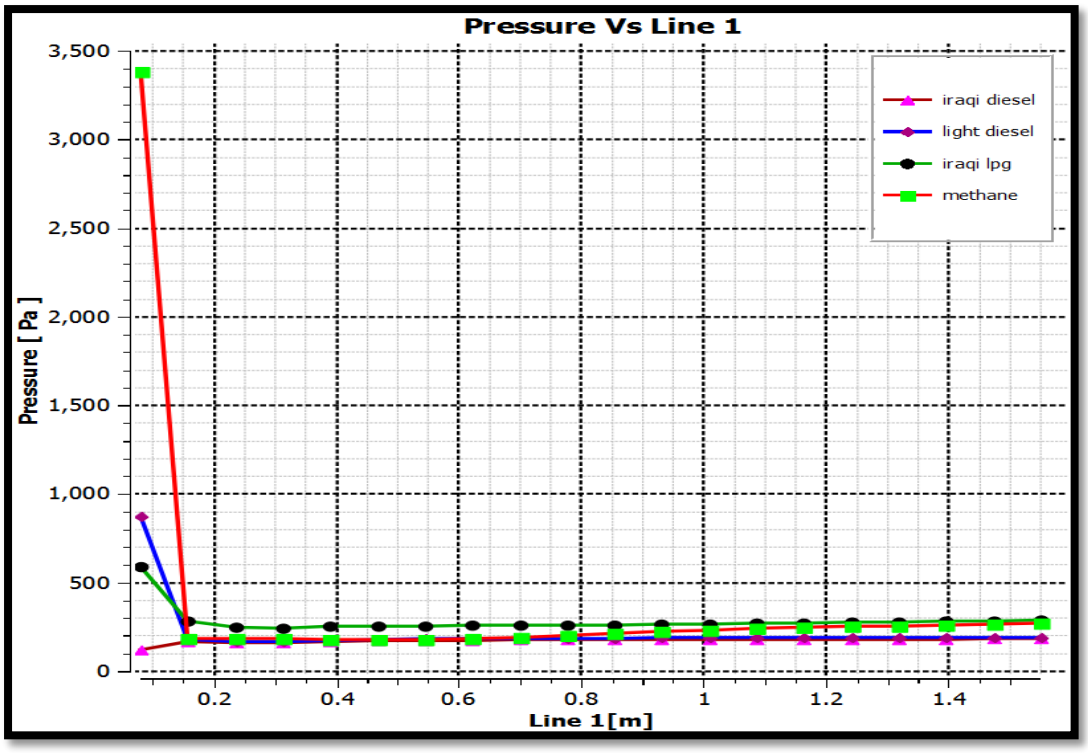

Figure (5-27) Pressure variation along line1.

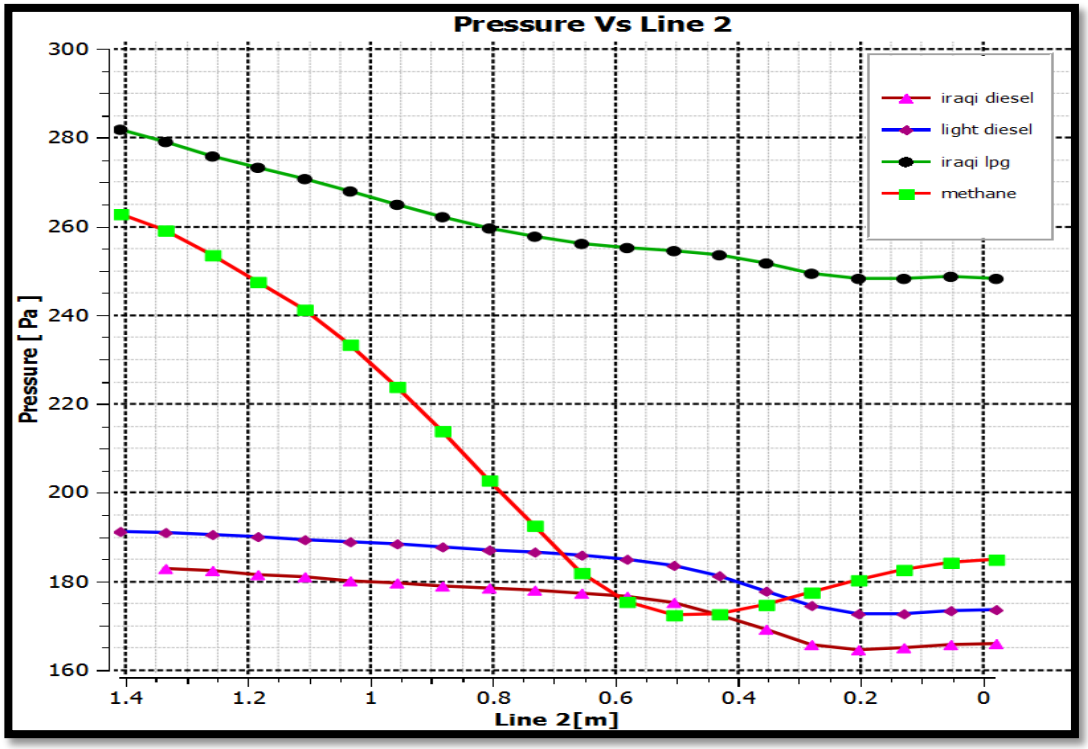

Figure (5-28) Pressure variation along line2.

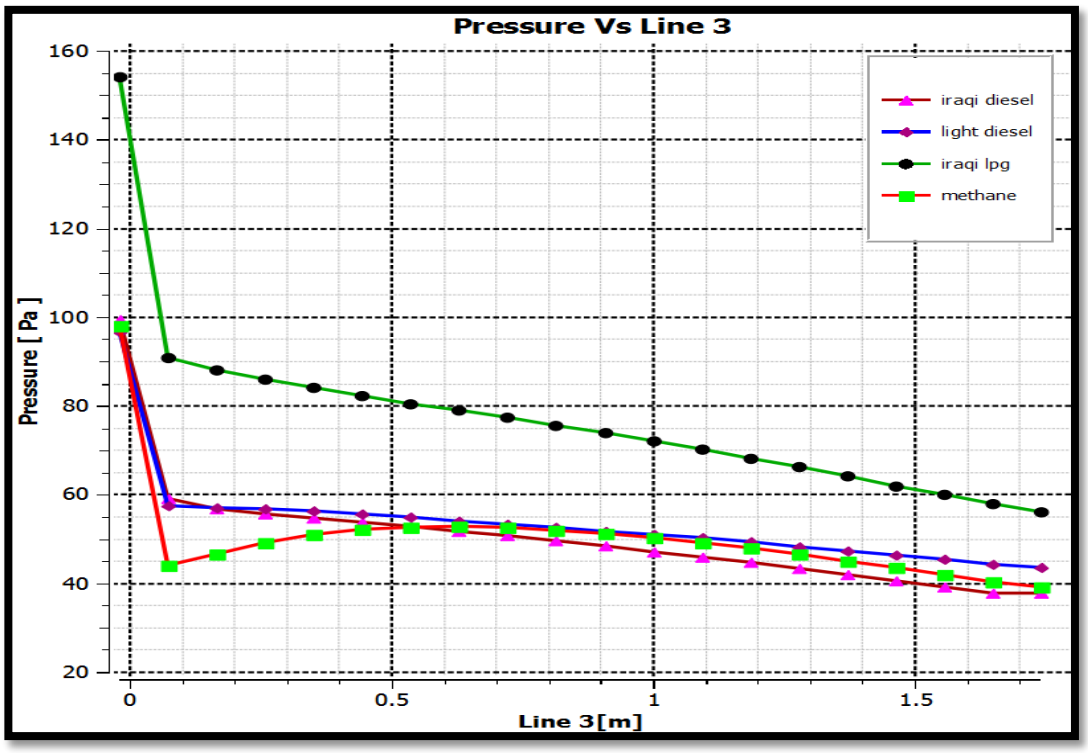

Figure (5-29) Pressure variation along line 3.

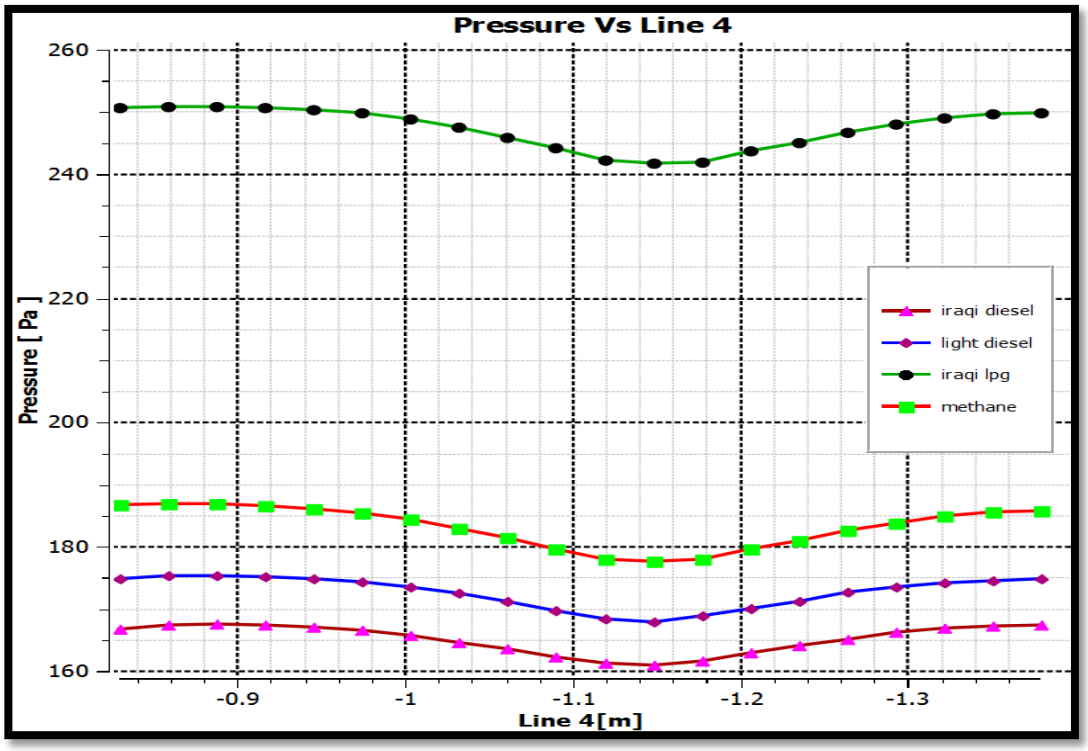

Figure (5-30) Pressure variation along line 4.

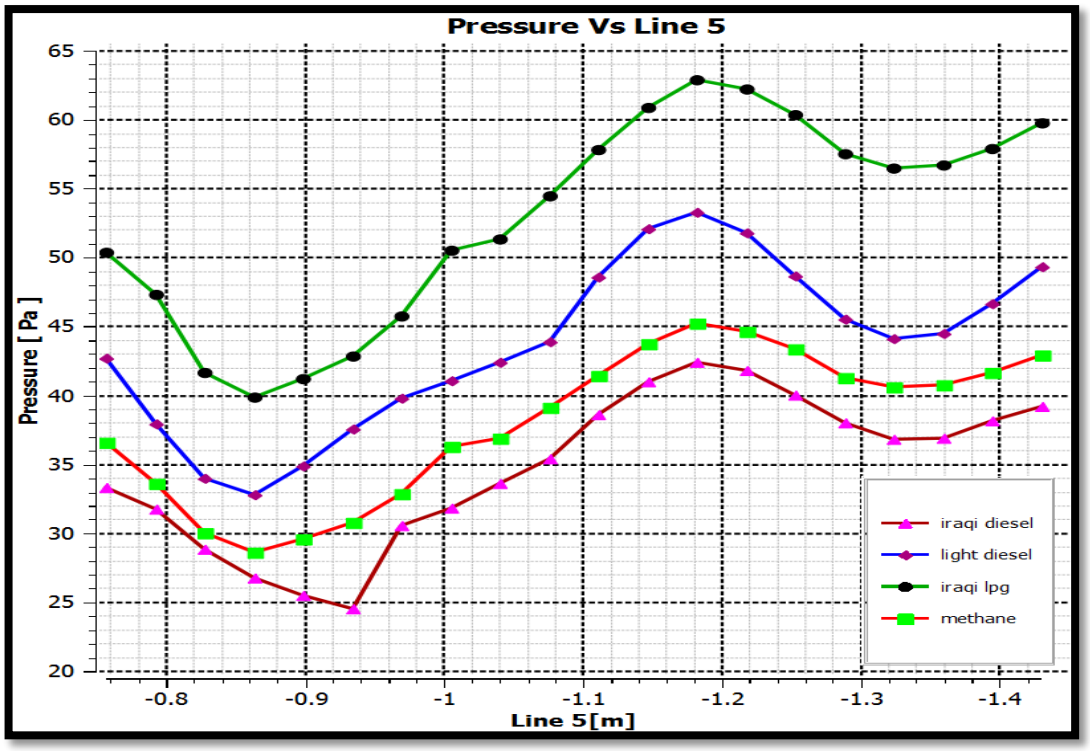

Figure (5-31) Pressure variation along line 5.

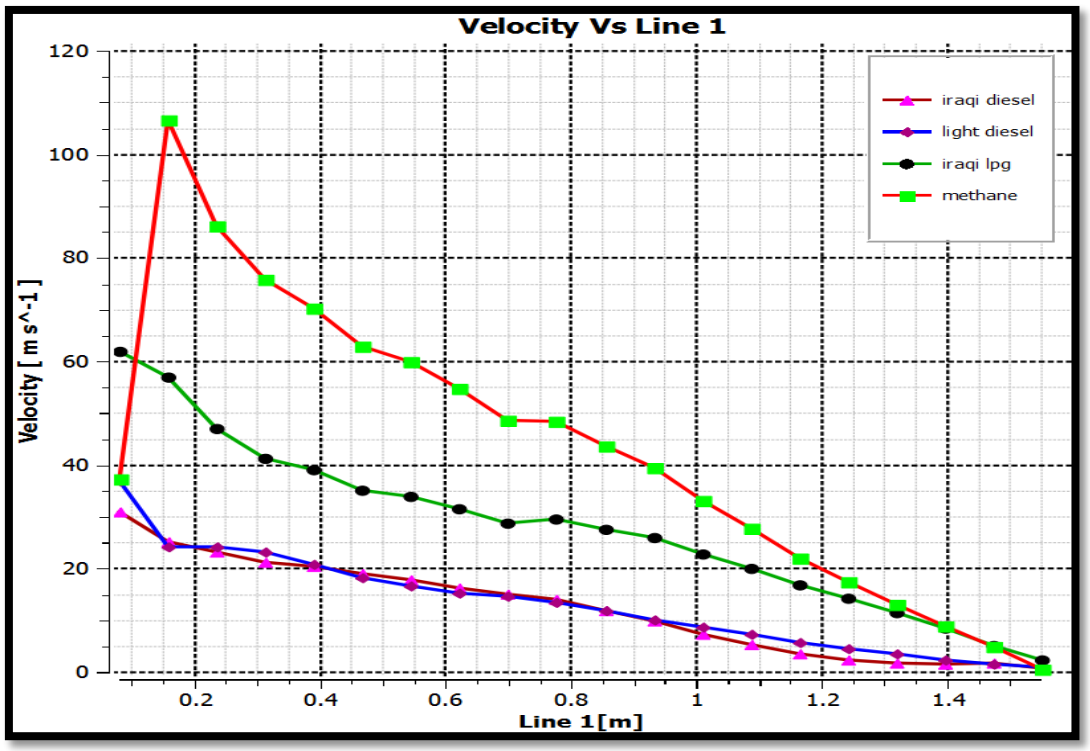

Figure (5-32) Velocity variation along line1.

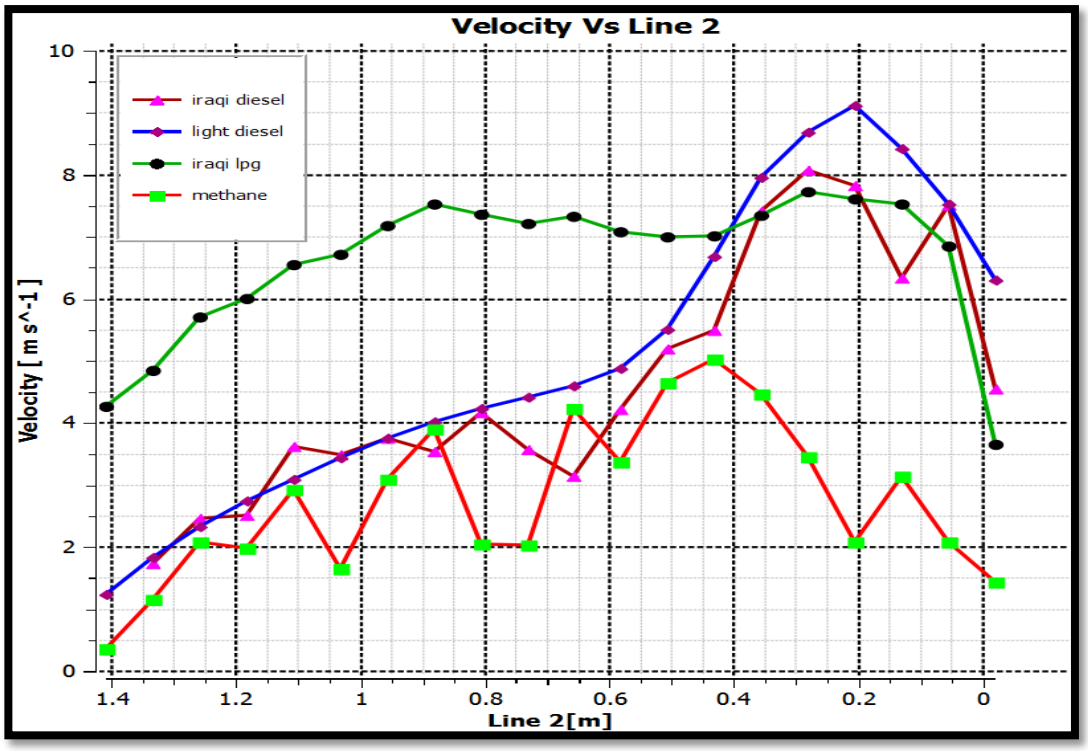

Figure (5-33) Velocity variation along line 2.

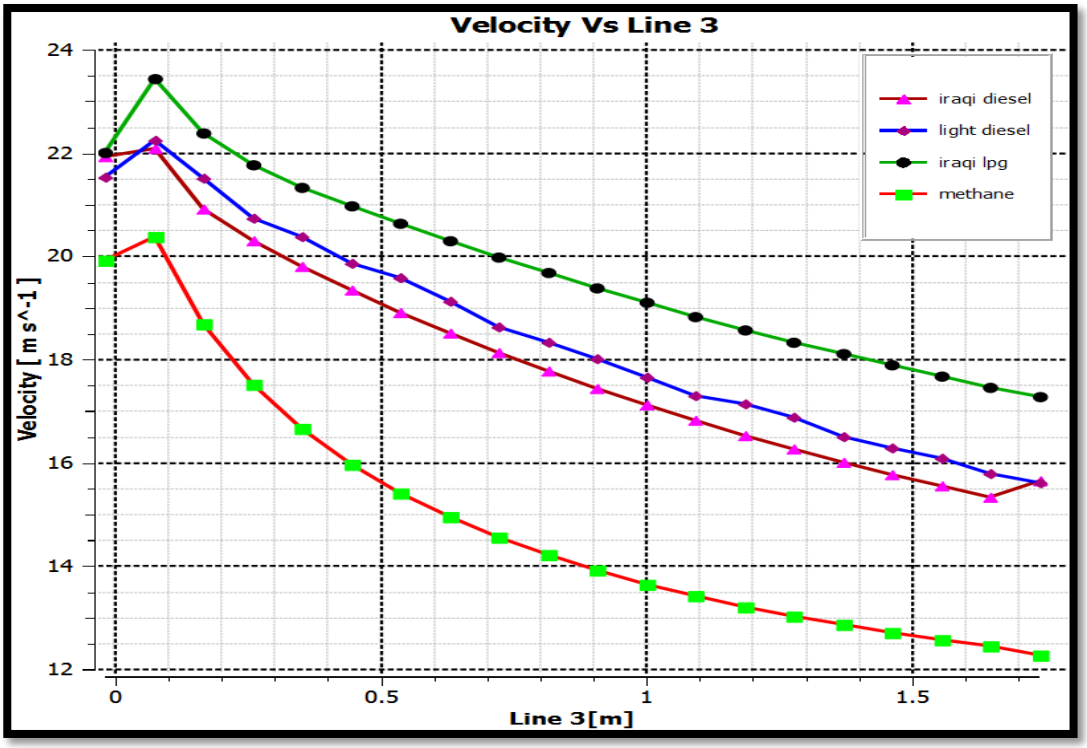

Figure (5-34) Velocity variation along line 3.

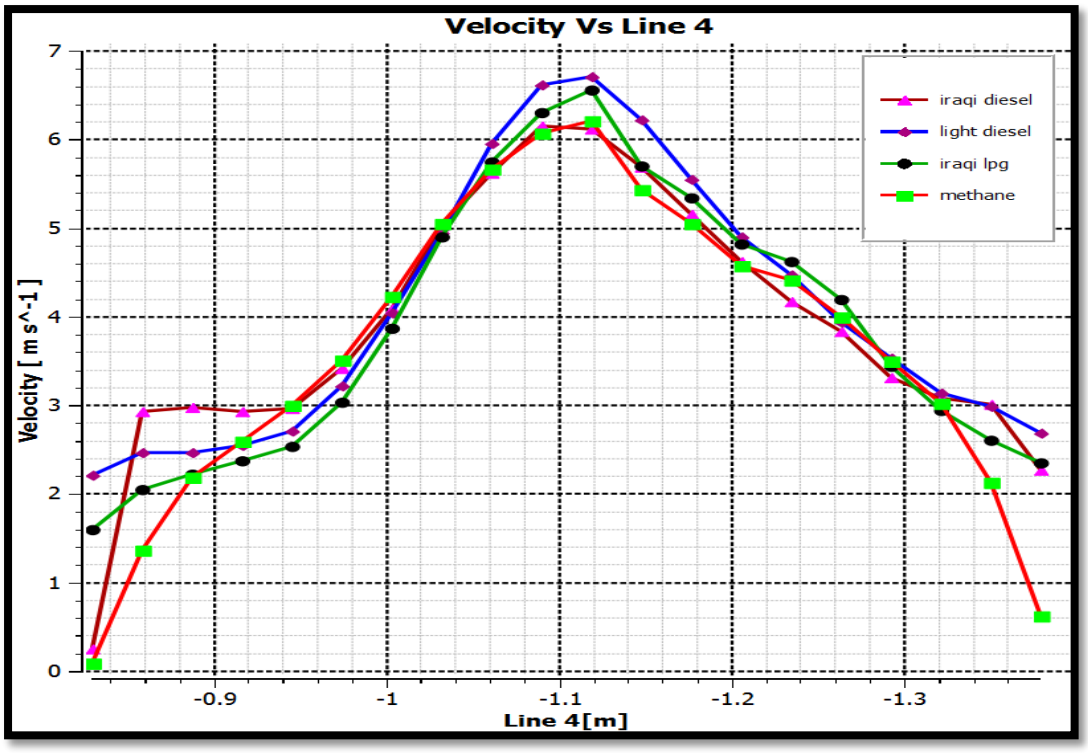

Figure (5-35) Velocity variation along line 4.

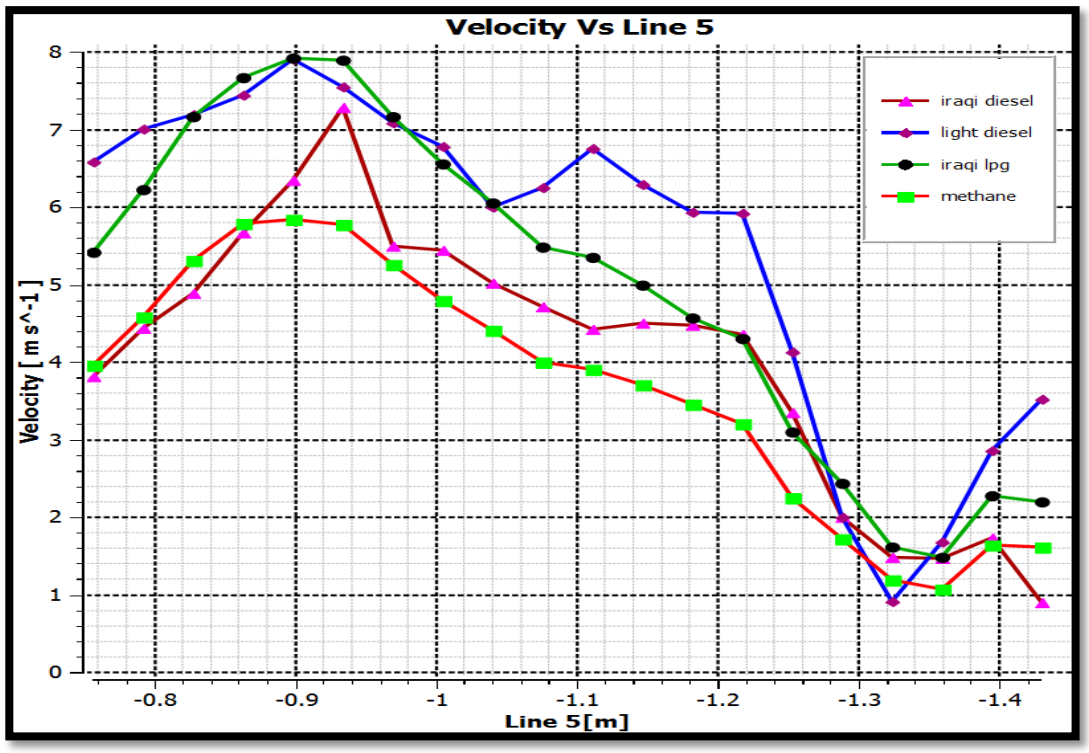

Figure (5-36) Velocity variation along line 5.

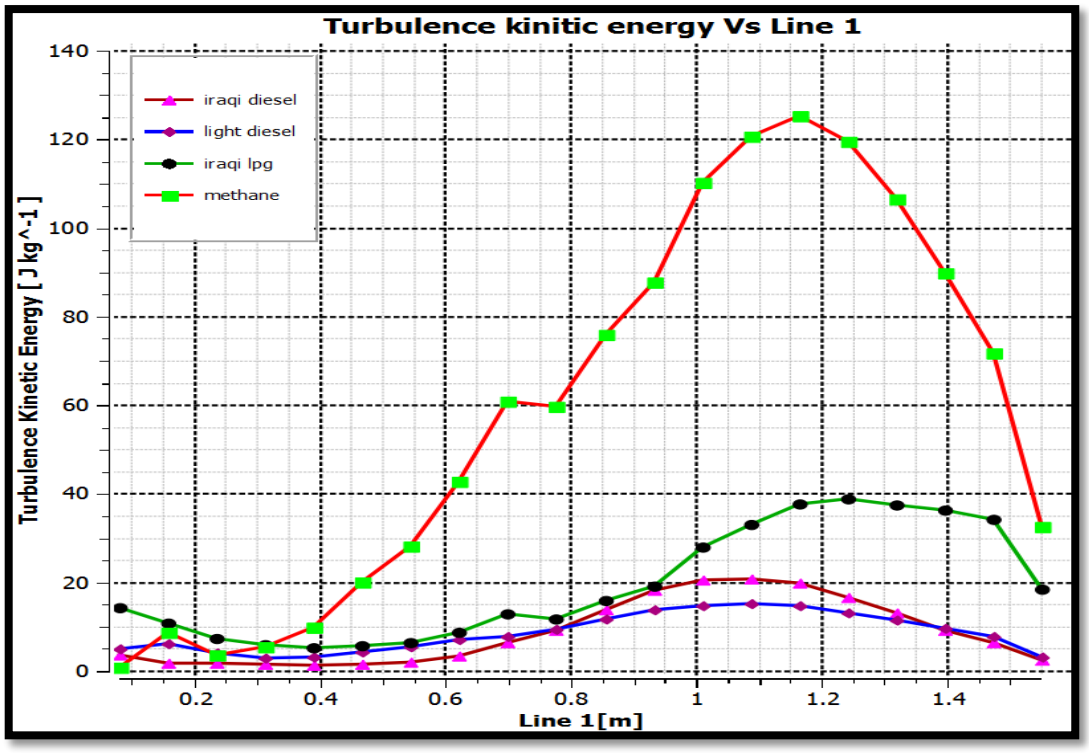

Figure (5-37) Turbulence Kinetic Energy variation along line1.

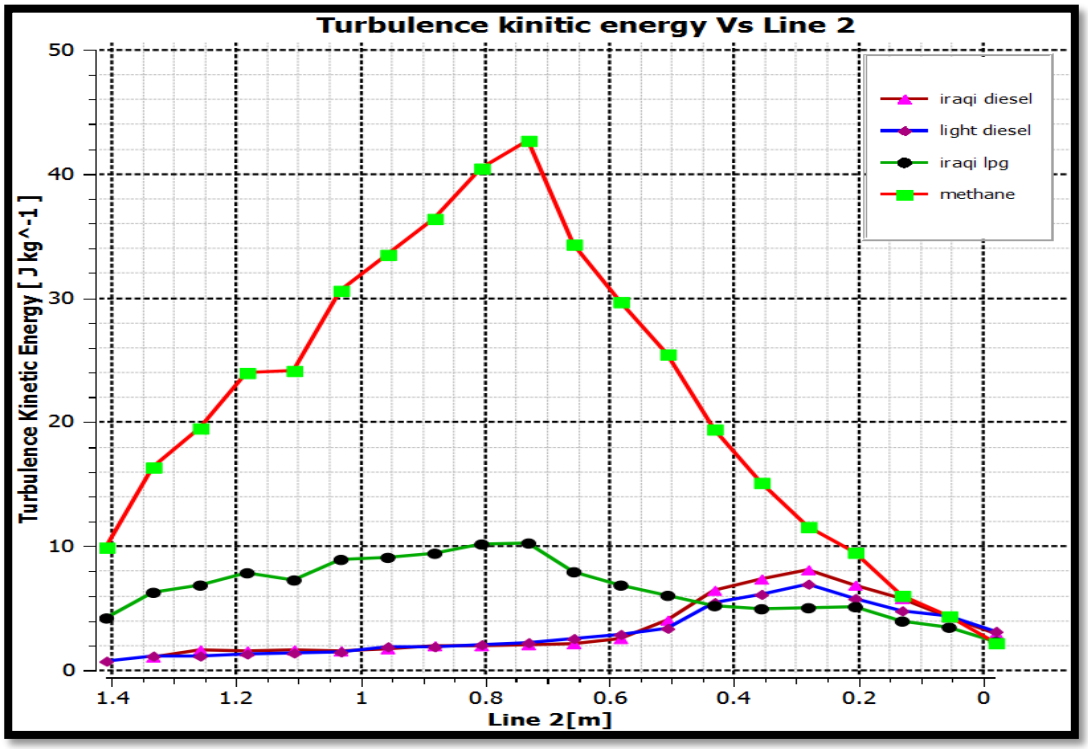

Figure (5-38) Turbulence Kinetic Energy variation along line 2.

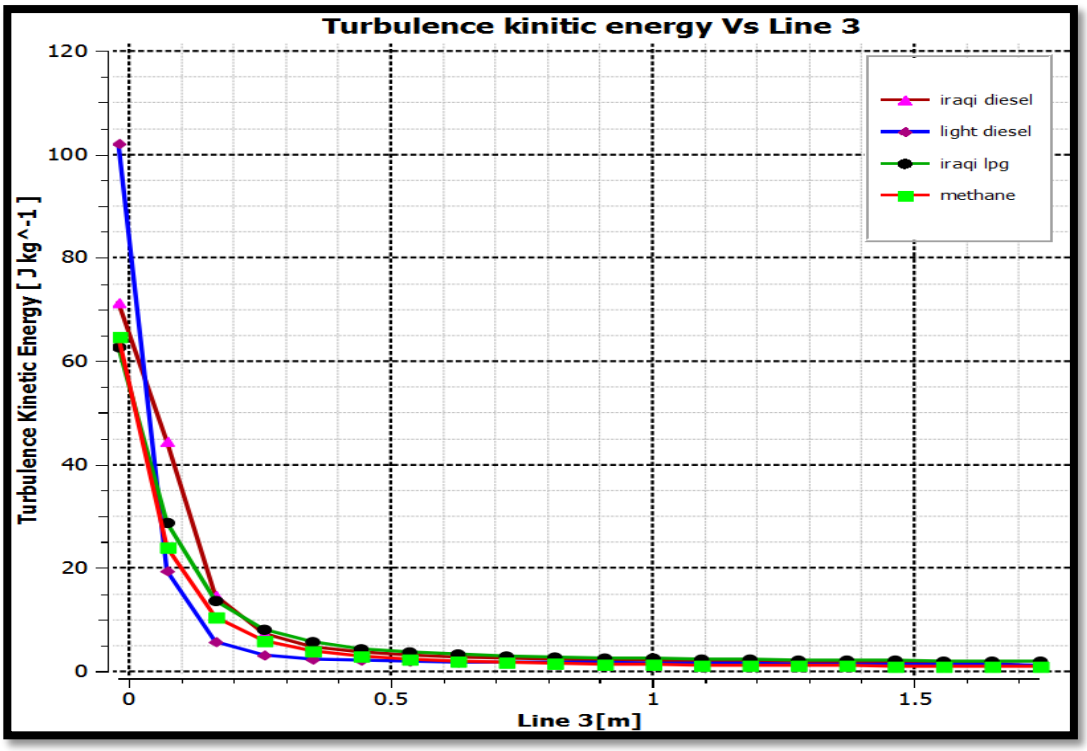

Figure (5-39) Turbulence Kinetic Energy variation along line 3.

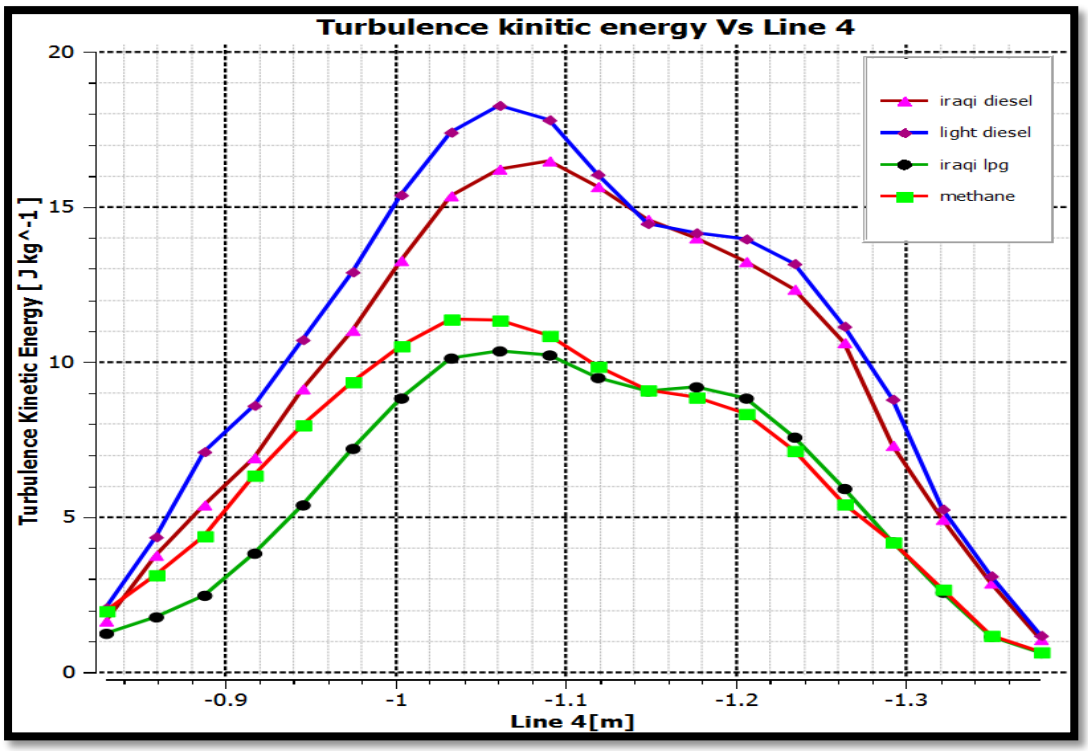

Figure (5-40) Turbulence Kinetic Energy variation along line 4.

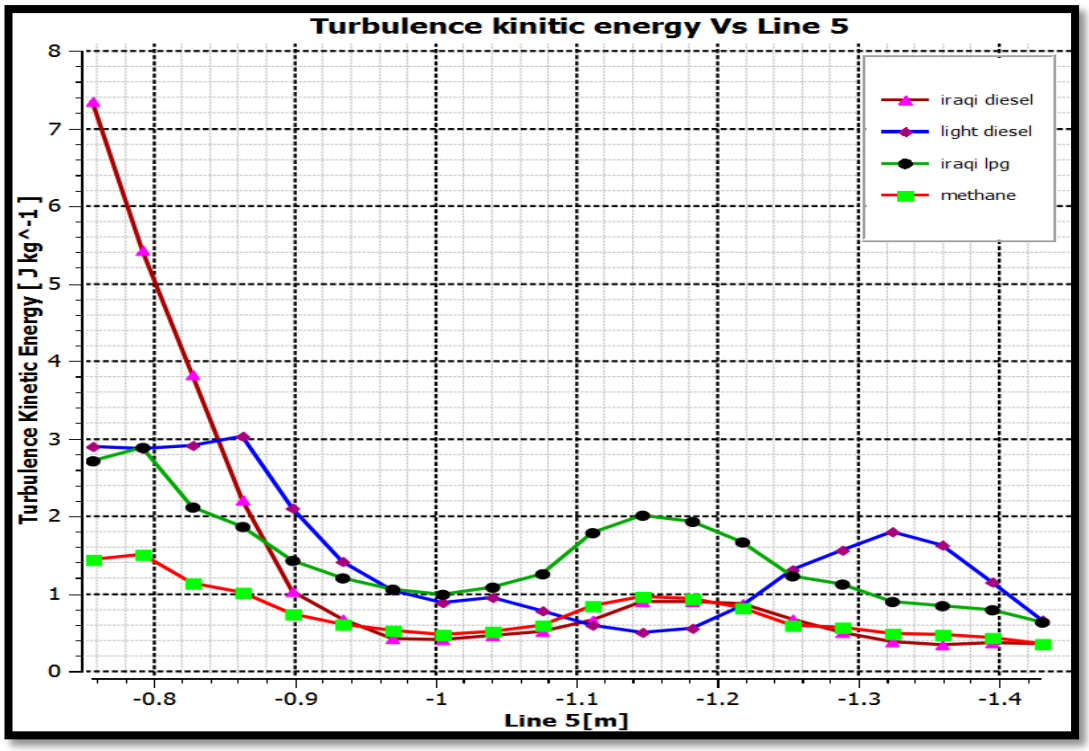

Figure (5-41) Turbulence Kinetic Energy variation along line 5.

5-6 Numerical Results

This section of the chapter contains two tables showing summaries for the numerical results of this study for the Iraqi Diesel, Light Diesel, Methane and Iraqi LPG and the results of Raja Saripalli study [21].

Table (5-5) demonstrates the results at the whole domain, while table (5-6) demonstrates the results at the outlet only (chimney inlet section).

Table (5-5) Numerical results at the whole domain.

Parameter	Iraqi Diesel	Light Diesel	Iraqi LPG	Methane	Raja Saripalli [21]
Maximum temperature (K)	1986.007	1955.405	1705.732	1631.411	1630
Maximum pressure (Pa)	413.774	2116.058	1288.754	3445.439	3459.29
Maximum velocity (m/s)	34.2	49.947	66.63	106.39	110
Peak turbulent kinetic energy (m^2/s^2)	116.2115	154.429	88.648	171.1152	173.23

Table (5-6) Numerical results at outlets.

Parameter	Iraqi Diesel	Light Diesel	Iraqi LPG	Methane	Raja Saripalli [21]
Temperature (K)	930.716	948.4596	734.7019	564.5367	563.8
Velocity (m/s)	11.809	13.79	12.9129	9.4236	10.37
CO_2 mass fraction	0.207083	0.177848	0.13041	0.111288	0.11129
CO mass fraction	0.025137	0.004658	0.080973	-	-
O_2 mass fraction	1.8339×10^{-5}	0.017658	1.4352×10^{-6}	0.058728	0.05873
H_2O mass fraction	0.056172	0.078153	0.0478277	0.09111	0.09112
Fuel mass fraction	4.837×10^{-5}	3.9622×10^{-6}	3.33×10^{-4}	0	0

CHAPTER SIX

CONCLUSIONS AND RECOMMENDATIONS

CHAPTER SIX

CONCLUSIONS AND RECOMMENDATIONS

6-1 Conclusions:

The main objective of this work can be divided into two parts. Part one is the experimental work where test was performed on a combustion chamber of a boiler using Iraqi Diesel fuel. Part two is a numerical work capable of solving three dimensional, compressible and turbulent combustion for both gaseous and liquid fuels, where the program ANSYS 14.5 was employed. The produced results agree reasonably well with the other published computational data, FLUENT software and experimental tests. Many flow parameters were obtained and compared to understand how each parameter effect the flow pattern and the thermal field. From the prediction of state of the boiler with the obtained parameters, it may be concluded that:

1- ANSYS FLUENT program has been used may be for the first time, to simulate combustion for liquid fuels in a combustion chamber of a boiler. It was found to be an accurate and good method for CFD predictions of all physical and chemical properties of the combustion in the boiler as shown by the results and comparison.

2- This three dimensional study was found to be suitable to present the combustion process for both liquid fuels, (Iraqi Diesel and Light Diesel) and gaseous fuels, (Methane and Iraqi LPG) to predict the physical and chemical parameters produced by the combustion numerically. These results were compared with the experimental results and also with the other studies in the same field to enhance the performance of these fuels in future.

3- The increase of (C/H) ratio had led to an increase in the overall temperature of the fuel products of combustion, but, in spite of the high

(C/H) ratio of Iraqi Diesel, the overall temperature of it had reduced due to the sulfur contents in the fuel.

4- The heat of evaporation and mixing of liquid fuels had effected clearly the combustion process and it's parameters like temperature, because the liquid fuels needed more time to evaporate and then mix while the gaseous fuels needed mixing only.

5- There are two big vortices between the burner and the wall of combustion chamber near the inlet of front plenum that vortices had appeared due to the returned hot gases in opposite direction after hitting the closed end of combustion chamber and some of the air inlet that try to escape from the combustion chamber and enter the front plenum due to the trapped situation in the combustion chamber.

6- The maximum temperature inside the boiler for Methane is (1631K). It is close to burner but for Iraqi LPG (1706K) it's further away of that of Methane because it is a mixture of gases. For liquid fuels, it was for Iraqi Diesel (1986 K) and for Light Diesel (1955K). Both are further away from gaseous fuels, for the maximum temperature, because of their higher density and viscosity than that for gaseous fuels. The temperature distribution among all positions as a result to their higher turbulent velocity in addition to that the combustion process produces water vapor, it works as coolant to absorb some of heat. The water vapor percentages in the gaseous fuel combustion is more than that in liquid fuels.

7- The pressure of furnace at burning gaseous fuels was larger than that for oil fuels except the Iraqi LPG (because it is a mixture of many different species). This is in agreement with the literature, because of the difference in temperature of burned fuel and the density, which obey the general ideal gas law.

8- The turbulence kinetic energy of burning for gas fuel was higher than that for liquid fuels (171.1152m^2/s^2 for Methane, 88.648 m^2/s^2 for Iraqi LPG, 116.2115m^2 /s^2 for Iraqi Diesel and 154.429 m^2 /s^2 for Light Diesel) because of the density and adhesion among the fuel particles. In addition, higher kinetic energy was found at high temperature situations inside the boiler.

9- The dominated velocity at the furnace entrance (burner) is the axial velocity but the maximum axial velocity takes place close to the nozzle where the fuel injected.

6-2 Recommendations:

The following recommendations for future works may be suggested:

1- Study of (temperature, velocity, heat transfer, chemical reaction, corrosion and erosion) using FLUENT program for plate superheater, convective superheater, and radiant superheater economizer, reheater, and regenerative air heater by using the results of this work.

2- Modeling efficient design of furnace, after the study of all circumstances of operation for this furnace chamber.

3- Fabricate the suggested design of the burner and use it to study the Iraqi LPG or any gas fuel experimentally and compare the obtained results with this study results.

4- Continuous analysis of fuel since it affects the performance of operation cycle and for protecting the pipes of boiler against punches or accident fractures as a result to burning higher amount of fuel, or due to decreasing the efficiency of system. That is for improvement of fuel by adding special solutions.

5- Using different air / fuel ratios and study the effect of increasing the equivalence ratio on the combustion parameters.

REFERENCES

REFERENCES

[1] Jones W.P, PhD Thesis, Imperial Collage, London University, (1971).

[2] Jones W.P. and Launder B.E., "Prediction of Laminarization with a two – Equations Model of Turbulence", International Journal of Heat Mass Transfer, volume 15, pp.301-345, (1972).

[3] Chomiak J., "Combustion", ABACUS press, 1990, PP. 180-185.

[4] Jones J.C., "Combustion Science", Australian Print Group, Australia, (1993).

[5] Lefebure A.H., "Gas Turbine Combustion", Second Edition, Taylor and Francis Group, UK (London), 1999.

[6] Gupta A.K., Lilley D.G, syred N., "Swirl Flows", 1st edition, Abacus press, United Kingdom, 1984.

[7] Beer J.M. and Chigier N.A., "Combustion Aerodynamics", Applied Science, London (1972).

[8] Mohseni K, Kosovic B., Shkoller S. and Marsden J.E., "Numerical Simulations of the Lagrangian averaged Navier-Stokes equations for Homogeneous Isotropic Turbulence", physics of Fluids, Vol.15, No.2, 2003.

[9] Versteeg H.K. and Malalasekera W., "An Introduction to Computational Fluid Dynamics, the Finite Volume Method", Longman Group Ltd Copyright, England, 1995, (P.41).

[10] FLUINT 6.3.26, "User Guide and Manuals", 2008.

[11] Najim S.E., "An Aerodynamics Study of Cyclonic Combustion with Gaseous Fuels", Ph.D. Thesis, Mech. Eng. And Energy Studies Dept., Cardiff University, 1979.

[12] Arscott J.A., Chew P.E. and Lawn C.J., "Improvements in Combustion Efficiency through the Matching of Air and Fuel on an oil-Fired Boiler", Journal of Institute of Energy, LIII, pp. 3-15, (1980).

[13] Sislian J.P., Jiang L.Y. and Cusworth R.A., "Laser Doppler Velocimetry Investigation of the Turbulence Structure of Axisymmetric Diffusion Flames" Progress in Energy and Combustion Science, Vol.14, No.2, PP.99-146, (1988).

[14] Holmborn J., "Development of LPP-burner for Industrial Gas-Turbine Application", Ph.D. Thesis, Heat and power Eng. Department, Lund Institute of Technolgy, Lund, Sweden, (2003).

[15] Bruno C. and Losurdo M., "The Trapped Vortex Combustor: An Advanced Combustion Technology for Aerospace and Gas turbine Applications", Advanced Combustion and Aerothermal Technologies by Springer copyright pp. 365-384.

[16] Love N.D., Parthasarathy R.N. and Gollahalli S.R., "Rapid Characterization of Radiation and Pollutant Emissions of Biodiesel and Hydrocarbon Liquid Fuels", ASME, Journal of Energy Resources Technology, (2009).

[17] Gruenberger T.M., "Studies of Soot and Carbon Black Formation by Incomplete Combustion and Thermal Decomposition of Natural Gas", Ph.D. Thesis, University of Wales, Cardiff School of Engineering, Division of Mech. Eng. and Energy Studies., Dec. (2000).

[18] Azazi F.A., "Aerodynamics and Thermal Prediction of Al-Hartha Power Generation Plant Furnace", Ph.D. Thesis, College of Engineering, Basrah University, Iraq (2001).

[19] Alhabbubi M.M., "Radiative Heat Transfer in Boilers Using the Zonal Method", MSc. Thesis, Mechanical Engineering, Babylon University, (2002).

[20] Baranski J., "Physical and Numerical Modeling of Flow Pattern and Combustion Process in Pulverized Fuel Fired Boiler", Licentiate thesis, Royal Institute of Technology (KTH), Stockholm, Sweden (2002).

[21] Saripalli, Raja, "Simulation of Combustion and Thermal Flow in an Industrial Boiler",M.Sc thesis, University of New Orleans (2005).

[22] Syred N., "A Review of Oscillation Mechanisms and the Role of Precessing Vortex Core (PVC) in Swirl Combustion Systems ", progress in Energy and Combustion Science, 32(2006), pp.93-161.

[23] Soroka B.," Thermodynamics of Modern Low-Emission (Low-NOx) Processes in the Combustion of Hydrocarbon Fuels, "Advanced Combustion, and Aerothermal Technologies by Springer Copyright, pp. 37-85, (2007).

[24] Agranat V.M., Tchouvelev A.V., Cheng Z. and Zhubrin S.V.," CFD Modeling of Gas Release and Dispersion: Prediction of Flammable Gas Clouds", Advanced Combustion and Aerothermal Technologies by Springer Copyright, pp. 179-195, (2007).

[25] Snegirev A.YU. And Isaev S.A., "Turbulent Combustion and Thermal Radiation in a Massive Fire", Advanced Combustion and Aerothermal Technologies by Springer Copyright, pp. 197-209, (2007).

[26] Sigal A.I. and Dolinsky A.A., "The Influence of Moisture in Air on the Working Efficiency of Boilers in the Industrial and Municipal Energy Sectors", Advanced Combustion and Aerothermal Technologies by Springer Copyright, PP. 331-339, (2007).

[27] Sobolev V., Snegirev A., Shinder Y. and Lupulyak S., "Modeling of Turbulent Diffusion Combustion in the Jet Flames of the Rectilinear-Swirl Burners", The 3rd international conference "Heat and mass transfer and Hydrodynamics in swirling flows", 21-23 October, (2008), Moscow, Russia.

[28] Bird R.B.,Stewart W.E. and Lighfoot E.N., "Transport Phenomena", Wiley International Edition, (1995).

[29] Anand G. and Jenny P., "Stochastic Modeling of Evaporating Sprays within a Consistent Hybrid Joint PDF Framework", Journal of Computational Physics, 228(2009) PP.2063-2081.

[30] Stopper U., Aigner M., Merier W., Sadanandan R., Stohr M. and Kim I.S., "Flow Field and Combustion Characterization of Premixed Gas Turbine Flames by Planar Laser Techniques", Journal of Engineering for Gas Turbines and Power, ASME, Vol.131, March (2009).

[31] ICI Caldaie Company Experimental Document for ICI Sixen 1000 boiler

[32] Moore H., "Liquid Fuels", the technical press LTD, London, (1935), PP.237238.

[33] Rose J.W. and Cooper J.R., "Technical Data on Fuel", 7th Edition (1977), Copyright (The British National Committee World Energy Conference) London.

[34] Law,Chunk K., "Combustion Physics",1st edition, Cambridge University Press (2006).

[35] FLUENT 14.5 "USER GUIDE", (2013).

[36] Lawn C.J., "Principles of Combustion Engineering for Boilers", Combustion Treatise, Academic Press Inc., Florida (USA), (1987).

[37] Nemoda S., Bakic V., Oka S., Zivkovic G. and Crnomarkovic N., "Experimental and Numerical investigation of gaseous fuel combustion in swirl chamber", International Journal of Heat and Mass Transfer, 48, P.P. 4623-4632, (2005).

Appendix A

APPENDIX A

The Qualitative Results of the Fuels

A-1 Light Diesel fuel

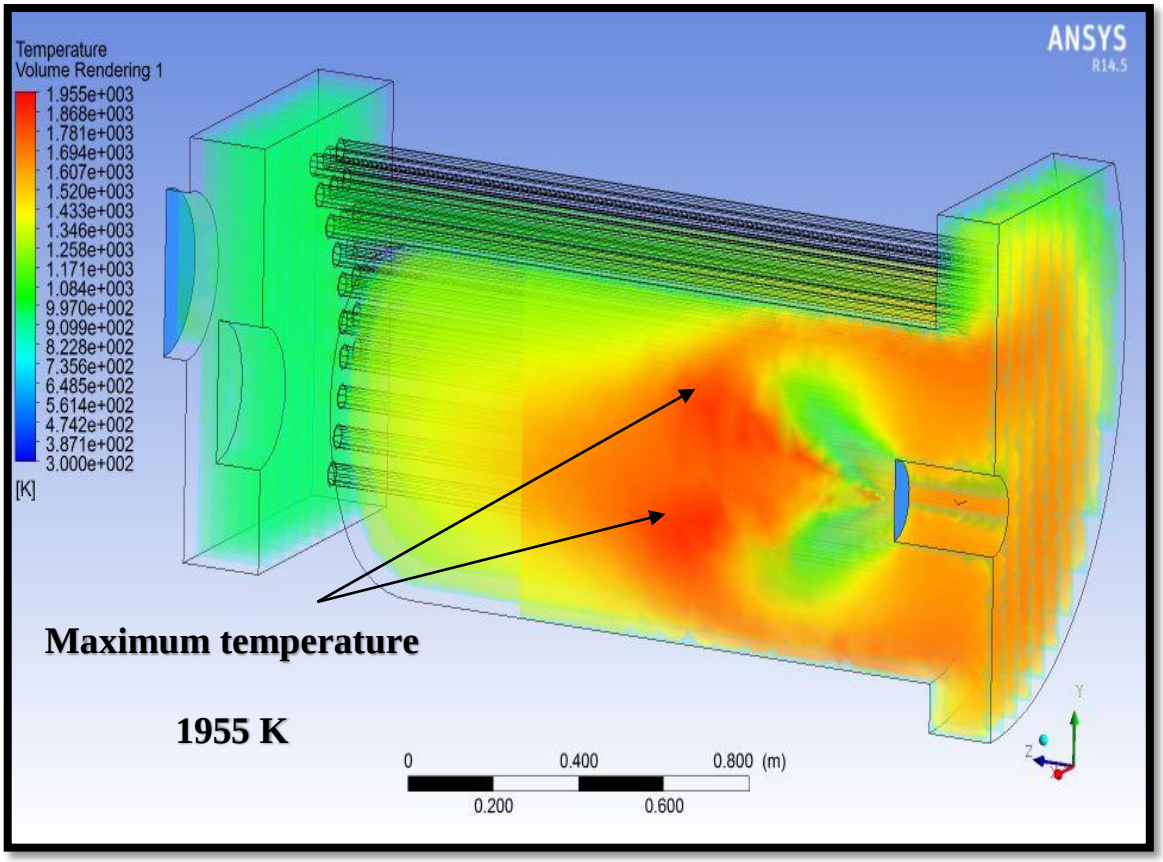

Figure (A-1) Temperature distribution of Light Diesel at the whole domain.

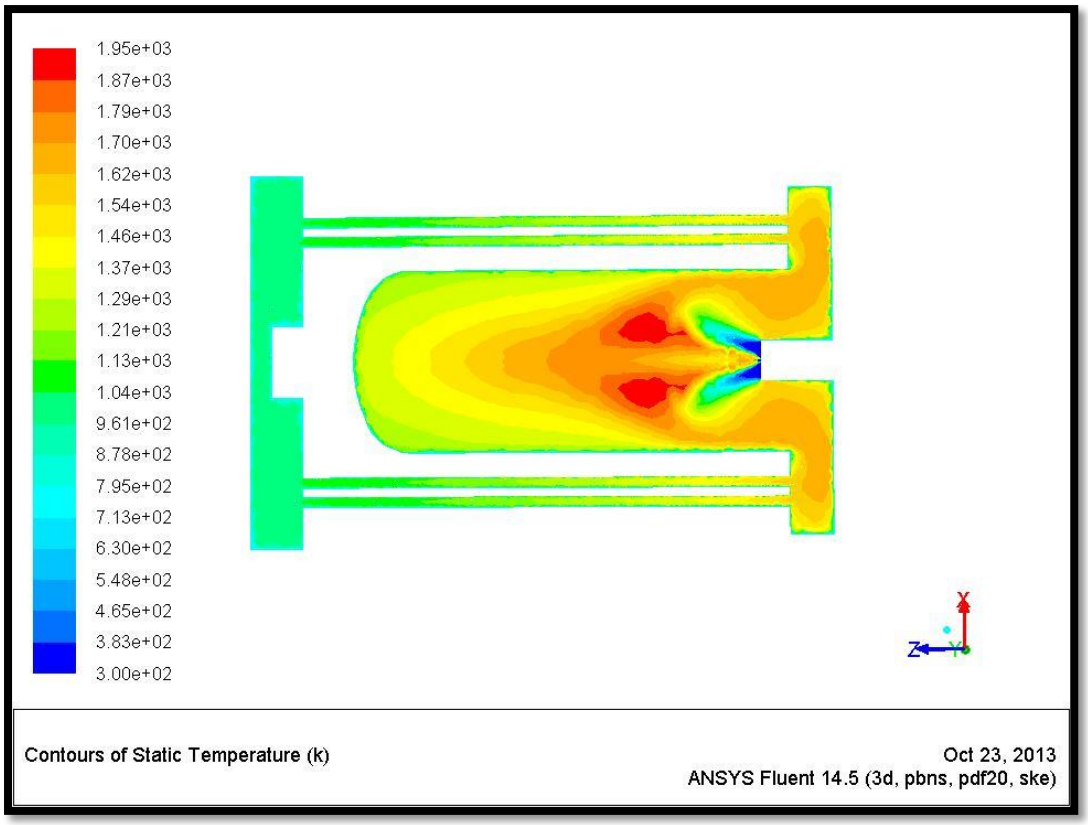

Figure (A-2) Temperature contours of Light Diesel at Y1 plane.

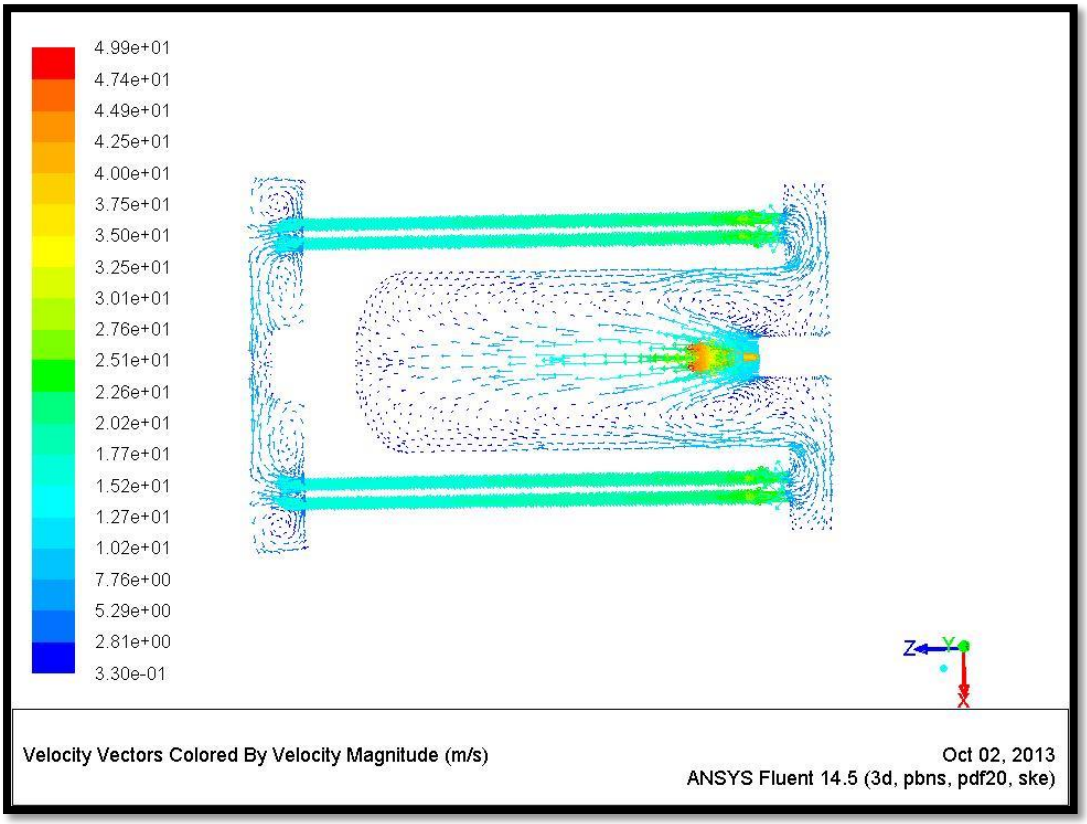

Figure (A-3) Velocity vectors of Light Diesel at Y1 plane.

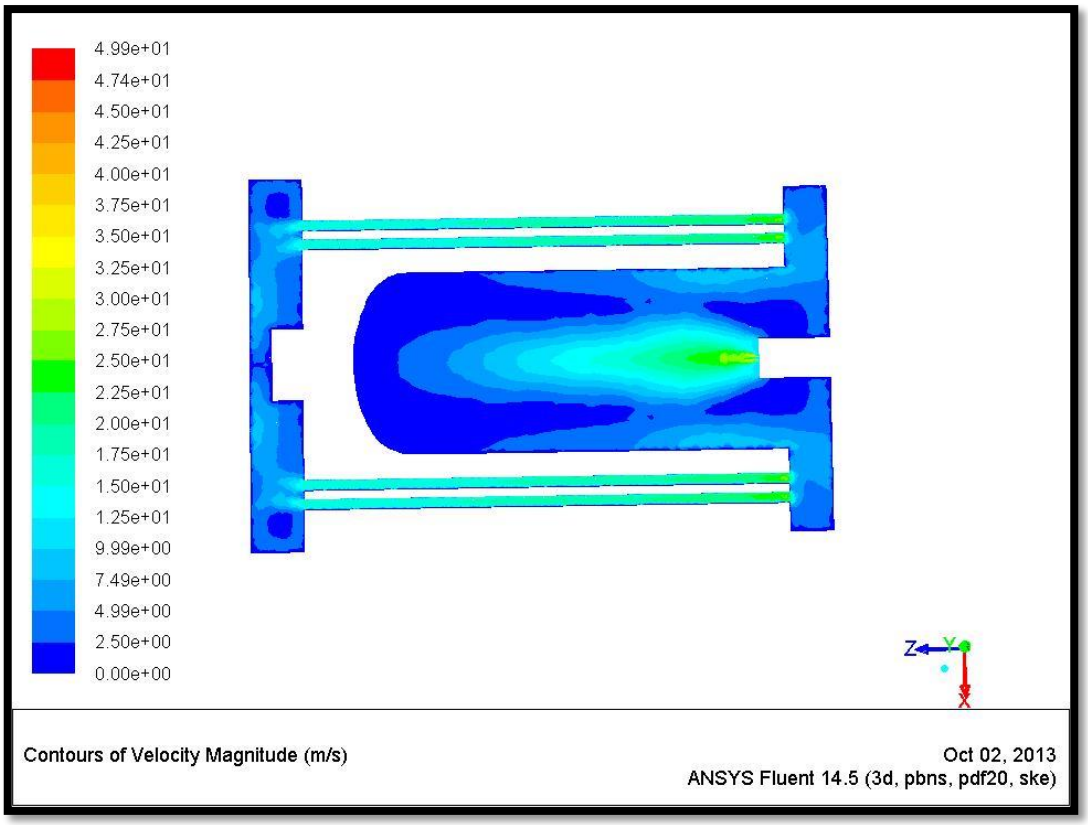

Figure (A-4) Contours of Velocity Magnitude of Light Diesel at Y1 plane.

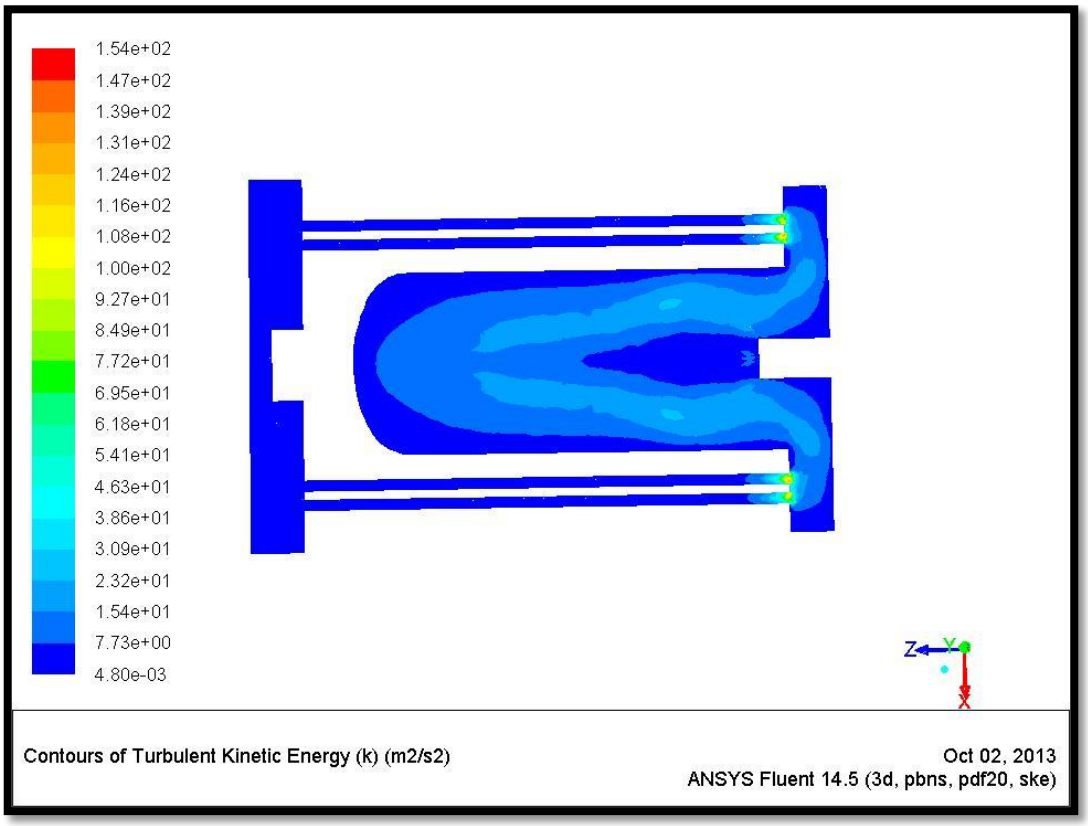

Figure (A-5) Contours of Turbulence Kinetic Energy of Light Diesel at Y1 plane.

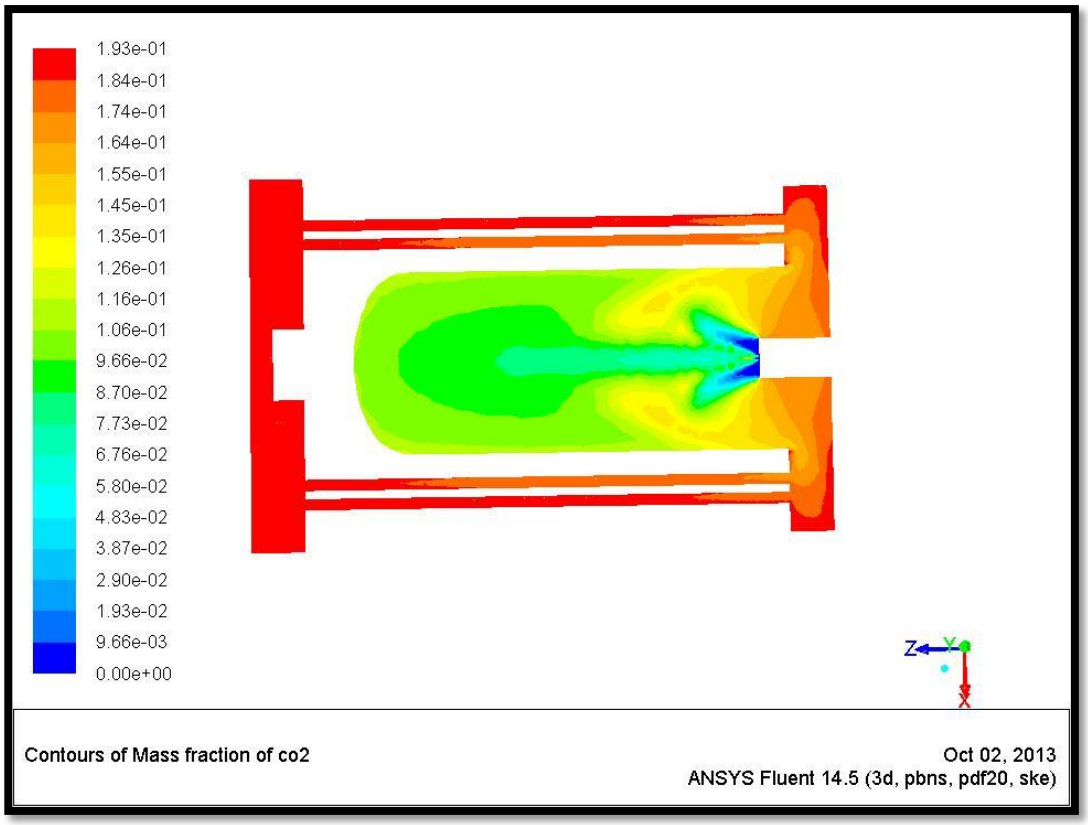

Figure (A-6) Contours of CO_2 mass fraction of Light Diesel at Y1 plane.

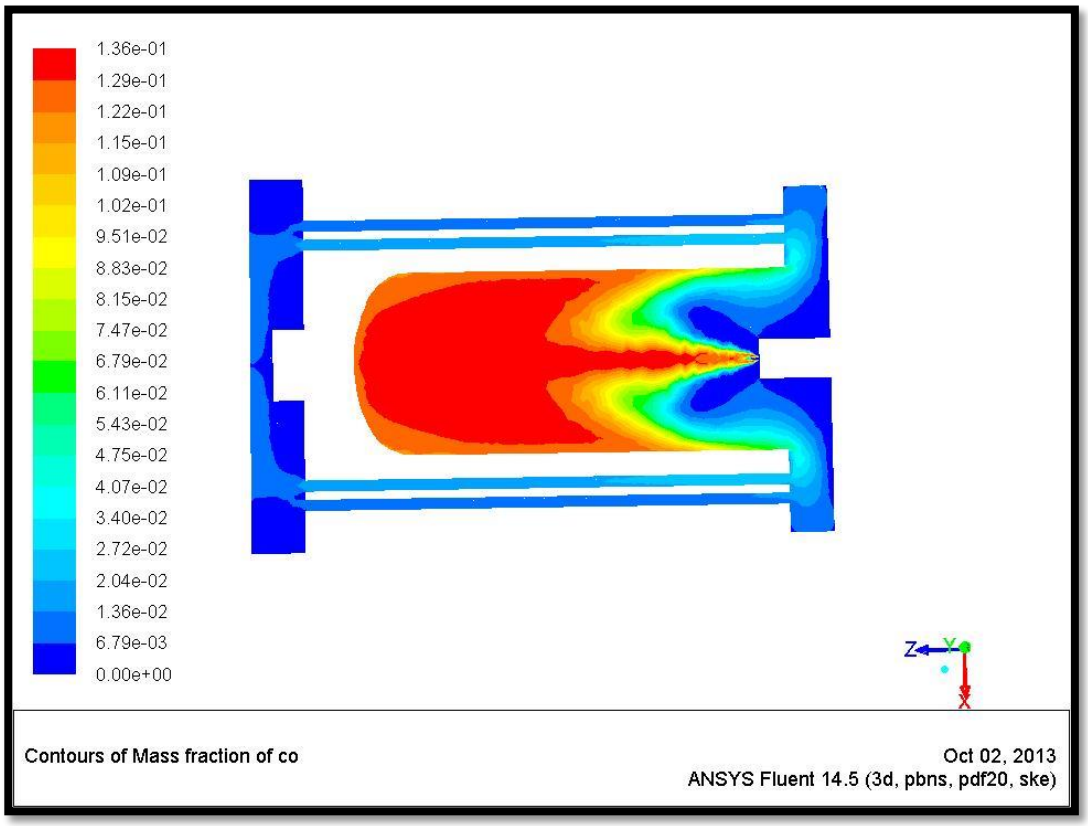

Figure (A-7) Contours of CO mass fraction of Light Diesel at Y1 plane.

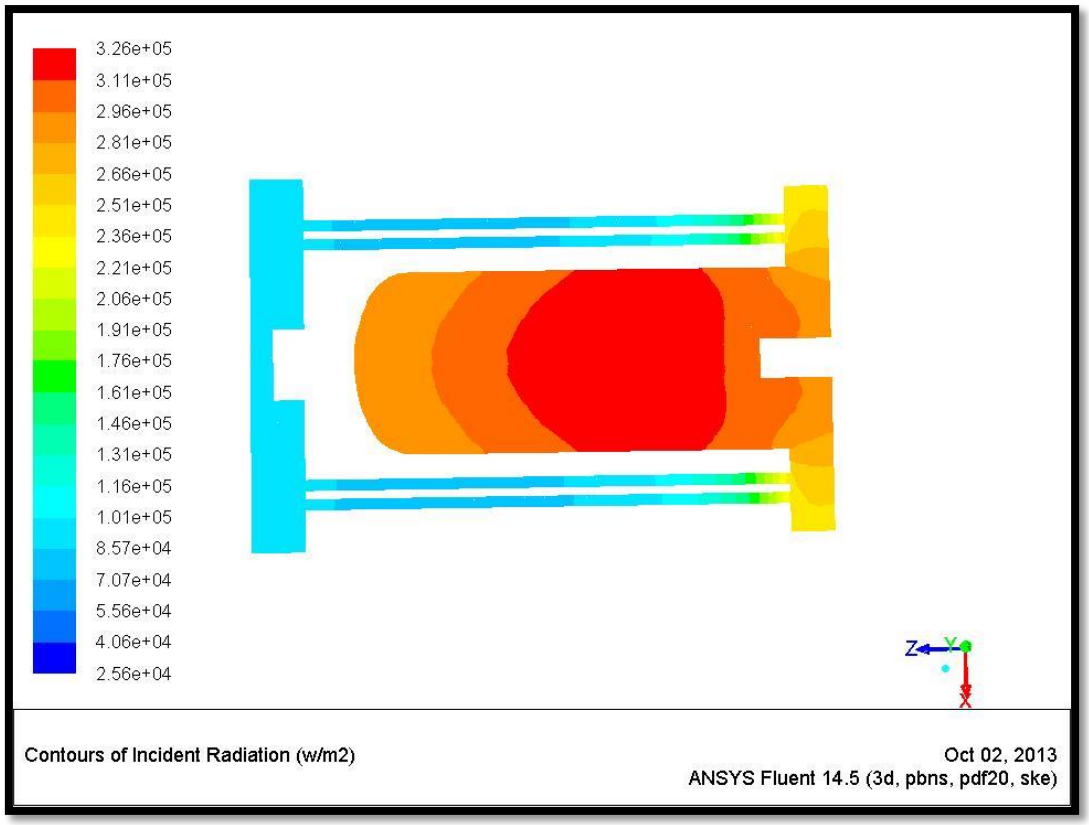

Figure (A-8) Contours of Incident Radiation of Light Diesel at Y1 plane.

A-2 Methane

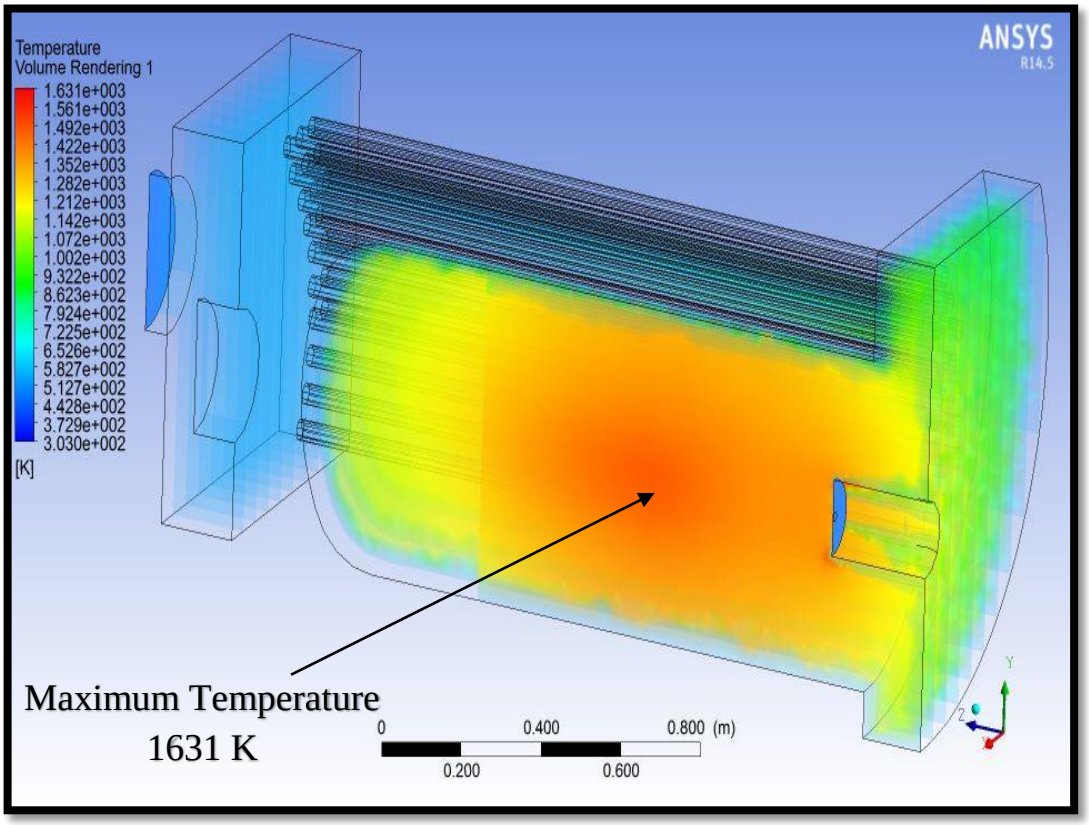

Figure (A-9) Temperature distribution of Methane at the whole domain.

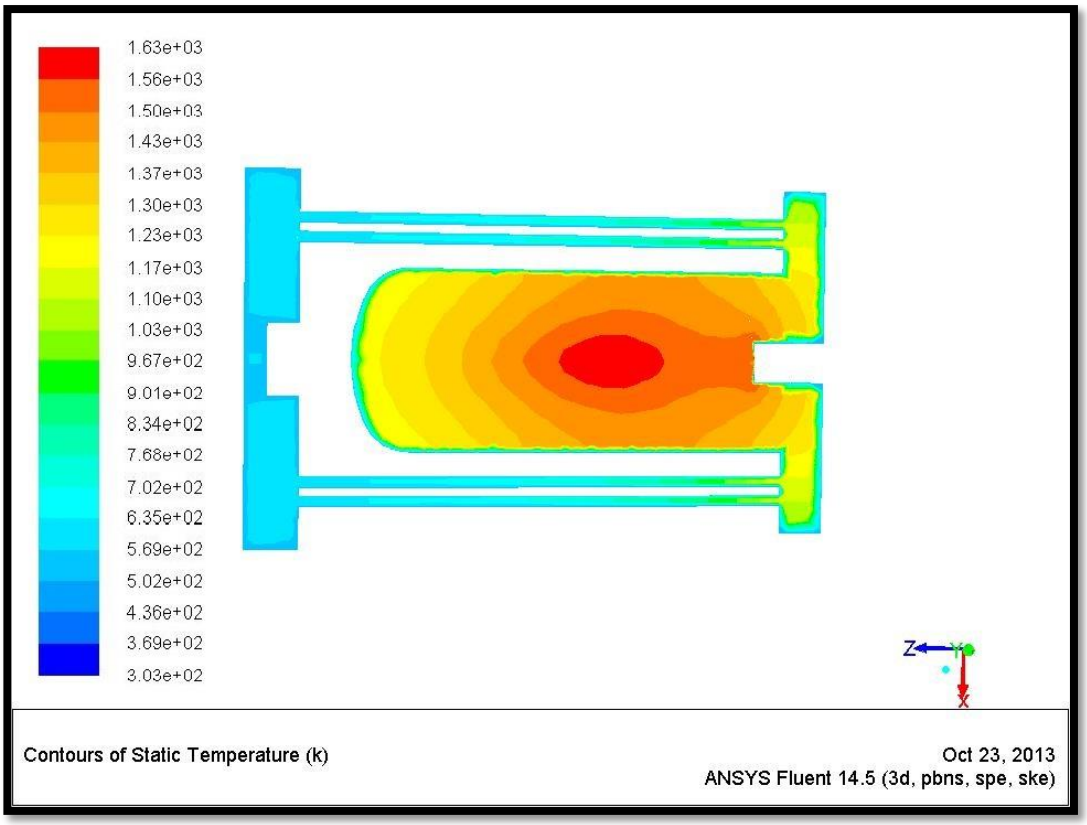

Figure (A-10) Contours of Temperature of Methane at Y1 plane.

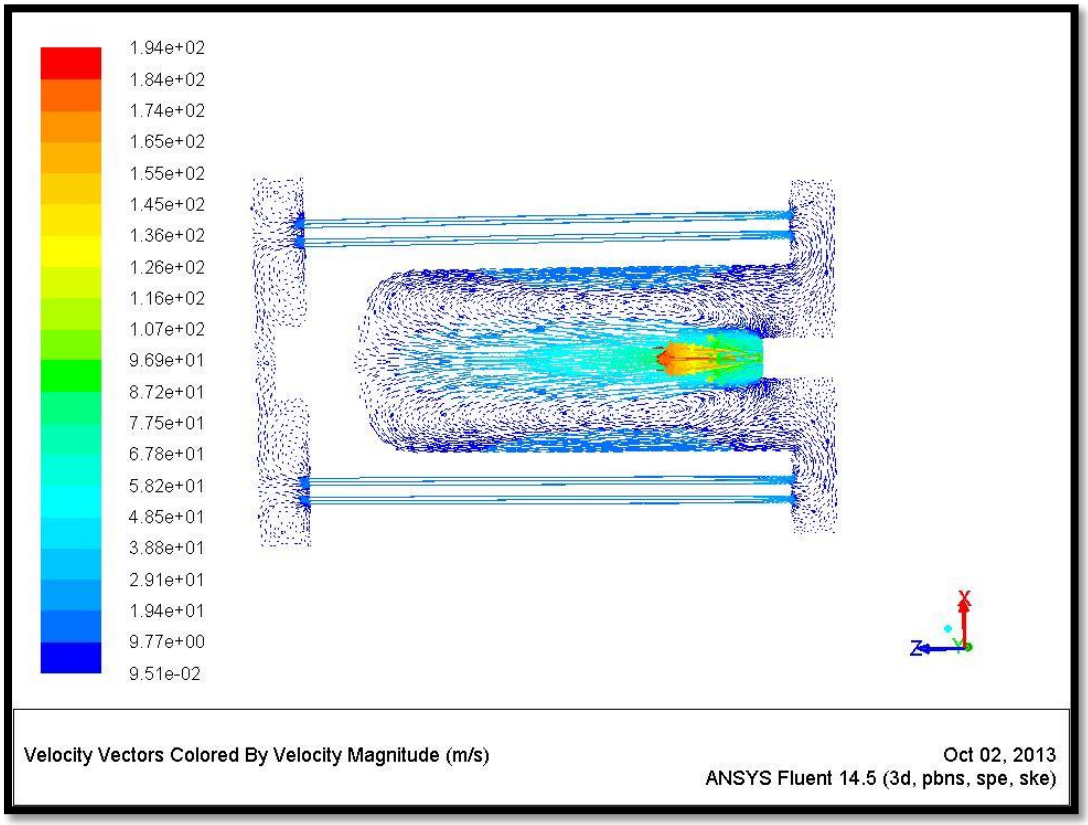

Figure (A-11) Velocity vectors of Methane at Y1 plane.

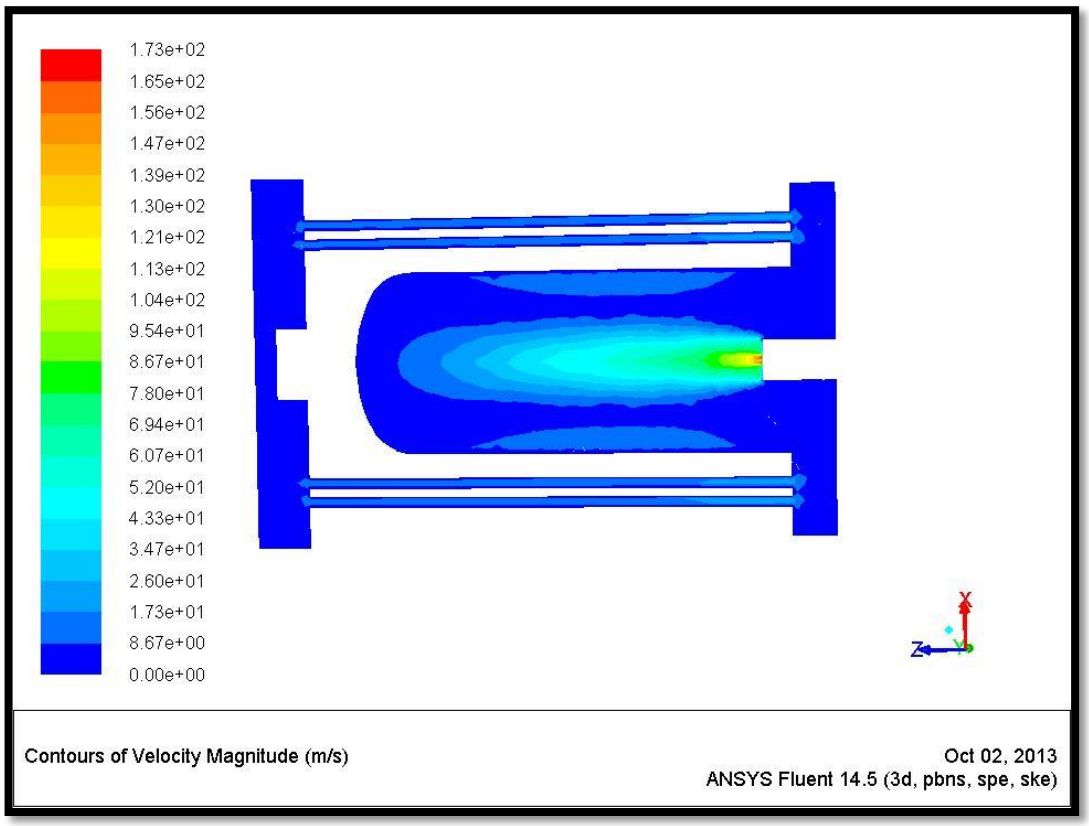

Figure (A-12) Velocity contours of Methane at Y1 plane.

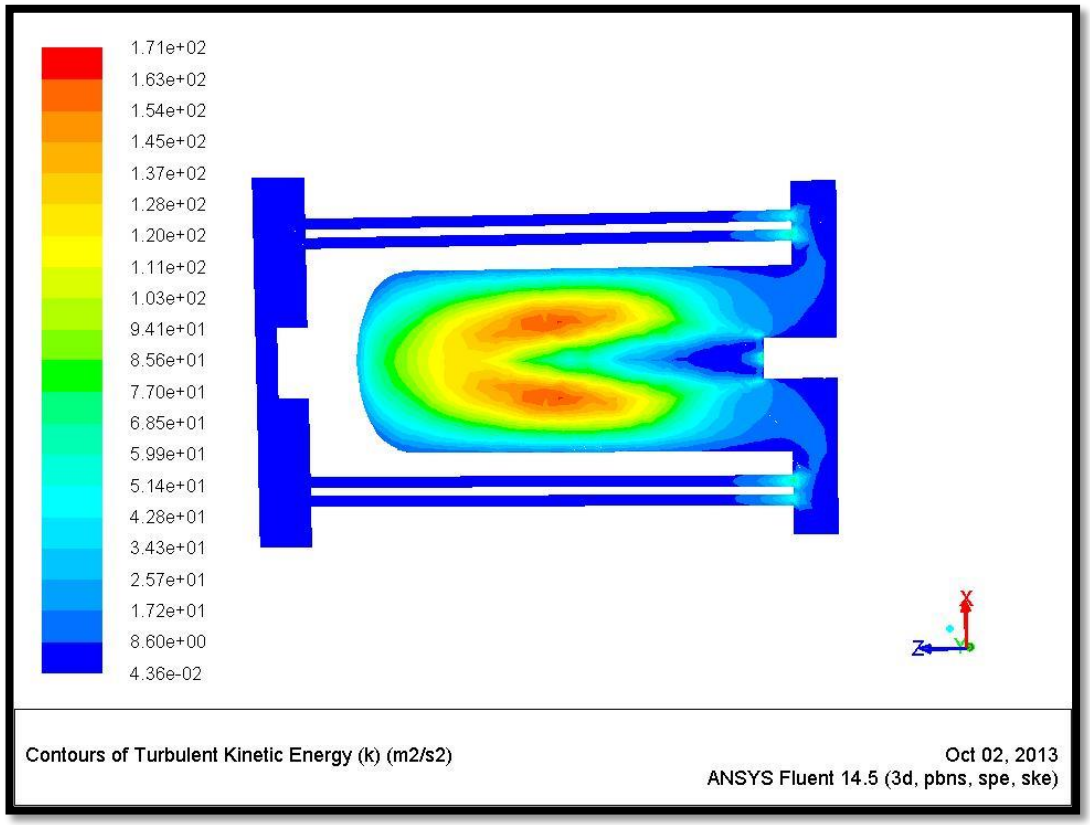

Figure (A-13) Contours of Turbulence Kinetic Energy of Methane at Y1 Plane.

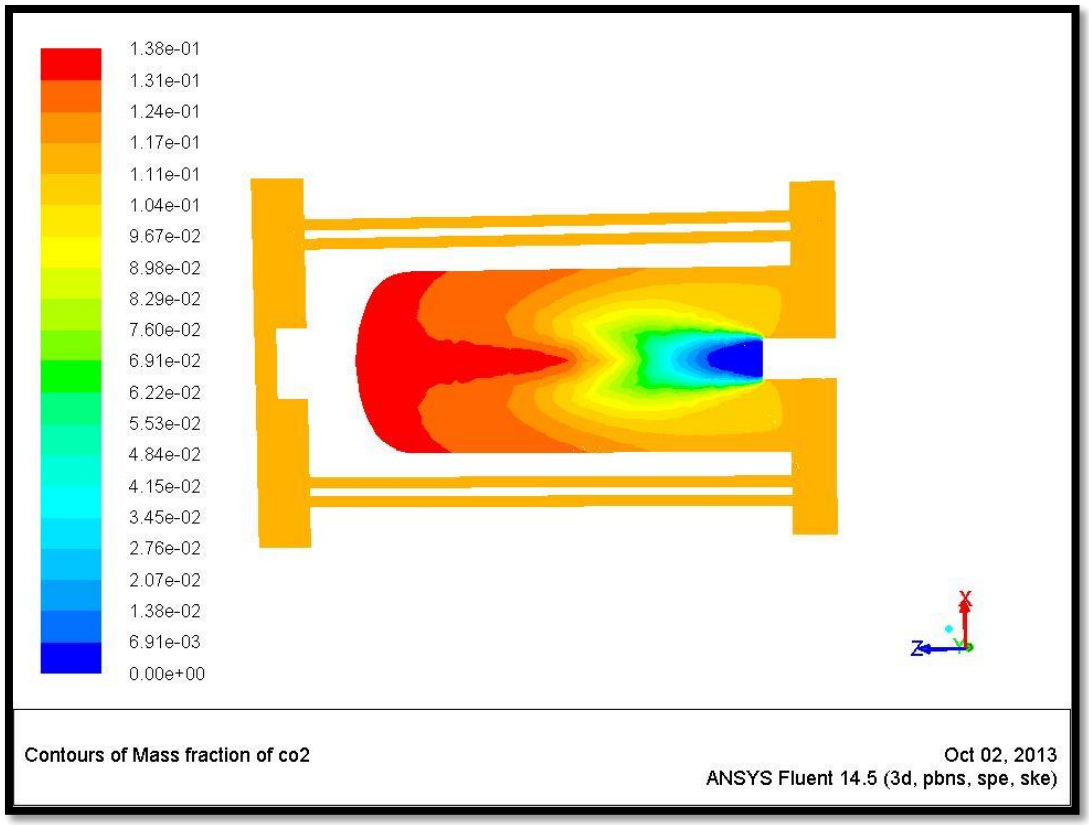

Figure (A-14) Contours of CO_2 mass fraction of Methane at Y1 plane.

A-3 Iraqi LPG fuel

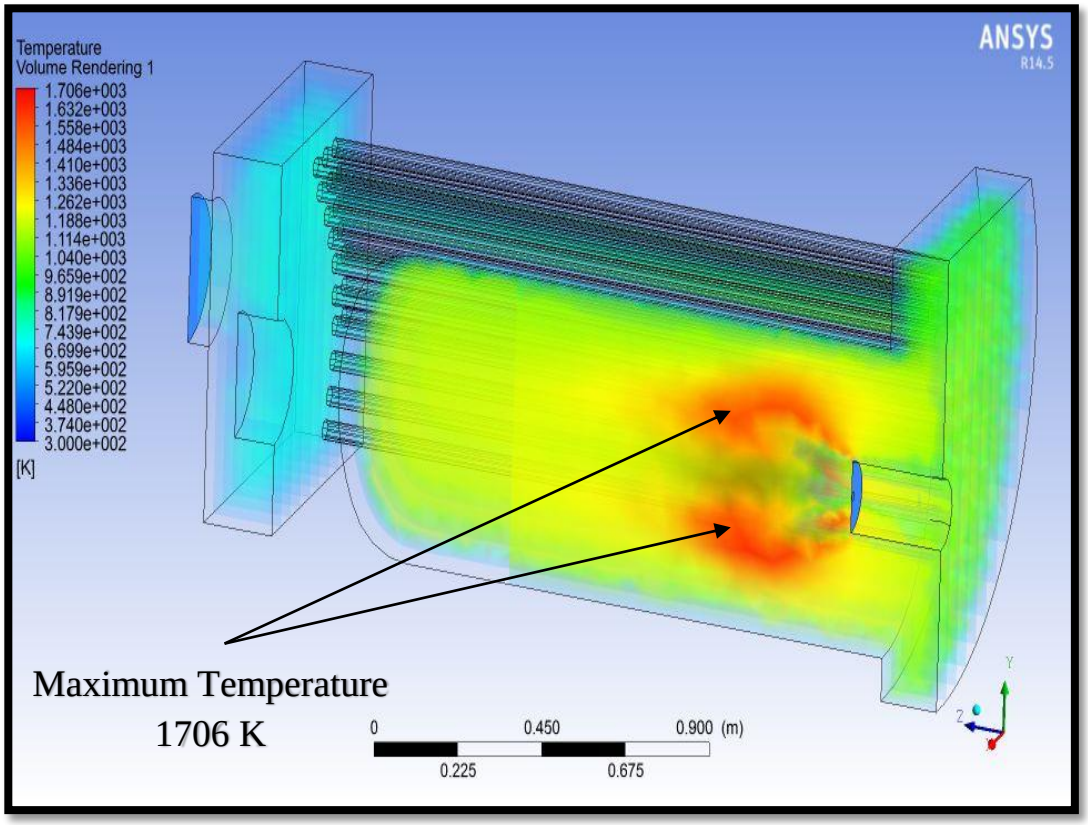

Figure (A-15) Temperature distribution of Iraqi LPG at the whole domain.

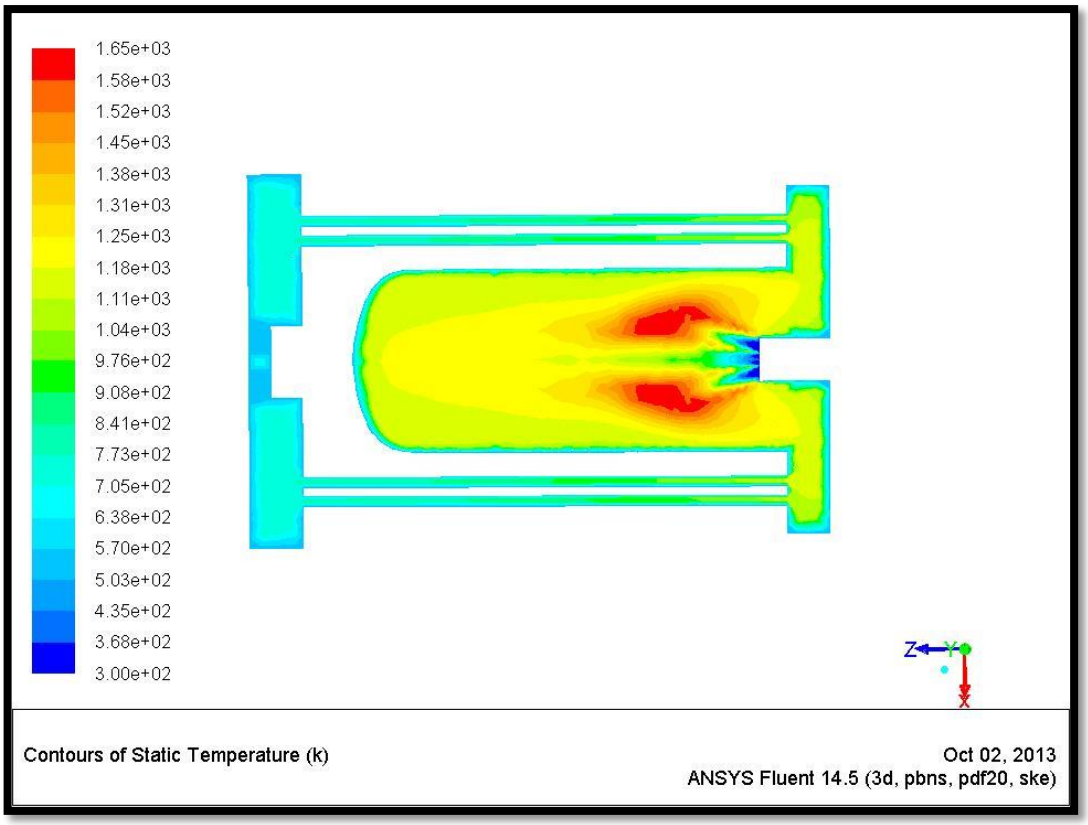

Figure (A-16) Contours of Temperature of Iraqi LPG at Y1 plane.

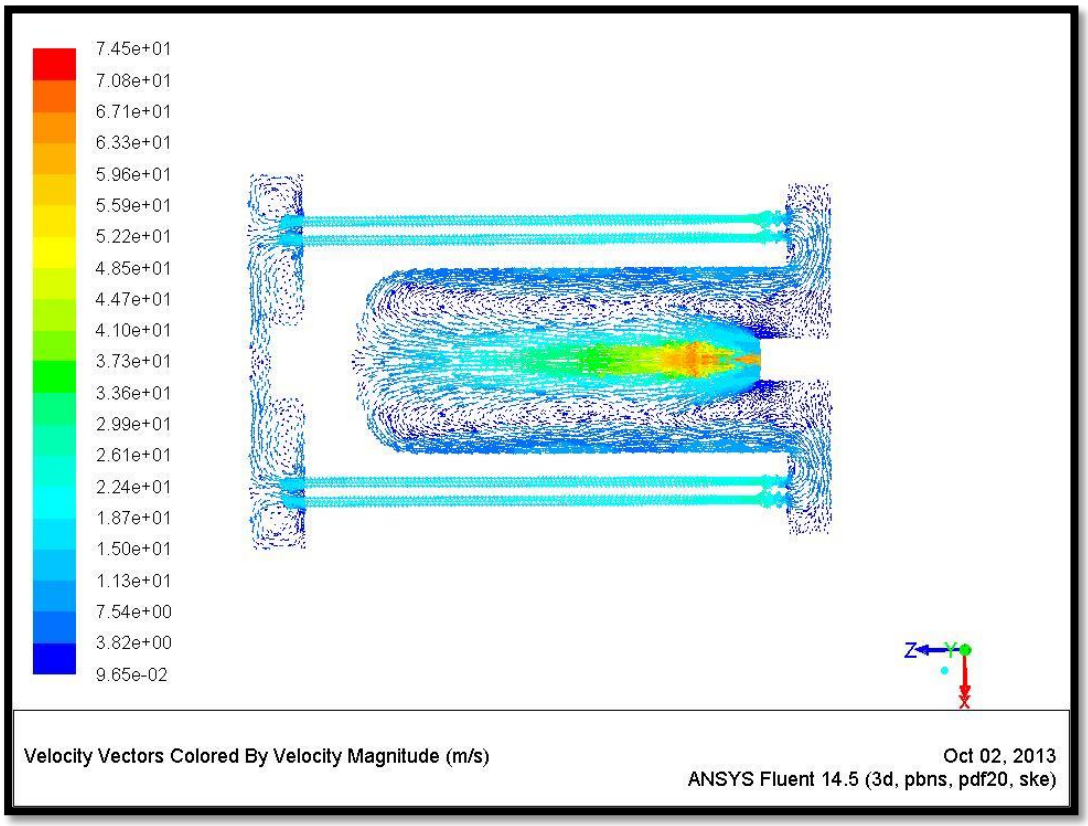

Figure (A-17) Velocity vectors of Iraqi LPG at Y1 plane.

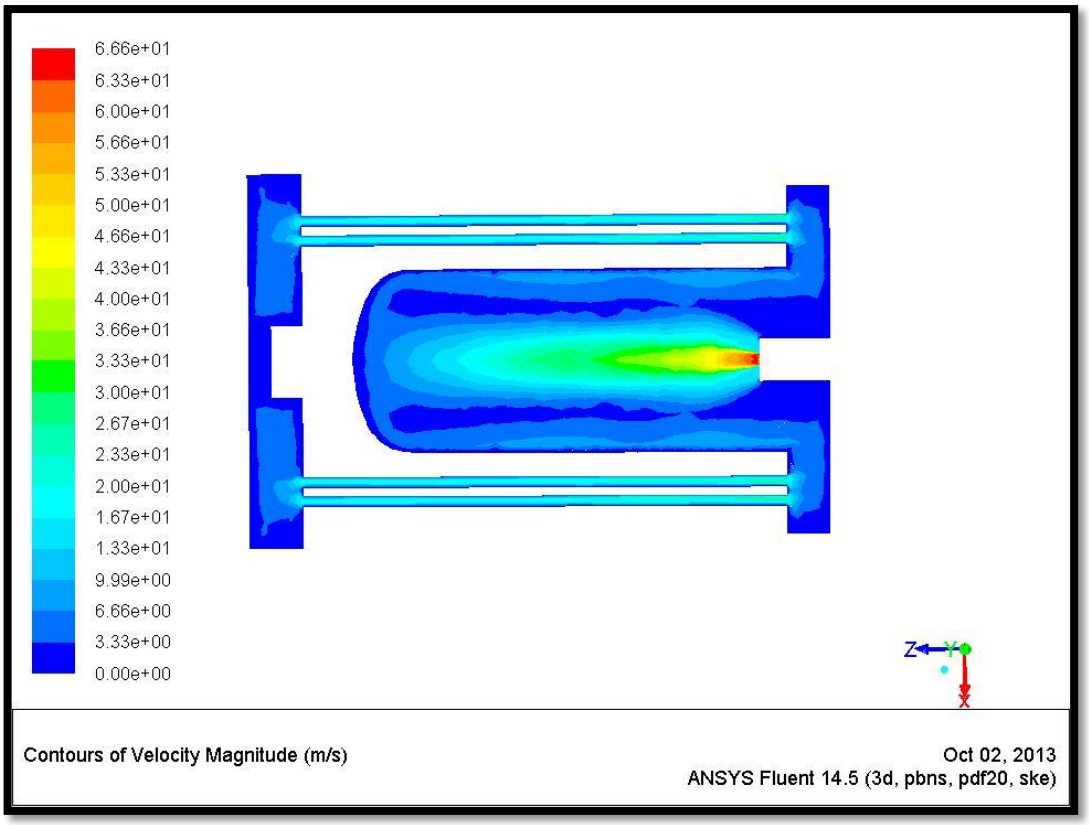

Figure (A-18) Contours of Velocity of Iraqi LPG at Y1 plane.

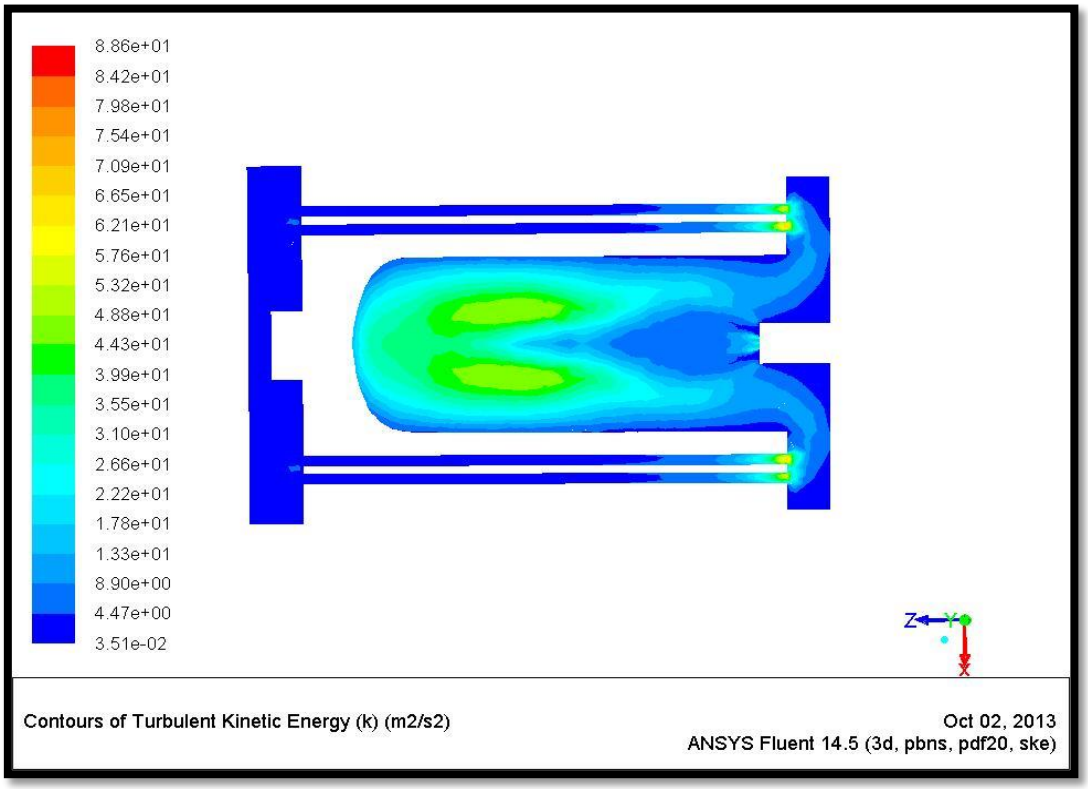

Figure (A-19) Contours of Turbulence Kinitic Energy of Iraqi LPG at Y1 plane.

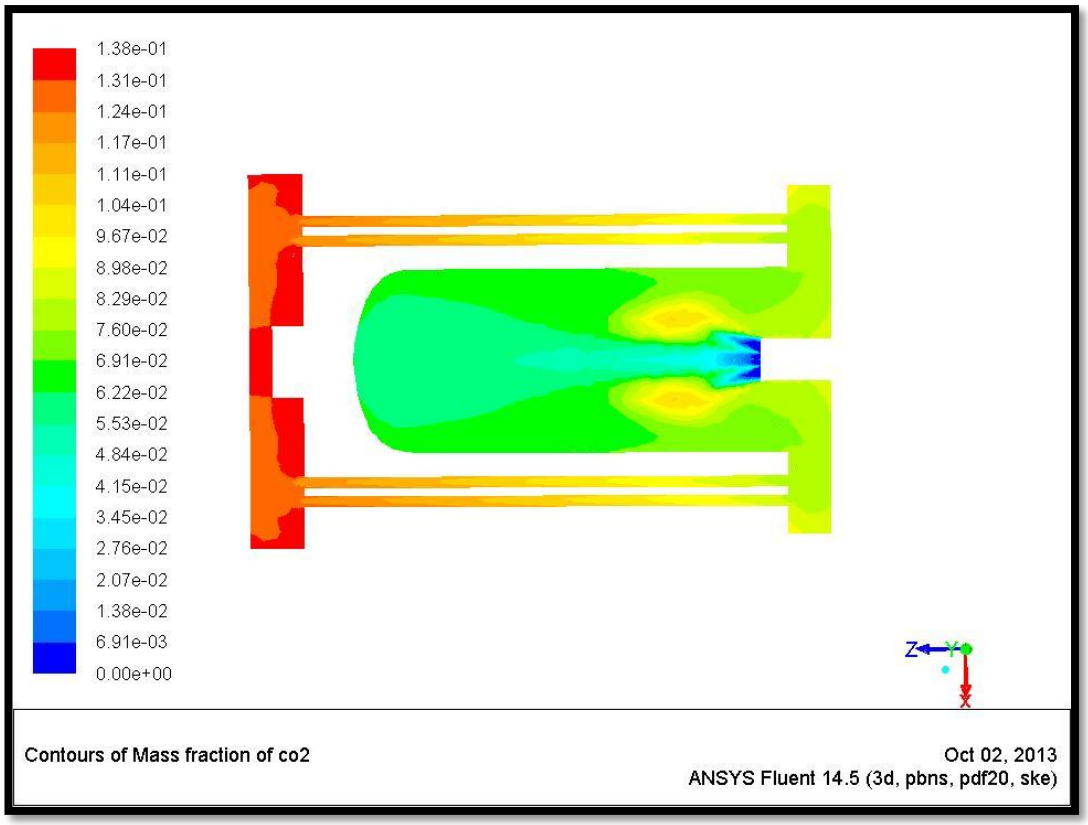

Figure (A-20) Contours of CO_2 mass fraction of Iraqi LPG at Y1 plane.

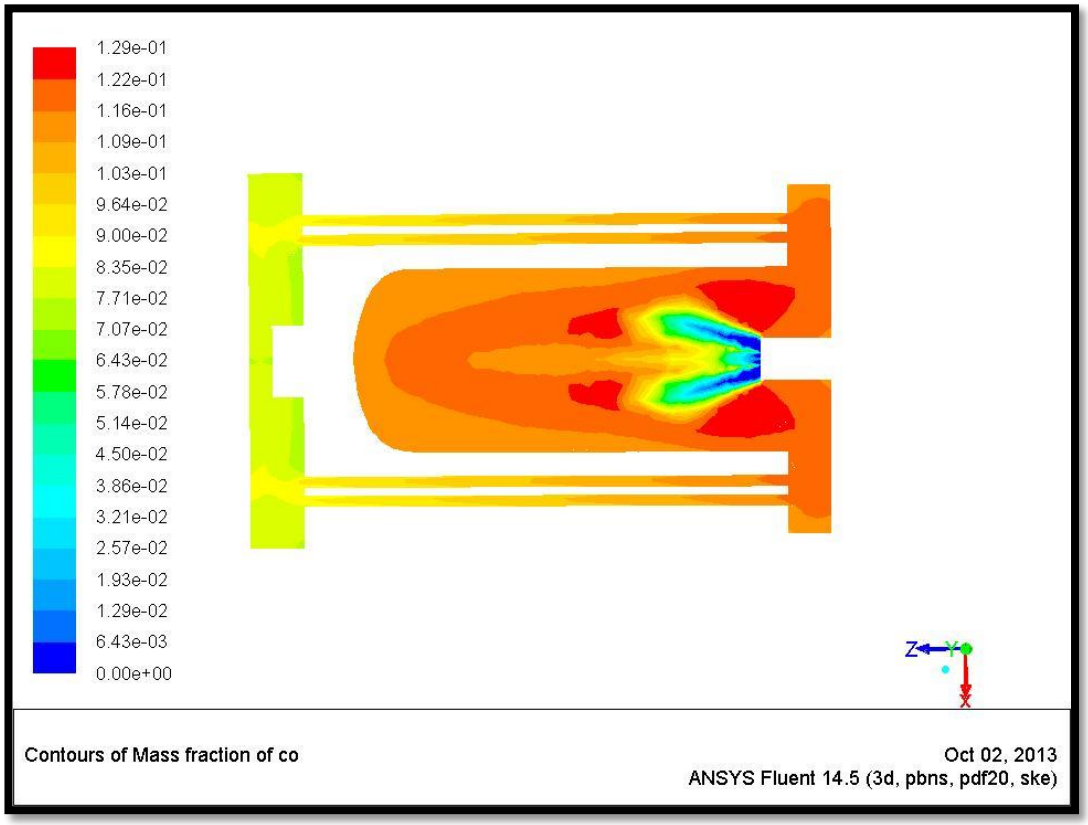

Figure (A-21) Contours of CO mass fraction of Iraqi LPG at Y1 plane.

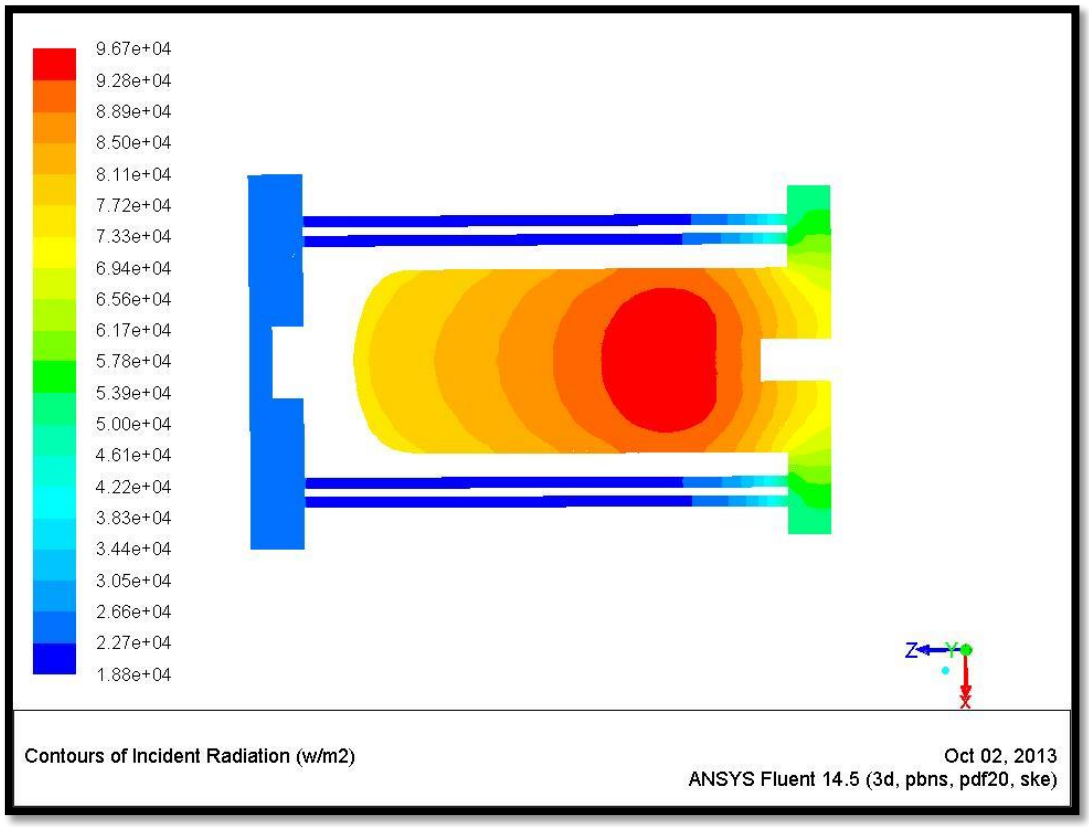

Figure (A-22) Contours of Incident Radiation of Iraqi LPG at Y1 plane.

A-4 Raja Saripalli study [21]

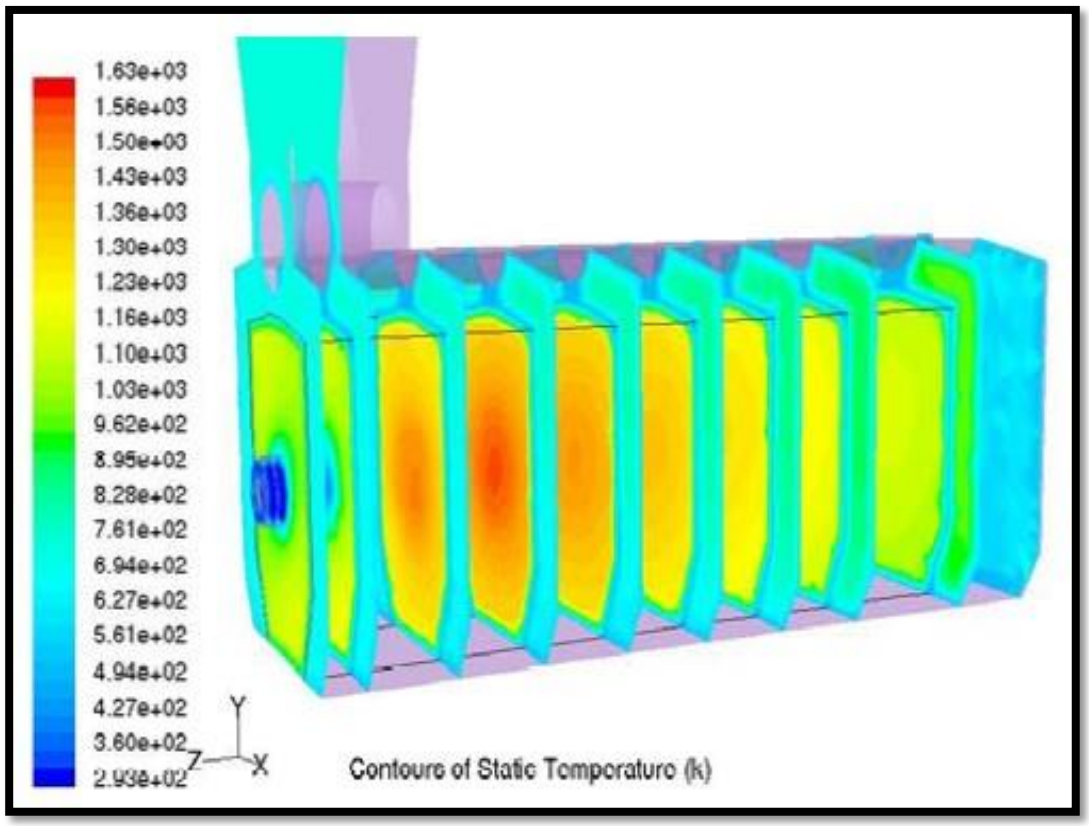

Figure (A-23) Contours of Temperature of Raja Saripali study [21] at the whole domain.

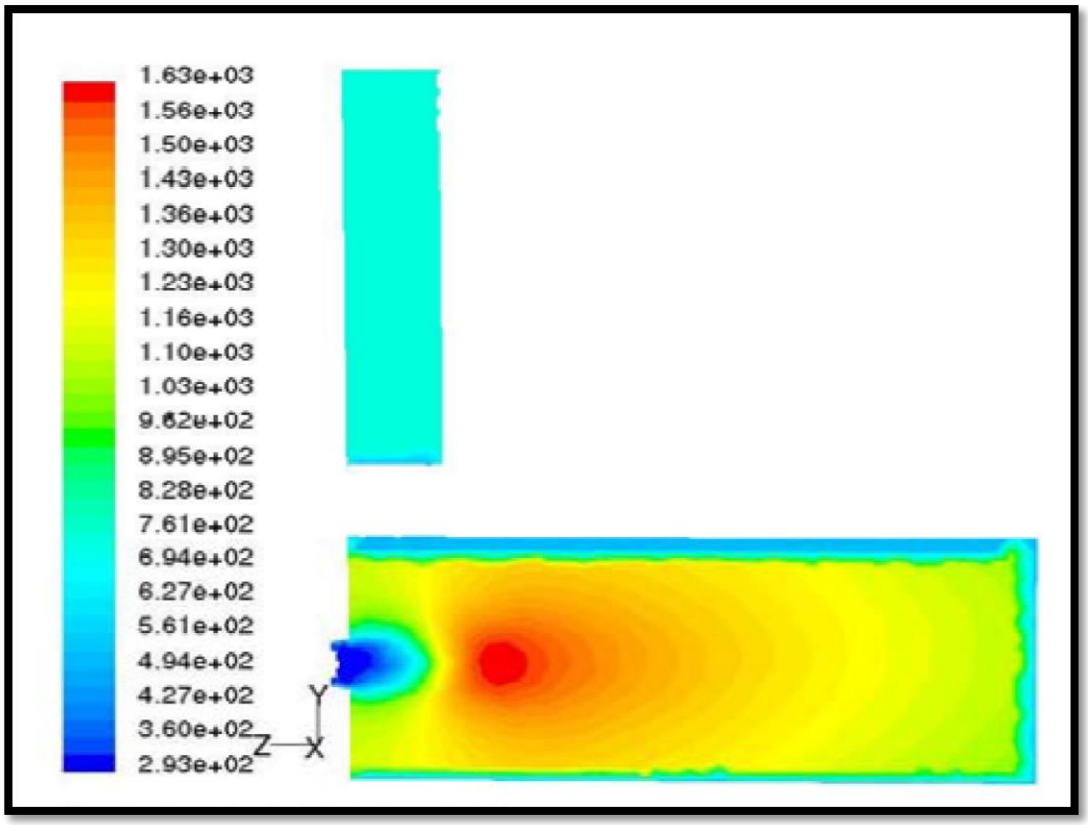

Figure (A-24) Contours of Temperature of Raja Saripali study [21] at side plane.

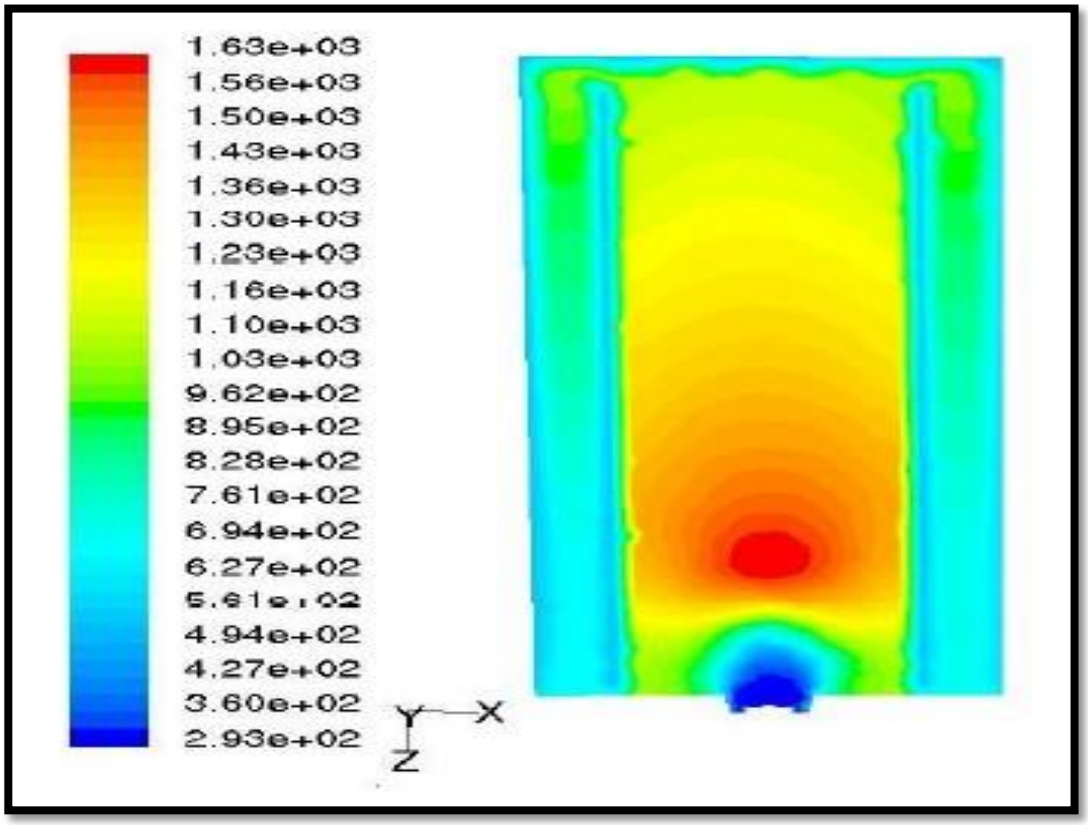

Figure (A-25) Contours of Temperature of Raja Saripali study [21] at Y plane.

A-5 Azazi study [18]

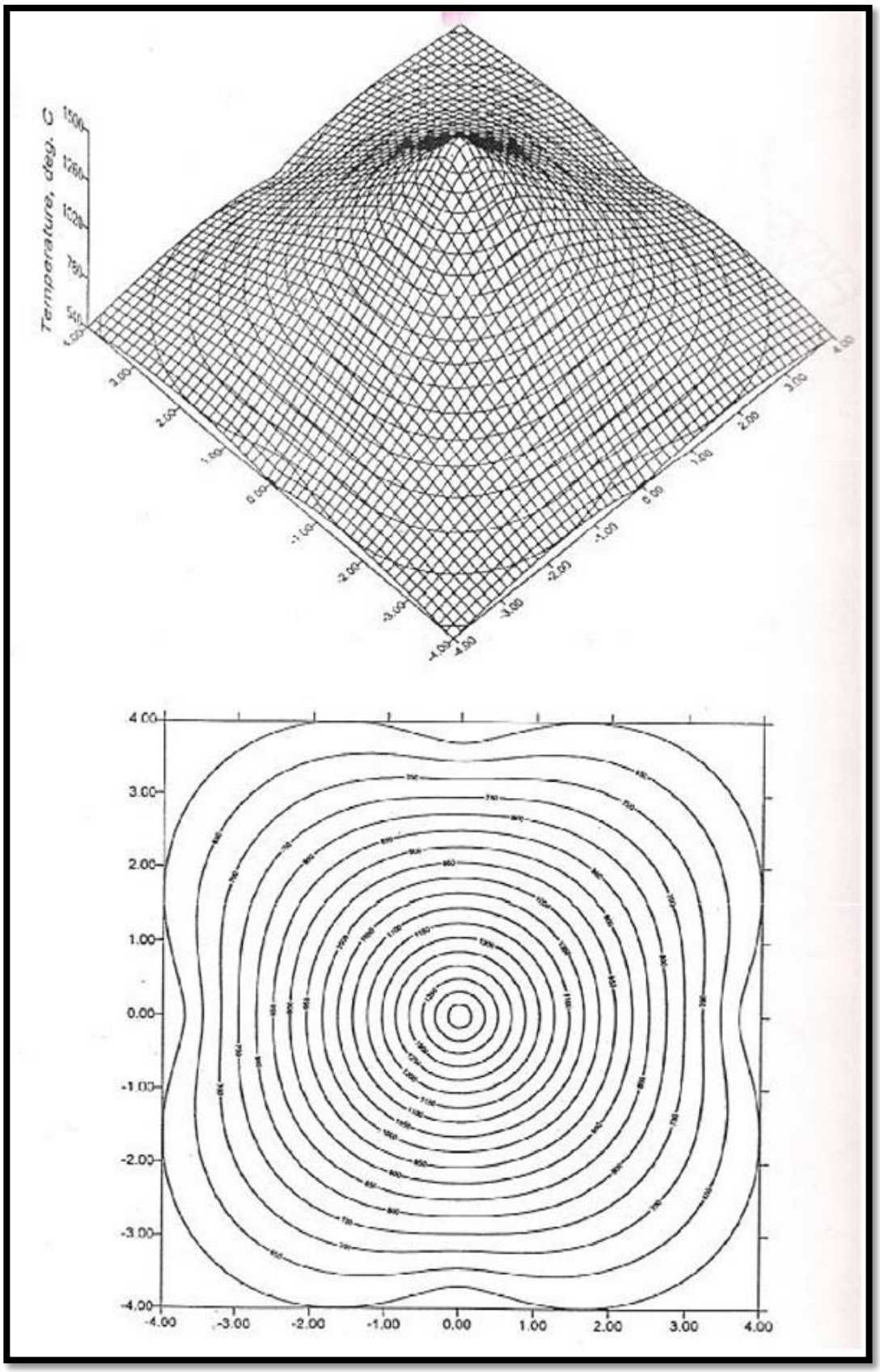

Figure (A-26) Temperature gradient of crude oil firing in Al-Hartha power plant [18].

A-6 Alhabbubi study [19]

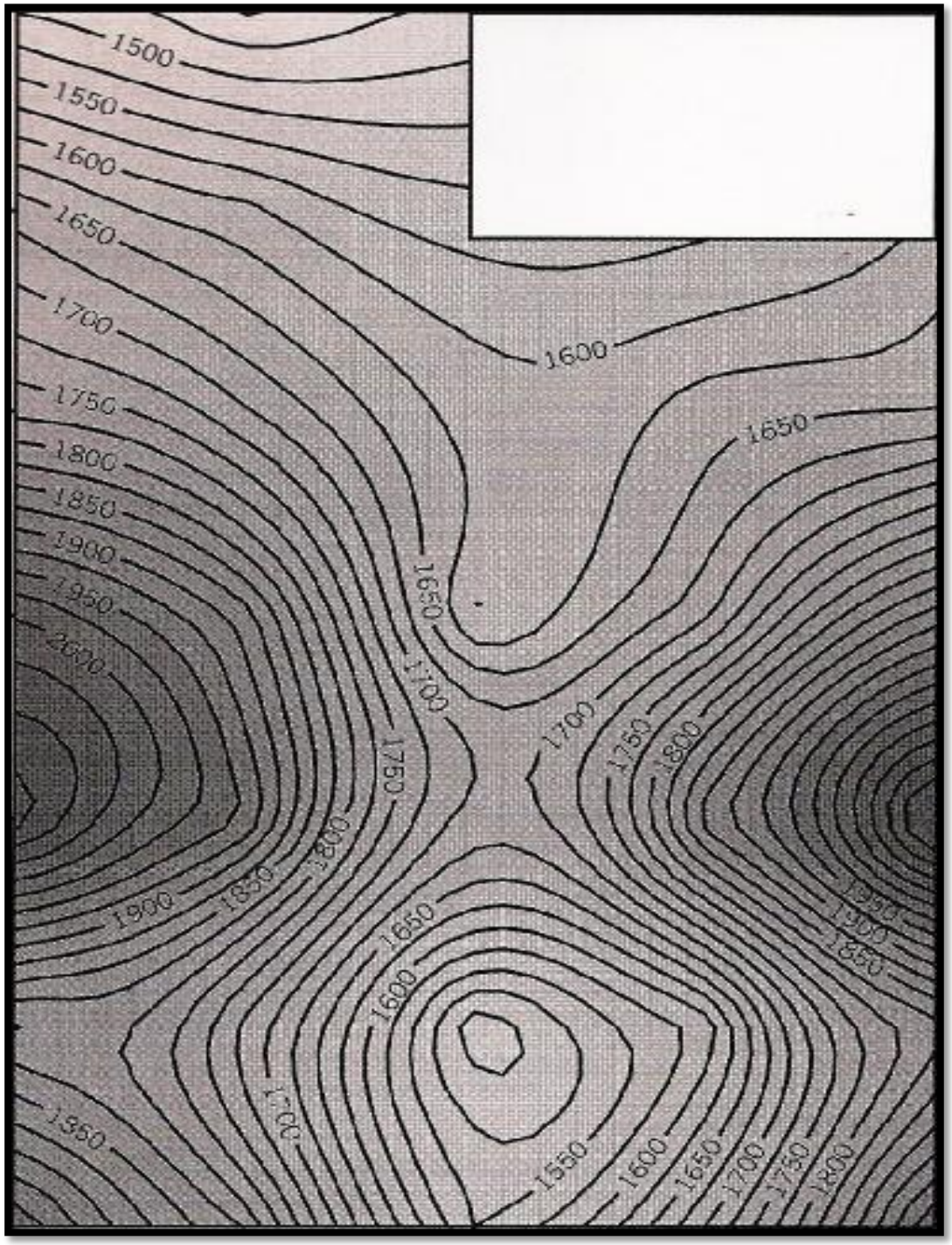

Figure (A-27) Temperature gradient inside Mussaib power plant furnace at oil firing (horizontal and opposite burners) [19].

للشركة المصنعة) و (564.5 كلفن) عند أستخدام البرنامج. وكانت كل النتائج المقاسة عمليا والمحسوبة نظريا متطابقة بشكل ممتاز.

عرضت النتائج على شكل مخططات مع مناقشة كافة المتغيرات مثل درجة الحرارة، الضغط، السرعة والطاقة الحركية للأضطراب لغرض مقارنه هذه المتغيرات لأربعه انواع من الوقود هي: الديزل العراقي، الديزل الخفيف، الميثان والغاز العراقي.

تم الحصول على أقصى سرعة داخل المرجل (34.2، 49.9، 106.39، 66.63) متر\ثانية عند حرق الديزل العراقي، الديزل الخفيف، الغاز العراقي، غاز الميثان على التوالي حيث تحدث هذه السرع بالقرب من الضرام.

كذلك قدمت هذه الأطروحة تصميما مقترح لضرام (محرقه) يعمل على الغاز العراقي او أي غاز اخر وذلك لتشغيل المرجل على الغاز بنفس كفائتة فيما لو تم استخدام الديزل العراقي.

أجريت مقارنة للعمل الحالي والاعمال السابقة ووجدت انها متوافقة تماما.

الخلاصة

قدمت هذه الأطروحة دراسة ثلاثية الأبعاد لمحاكاة حساب ديناميكية الموائع لأحتراق بعض أنواع الوقود السائل والغازي العراقي. كما قدمت بعض النتائج العملية لأحتراق الديزل العراقي.

تضمنت هذه الدراسة تأثير زيادة نسبة ذرات (الكاربون \ الهيدروجين) في الوقود والذي يؤدي الى زيادة المعدل العام لدرجات الحرارة بأستثناء الوقود العراقي بسبب وجود الكبريت الذي يمتص جزء من الحرارة المتولدة من عملية الأحتراق. كما تؤدي هذه الزيادة الى زيادة نسبه الوقود الغير محترق في غازات العادم.

تمت اضافه الديزل العراقي والغاز العراقي مع كافة خواصهما الى بيانات برنامج FLUENT بينما بيانات الديزل الخفيف وغاز الميثان موجودة ضمن بيانات البرنامج. تم استخدام نموذج الاضطراب ($k-\varepsilon$) لمعدل الضائعات مع الطاقة الحركية المضطربة لتحليل عملية الجريان المضطرب.

اجري التحليل بأستخدام طريقة الحجوم المحددة وطريقة الحساب لديناميك الموائع المعالج بالحاسبة CFD.

لأول مرة وباستخدام نموذج الطور المنفصل، تم تحليل احتراق الوقود السائل (الديزل العراقي والديزل الخفيف) للحصول على نتائج دقيقة ومقبولة لتوزيع درجة الحرارة والسرعة.... الخ. تم قياس درجه حرارة الغازات الخارجة من المرجل للديزل العراقي عمليا وكانت تساوي (930 كلفن) اما بالنسبة للديزل الخفيف فكانت درجه حرارة الغازات الخارجة (948 كلفن) وفقا للتجارب العملية للشركة المصنعة للمرجل. ولكن هذه النتائج تم حسابها نضريا بواسطة برنامج FLUENT فكانت درجه حرارة الغازات الخارجة للديزل العراقي (930.7 كلفن) وللديزل الخفيف (948.459 كلفن). أما بالنسبة لغاز الميثان فكانت درجه حرارة الغازات الخارجة (564 كلفن) (وفقا للنتائج العملية

جمهورية العراق
وزارة التعليم العالي والبحث العلمي
الجامعة التكنولوجية
قسم هندسة المكائن والمعدات

محاكاة حساب ديناميكية المائع لأحتراق بعض أنواع الوقود السائل والغازي العراقي

أطروحة مقدمة الى
قسم هندسة المكائن والمعدات في الجامعة التكنولوجية كجزء من متطلبات
نيل درجة ماجستير علوم في الهندسة الميكانيكية

أعداد المهندس
حيدر محمد عباس
بكالوريوس هندسه ميكانيك. 2002

أشراف
أ.م. د. قتيبة جميل مهدي
أ.م. د. عادل محمود صالح

2013